THE UNIVERSITY *of* EDINBURGH

THE UNIVERSITY *of* EDINBURGH

Understanding and utilising bacterial growth rate changes at high external osmolarities

Doctorate of Philosophy Thesis

Examiner:	Matt Scott, Andrea Weisse
Chair:	Prof. Dr. Steven Spoel
Principal Supervisor:	Prof. Teuta Pilizota
Assistant Supervisor:	Prof. Alexander Medvinsky
Study Program:	Ph.D in Biology
Submitted by:	Mark Zurbruegg
Matriculation Number:	1476065
Defense Date:	10 October 2023
Submission Date:	11 January 2024

Abstract

Bacteria colonized nearly all corners of the globe because of their amazing ability to adapt and evolve. To humans, bacteria represent both an incredible tool, that can be harnessed for food production, medicine, and biotechnology; and a danger that can cause famine and disease. Understanding what drives bacterial growth is therefore of great importance to harness the power of microbes both good and bad. The traditional model bacterium, *Escherichia coli*, can survive and grow in a variety of different environments, that vary in pH, temperature, osmolarity, and other physical parameters. However, our understanding of how *E. coli* manages to overcome these adverse conditions to continue growth is incomplete. Determining the physical limits imposed on growth by the external environment holds significant scientific importance, as it helps prevent unwanted bacterial growth and enables increased industrial bacteria production for biotechnology and agriculture applications.

For more than a century, scientists have extensively studied the growth rate of bacteria. When bacteria are allowed to adapt to their environment, they exhibit constant growth. However, the speed at bacteria grow varies significantly and depends on the strain of bacteria as well as the conditions in which it is grown. Unraveling the specific mechanisms that govern growth is challenging due to the complexity of biological systems, such as *E. coli*. Growth can be viewed as the process in which bacteria transform nutrients from their environment into more cellular material. Growth, therefore emerges from the metabolic flux of nutrient substrates to bacterial products, catalyzed by bacterial enzymes, raising questions about what limits the rate of metabolic flux under specific conditions. How does the cell effectively balance metabolic flux across diverse environmental circumstances to optimize its growth rate? Previous studies have extensively explored the relationship between the nutritional composition of growth media and the rate of growth.

However, nutrient limitation is just one of the many stresses bacteria face in nature. They also encounter other challenges, such as oxygen limitation, extreme temperatures (both low and high), pH variations, and fluctuations in osmolarity, all of which

can impact their growth rate. This thesis aims to investigate how hyperosmotic stress affects bacterial growth.

I demonstrate that increasing the media osmolarity does not affect the growth rate by providing an energy burden, or a proteome burden on the cell. I also show that the growth rate slow down is not caused solely by a decrease in cytoplasmic water concentration. I present evidence that a similar slow down can be achieved by loading the *E. coli* cytoplasm with compatible solutes that do not cause osmotic stress. Therefore, the decrease in growth rate seems to be independent of osmotic stress. Instead data suggests osmotic stress causes cell-wide changes in metabolic efficiency. I hypothesize that the reduced growth is the result of increased cytoplasmic viscosity decreasing the rate of metabolic flux.

Finally I apply knowledge gained during this fundamental scientific investigation to explore whether lactobacillus experience osmotic stress during industrial fermentation and whether strategies used by *E. coli* can lead to potential improvements of the growth rate and yield. I find that there is minimal osmotic stress during fermentation and that addition of osmotic stress by addition of NaCl reduces yield after culture and does not provide any additional benefits when freezing or freeze-drying bacteria.

Keywords: Bacterial Growth, Osmotic Stress, Bacterial Biophysics, Compatible Solutes, Trehalose

Lay Summary

Bacteria are all around us. In fact they are inside us as well. They are important for keeping us healthy and for making us sick. We use them to make food and to produce medicine. Yet until recently we didn't really understand why bacteria grow fast or slow, what makes them thrive and what makes them struggle. We know that when we give them food and good conditions they will rapidly double their numbers until they use up all the resources.

We want to make bacteria grow quicker in some cases and stop their growth in other cases, so we need to understand what drives their growth. For the bacteria to grow they need to take food from the environment and turn it into more bacteria, just like how humans grow. We understand why giving them good food makes them grow fast. However, we do not understand how adding salt or sugar to the solution bacteria grow in affects growth. It was already well known that adding too much salt slows or stops bacterial growth, this is used for example to make cured meats. Adding salt or sugar or really anything that dissolves in water is a problem for the bacteria because it will suck the water out of them and cause them to shrivel up. This is because water flows wherever the most other stuff is. However, bacteria can counteract the loss of water by bringing stuff into the cell. This causes the water to go back into the cell. We thought maybe the bacteria needs to spend a lot of energy or resources on bringing stuff into the cell but this was not the case.

Instead the stuff bacteria make or bring into the cell itself is slowing their growth. I show that even if cells don't lose water they still grow slower if a lot of stuff is in the cell. I propose a new theory, enzymes the workers of the cell that convert nutrients to more cell have a difficult time moving around as the cell brings in stuff. Just like it is more difficult moving your arms about in water than it is in air. This causes everything inside the cell to happen slower. Overall, this work can be important for a lot of different applications ranging from food preservation to fighting bacterial infections.

Contents

List of Figures

List of Tables

List of Abbreviations

4-MUG	4-Methylumbelliferyl-β-D-galactopyranoside
ATP	Adenosine triphosphate
BetA	choline dehydrogenase
BetB	betaine aldehyde dehydrogenase
BetT	choline:H^+ symporter
CAA	casamino acids
CFU	colony forming units
complex media	Complex Media
CTC	Chlorotetracycline
DMSA	dimethylsulfonioacetate
DMSP	Dimethylsulfoniopropionate
DNA	deoxyribonucleic acid
E. coli	*Escherichia coli*
EF-Tu	Elongation Factor thermo unstable
EG	Ethylene Glycol
FACS	Fluorescence Assisted Cell Sorting
G6PDH	glucose 6-phosphate dehydrogenase
GAPDH	glyceraldehyde-3-phosphate dehydrogenase
GDH	glutamate dehydrogenase
GlpF	Glycerol facilitator protein
GOGAT	glutamine oxoglutarate aminotransferase

GTP	guanosine-5'-triphosphate
HPLC	High-Performance Liquid Chromatography
IPTG	isopropyl-β-d-thiogalactopyranoside
KdpFABC	K+ transporting P-type ATPase
KGlu	potassium glutamate
L. animalis	*Lactobacillus animalis*
LAB	Lactic Acid Bacteria
LB	Luria-Bertani liquid medium
MOPS	morpholinepropanesulfonic acid
mOsm	milliosmoles
mRNA	messenger RNA
MRS	De Man–Rogosa–Sharpe
NAD	Nicotinamide adenine dinucleotide
NADH	Nicotinamide adenine dinucleotide H
OD_{600}	OD_{600}
OtsA	trehalose-6-phosphate synthase
OtsB	trehalose-6-phosphate phosphatase
PCR	Polymerase Chain Reaction
PGK	phosphoglycerate kinase
ppGpp	guanosine-3',5'-bispyrophosphate
ProP	osmolyte:H^+ symporter
ProU	glycine betaine ABC transporter
ptsG	glucose-specific PTS enzyme IIBC component
relA	GDP/GTP pyrophosphokinase
RFU	Relative Fluorescence Units
RNA	ribonucleic acid
rRNA	ribosomal RNA

sfGFP	super-folder green fluorescent protein
spoT	bifunctional (p)ppGpp synthase/hydrolase SpoT
TC	ternary complexes
TreA	periplasmic trehalase
TreB	trehalose-specific PTS enzyme
TreC	trehalose-6-phosphate hydrolase
TreF	cytoplasmic trehalase
TreP	trehalose phosphorylase
TrkGH	K+ transporter
tRNA	transfer RNA
TST	Transition state theory
WT	Wild-Type

Acknowledgements

This thesis could not have happened without the input of many talented people who supported and guided me through it. First I would like to thank my fiancee Man-Ying, who kept me sane and insisted that I go outside for at least 5 minutes a day. I would also like to thank Teuta who has been an excellent supervisor, our vivid discussions pushed me to learn more and I could not have completed this thesis without her support. Despite having multiple other students and starting her own company it always felt like she responded to my e-mails with almost too much enthusiasm. Her input on this project helped guide and shape this project and her guidance and support inspired me. I always tell prospective Ph.D. students that scientific arguments with her may be intense but at the end you do not need to be worried about the Viva. I would also like to thank my industrial mentor Zuzana Mladenovska who taught me a lot about work in an industrial setting and lactic acid bacteria. Working at Chr. Hansen was an amazing opportunity and I cherished working in this fast paced environment with many talented colleagues. I would also like to thank Chr. Hansen for part funding this Ph.D. together with the EPSRC. Thanks also goes out to Smitha Hegde for her guidance and entertaining discussions as well as teaching me how to run and operate our microscope. The same goes to Dario Miroli, who laid a lot of the ground work for my project. Jill Howie and Francesca Galdi who are now with Ogi bio also gave me a lot of support with operating and running micro bioreactors and it has been a joy to watch the evolution of this product. Finally from the Hwa lab I would like to thank Hiroyuki Okano who guided me and taught me a lot about scientific precision, HPLC and a lot of other topics, as well as Zhongge Zhang who rapidly generated three different strains for me. Finally, a special thanks to Terry Hwa who provided a huge amount of insight into my project and provided so much insider knowledge that really boosted my understanding of bacteria in general.

Quotations

> ”There is always a way to water.”
> —-Fremen saying from Dune by Herbert Frank

> Everything that happens, happens as it should, and if you observe carefully, you will find this to be so.
> —Marcus Aurelius

1. Introduction

1.1 Introduction to Thesis

Biology is nothing more than the laws of physics and chemistry applied to life. In fact all of life can be characterized as a series of self-sustaining chemical reactions. Erwin Schrödinger pointed out that one of the distinguishing characteristics of life is the ability to resist entropy. While most systems get more disordered with time living things oppose this natural descent into disorder by using energy from their surroundings. While this view of life may seem nihilistic it is in fact the opposite, it shows that despite the inexorable pull towards chaos, intricate complexity can arise. It is from this view point that I would like to approach my thesis, the idea that complex biological systems must deal with the harsh reality of physical laws that govern all matter and energy.

One of the physical constraints all organism face is the need for water. Water is essential for life, providing the solution for the molecular machinery present inside the cells of organisms. Therefore two opposing constraints are placed on cells, there has to be free movement of water required for functioning of cellular components, as well as preventing the loss of other cellular content. The problem is solved by using a semi-permeable phospholipid bilayer to form the cell membrane. The membrane retains all the constituent components while permitting free exchange of water. However, having a semi-permeable membrane means that water flows into or out of the cell by osmosis. The direction of the flow is determined by a simple equation

$$\Pi = (c_i - c_e)RT. \tag{1.1}$$

Here we calculate the osmotic pressure Π by taking the difference in the number of solutes inside c_i and outside the cell c_e and multiplying it by the gas constant and temperature RT. If solutes outside the cell are higher than inside the cell then water will flow out of the cell. If solutes inside the cell are higher than outside water will flow into the cell. Most human cells are iso-osmotic with their surroundings meaning that the

concentration of solutes inside and outside the cell is approximately equivalent and osmotic pressure is close to 0. Bacteria and many other single celled organisms have a higher solute concentration inside than outside leading to a net influx of water which generates osmotic pressure. The pressure inflates the cell membrane creating outward pressure. The outward pressure is counteracted by the rigid cell wall exerting an inward pressure. However, single celled organisms such as *Escherichia coli* (*E. coli*) face a fundamental problem. The osmolarity of their surroundings (c_e) varies wildly. These cells therefore have to be able to adapt to external osmolarity changes. Indeed *E. coli* can grow at osmolarities ranging from 0.04 to 3 osmole (*1*). However,with increasing osmolarity the rate at which *E. coli* grows decreases, an effect that has been known for nearly a century (*2*). Despite there being many attempts to explain the cause of the growth slowdown no definitive answer is given.

The main aim of this thesis is to attempt to answer what is the origin of the growth slowdown at increased external osmolarities, and in a broader sense investigate the impact of changes in the external osmolarity on *E. coli* and other bacteria. To accomplish this task I will first give a brief overview of the history of microbiology and focus on how quantitative biology allows us to develop biophysical models that can answer important biological questions. I will then focus on how biophysical models can be used to test and understand the effect of osmolarity on the growth rate of bacteria. However, first I would like to outline why the growth rate of bacteria is so important.

1.2 Why Growth Rates Matter

One of the most important characteristic of a bacterium is how fast it grows. Growth here is defined as the process of binary fission turning one cell into two. The ability to grow implies that the cell can copy its genetic material, as well as, double all the proteins, lipids, ribosomes and other cellular components. At the same time cells have to ensure that the metabolic fluxes of precursor and intermediaries provide the cell with a constant source of new material required for growth. The growth rate is therefore an amalgamation of all these variables and can be regarded as a window into all other cellular functions. Like all living things bacteria must deal with a variety of physical constraints that put limits on their behaviour. Understanding what these constraints are and how the cell optimizes its growth rate in different circumstances will allow us to control when and how cells grow.

Understanding bacterial growth can help us build knowledge about cell and molecular biology. *E. coli* is one of the most studied organisms and has provided insight into the nature of all organisms. Bacteria represent a simplified system to investigate

resource allocation, cell division, gene regulation and many other fundamental processes in biology. Bacteria also have many practical applications and are used for everything from molecular biology, to producing the food we eat. Understanding their growth and metabolism is crucial for optimizing production processes, such as the manufacturing of pharmaceuticals, enzymes, starter cultures, and biofuels. Additionally, the bacteria that inhabit our body play an essential role in preventing disease, and keeping us healthy (*3*). Conversely, bacteria have the ability to cause disease. Understanding bacterial growth helps us investigate how these microorganisms multiply, survive, and spread. Knowledge of bacterial growth is essential for developing strategies to prevent and control illness. Understanding bacterial growth allows for prevention strategies such as proper hygiene practices, antibiotic use, and vaccination. Bacteria also play a critical role in spoiling food and undesired growth can cause serious food safety issues. Preventing bacterial spoilage of food can help alleviate food shortages and improve population health. Improving food safety was a major achievement of microbiology. Furthermore, inhibition of growth plays a major role in the emergence of antibiotic resistance (*4*). Antibiotic resistant bacteria are named as one of the biggest threats to global health, food security, and development by the world health organisation. An estimated 4.95 million deaths are associated with antibiotic resistance and 1.27 million deaths are caused directly by antibiotic resistance (*5*, *6*). Understanding what drives bacterial growth will give us insight into how we can change bacterial growth to our advantage, helping us improve food security and global health.

Now that it is clear why bacteria and their growth matter, I would like to honour the history of microbiology which is in itself a fascinating topic. Advancements in microbiology such as sterile surgery and the discovery of penicillin has undoubtedly saved millions of lives.

1.3 The Early History of Microbiology

Humans have a long history of using microorganisms in food and agriculture, such as turning milk into cheese. Some studies suggest that use of micro-organisms happened as early as 7200 years ago (*7*, *8*). This mirrors findings on alcohol production that uses yeast and was produced approximately 7000-6600 B.C. (*9*). The relationship between humans and bacteria therefore has ancient roots.

Human understanding of bacteria and their role in disease also predates recorded history. For example neolithic humans were aware of illnesses and had some basic medicines to treat them. Ötzi the remarkably well-preserved mummy of a man that

lived 5250 years ago had genetic traces of *Borrelia burgdorferi* in his blood. Among his possession were *Piptoporus betulinus* fungi known to possess antibiotic properties. Demonstrating that people may have utilized antibiotics for a long time (*10*).

Despite medicinal knowledge to treat bacterial disease, the nature of microbial pathogens was not well understood. Some of the earliest recorded believes about the origin of bacteria and mould were that they were created spontaneously. The early Greeks believed in abiogenesis, the creation of living from the non-living, thinking that mould on bread arose spontaneously. However as early as 384 B.C. humans at least partially understood that life is a continuous process but did not understand that this is true also for microbial organisms. Aristotle's writings described four ways in which life is created (*11*).

1. Spontaneously from mud (abiogenesis)
2. Budding of from other organisms (asexual reproduction)
3. Sexual reproduction without copulation
4. Sexual reproduction with copulation

The first recorded link between microbes and disease was made by the Greek physician Hippocrates, suggesting that supernatural forces were not the cause of illness. Instead, he proposed that illnesses were the result of natural causes from the patient's surroundings (*12*). The theory was elaborated on by Thucydides, who wrote about the Athenian plague, that wiped out one-third of the Athenian population at the time. He noted that the plague transferred from person to person. However, once the person had been infected, they would be immune to re-infection (*13*). Even the idea of microscopic organisms has existed at least since the times of ancient Rome. Marcus Terentius Varro mentions the idea of *animalia minuta*, animals so small they cannot be seen with the eye, that are the cause of disease (*14*).

However, it was not until the Age of Enlightenment that humans really started to understand the roots of phenomena such as fermentation, spoiling and bacterial disease. Like many advancements, this observation was driven by development of a new technology, the microscope. A Dutch merchant, named van Leeuwenhoek, was originally interested in better observing the quality of the cloth he was trading. To achieve better insight into his fabric, he built the first microscope powerful enough to observe the *animalia minuta* Varro hypothesized about nearly two-thousand years ago (figure 1).

It was through the experiments of Lazzaro Spallanzani that the spontaneous generation of life was really questioned. Armed with microscopes to see bacteria and other microscopic organisms growing, many researchers came to the conclusion that they spontaneously arise on certain substrates that had undefined life generating prop-

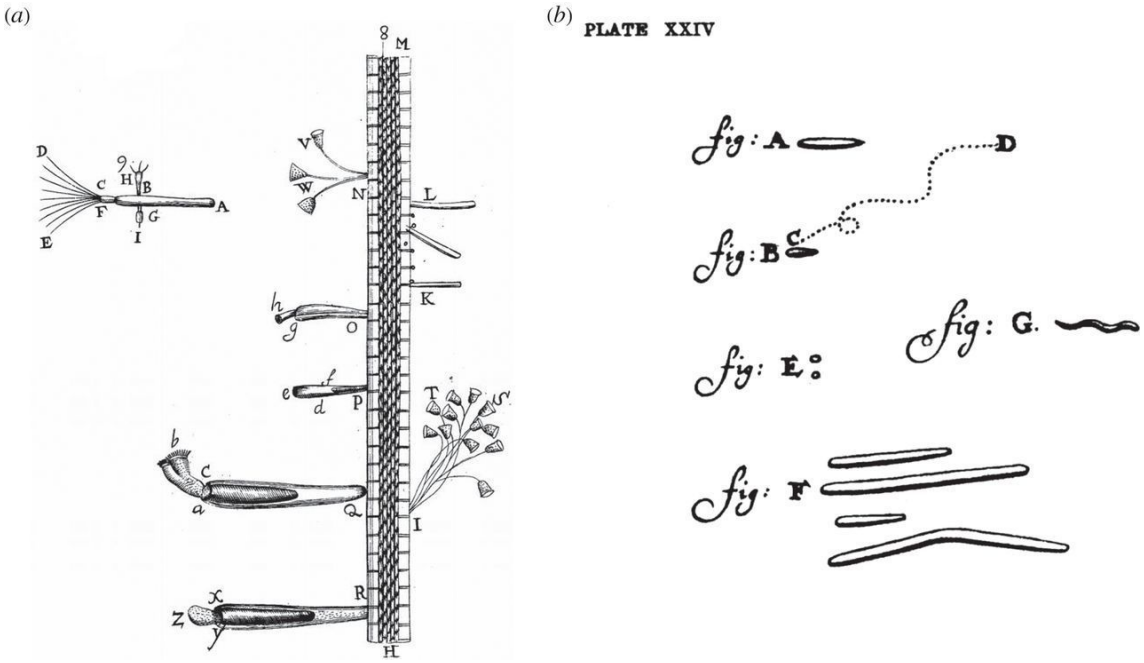

Figure 1: Drawings sent to the Royal Society from van Leeuwenhoek reproduced from his original letters (*15*). Reproduced with permission from (*16*).

erties. However, Spallanzani showed that boiling the life generating substrate and keeping it sealed stopped any growth of organisms. He hypothesized correctly that microbes spread through the air. The first direct evidence that microbes could cause disease were collected by Agostino Bassi around the 1820's who observed a fungal infection in silk worms. Furthermore, he showed that various chemicals could decrease the infection rate of the silkworms. He postulated that a similar process was responsible for human disease (*17*). These findings paved the way for Louis Pasteur's and Robert Koch's studies (*18*), as well as modern food preservation techniques (*19*).

It was in the mid 18th century that the golden age of Microbiology really began. Louis Pasteur figure 2 was a French chemist that had already made important contributions to science by discovering molecular chirality (*20*). Additionally, his remarkable achievements extended to the fields of microbiology and bacteriology. He conclusively disproved the theory of spontaneous generation by generating sealed environments and sterilizing them. As no life arose spontaneously in these environments, it showed that life must be continuous and non-living cannot become alive spontaneously (*21*). While these insight now seems common sense to us, they had huge ramifications for public health and disease treatment. It furthered the germ theory of diseases, leading to Joseph Lister, along with others, developing antiseptic methods in surgery. Antiseptic methods drastically reduced the death rate during surgery, as surgeons were no longer introducing infections into the body (*22*). Furthermore, Pasteur proposed the idea that fermentation was a microbiological process and not caused by decom-

position of chemical products, as was previously believed (*23*).

Simultaneously, Robert Koch (figure 2) showed that bacteria were the causative agent in cholera, anthrax and tuberculosis.

He made four fundamental observations:

1. A specific disease is always associated with a specific microorganism.
2. The microorganism can be isolated from an infected animal.
3. Transferring the microorganism to a healthy animal will result in that animal getting the specific disease.
4. The microorganism can now be isolated from the sick animal, whereas it could not be previously from the healthy animal.

Koch developed methods to culture bacteria in the laboratory on agar dishes. Petri dishes are named after his assistant, Julius Richard Petri. Finally, Koch made important contributions to microscopy, he was the first physician to use an oil immersion lens and condenser, and the first to take microphotography images of the bacteria he was studying (*24*), rather than relying on sketches.

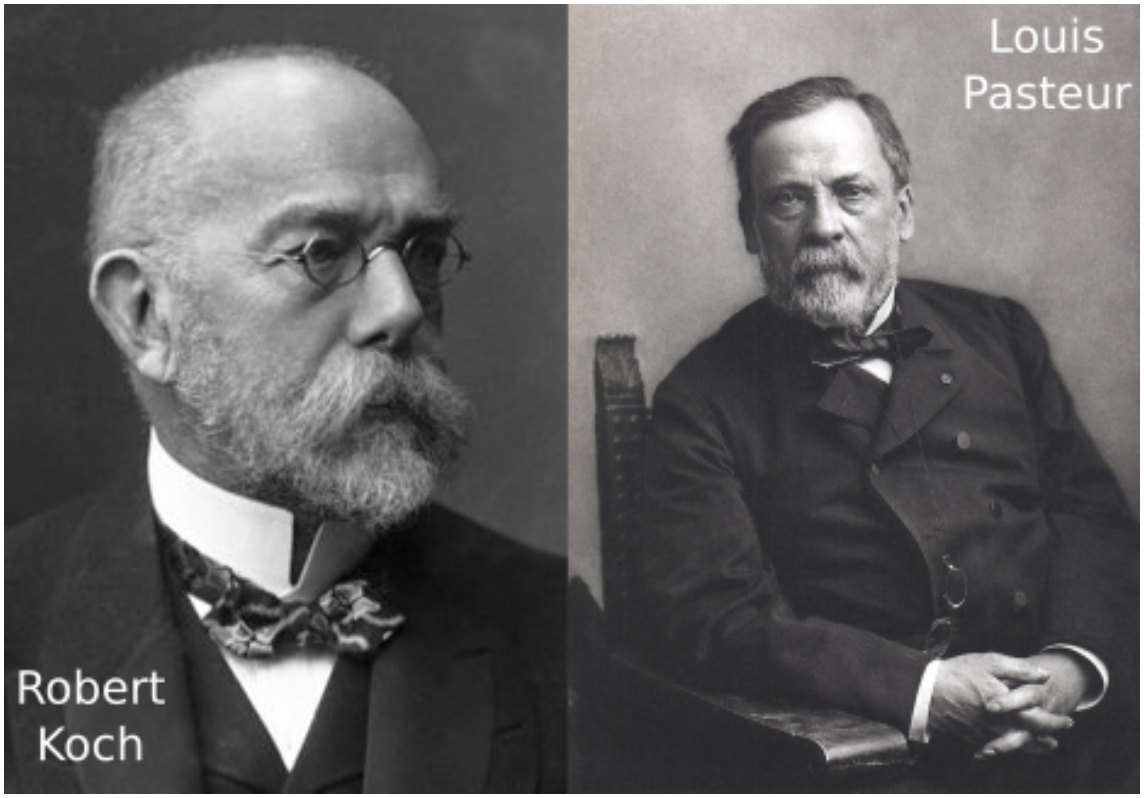

Figure 2: Robert Koch and Louis Pasteur are two of the most important figures in the history of microbiology. Their discoveries have undoubtedly saved millions of lives.

Historically, it becomes clear that microbiology has always been an interdisciplinary

subject. It was thanks to a textile merchant that we unlocked the wonderful world of microbes. The establishment of microbes as essential in industrial processes such as fermentation led to the birth of biotechnology. The insight that some bacteria could be helpful to society laid the groundwork for more than a century of follow-up research into how we can utilize these magnificent microbes to our benefit. Conversely, the acknowledgment that disease is caused by microscopic lifeforms paved the way to greatly improving human health. Thanks to understanding pioneered by Koch and Pasteur, that micro-organisms cause disease, we greatly reduced mortality of infectious disease. The discovery of antibiotics by Alexander Fleming, as well as antiseptic technique were all enabled by these early studies.

We can therefore conclude that understanding of microbes has had a tremendous impact on human society. However, these micro-organisms were still puzzling as scientists struggled to understand how these tiny organisms functioned and what drove their rapid growth. The next section will explore the intricate and complex networks that allow bacteria to survive and thrive in all corners of the globe and even space (*25*). I will then discuss how the development of quantitative biophysical models allowed scientists to quantify, understand and, model the biological processes underlying bacterial growth.

1.4 Introduction to Bacterial Biophysics

Given the importance of bacterial growth surprisingly little was understood about how bacteria regulate their growth. Early studies attempting to characterize bacterial cell growth noted that it proceeded in four distinct phases. First there is a period of adaptation during which bacteria do not grow. Then the cells undergo a period of exponential doubling. At a certain point the bacteria stop growing and enter a stationary phase. Finally, cell numbers will start declining as cells die figure 3 (*26*). However, there was no understanding of why bacteria grew in this specific way. Early speculations were that the growth curve was defined for a specific organism just like a human being grows to a certain size the bacterial population undergoes a fixed amount of growth and then stops (*27*).

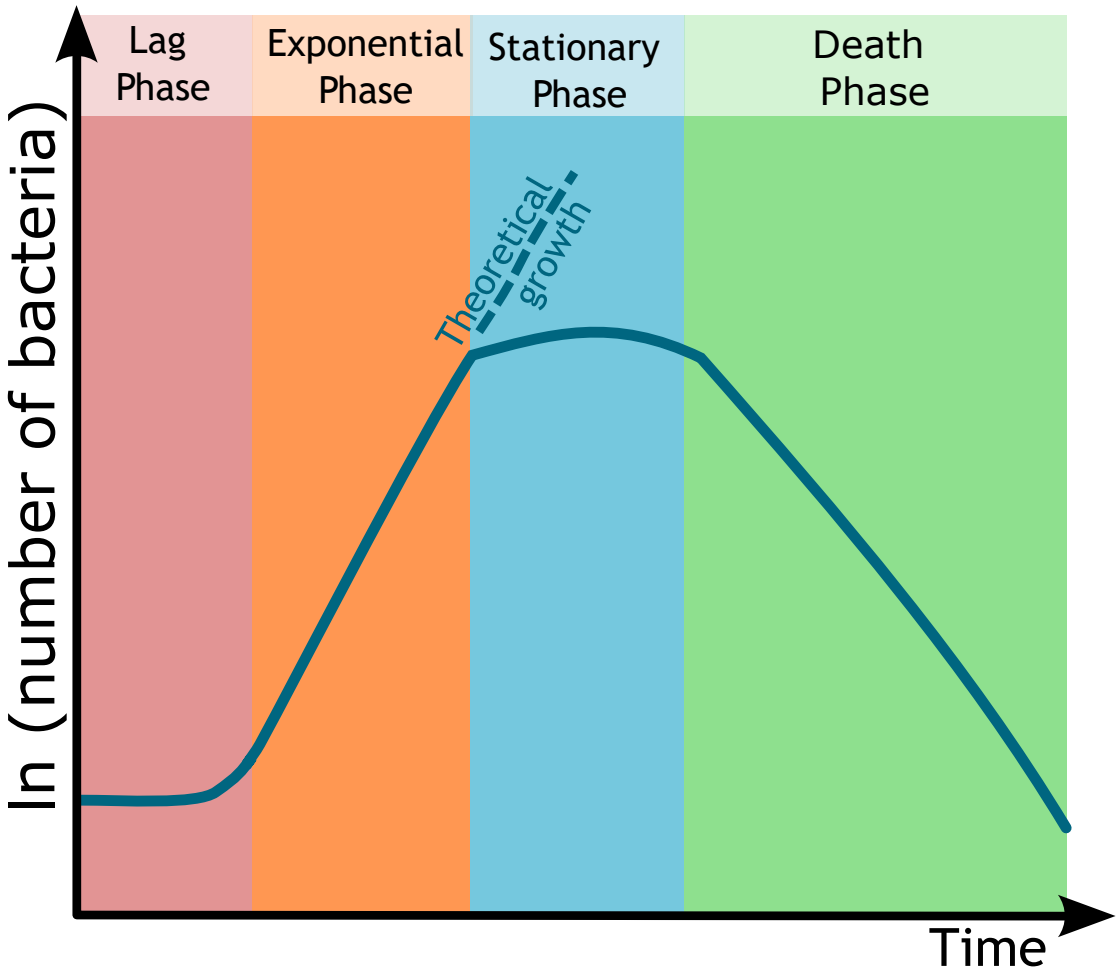

Figure 3: Representation of Bacterial Growth Curve

This meant that data collected at the time were mainly observational, with experiments looking at changes in the growth curve in different environmental conditions. These studies failed to understand the specific relationships between an environmental conditions and bacterial growth. The important question is: are there underlying

principles that can be used to predict how bacteria will grow in different environmental conditions? To answer this question we first need to define growth. Growth can be defined as the biosynthetic flux of substrate molecules into the complex chemical products we associate with life such as deoxyribonucleic acid (DNA), ribonucleic acid (RNA), lipids and proteins. Additionally, there has to be some regulation of the biosynthetic flux. The creation of new cell wall material needs to be in proportion to the rate of DNA synthesis so that division can happen when the cell has generated one nucleoid per cell. Therefore, to understand what drives growth in these bacteria we have to understand the biosynthetic flux and how it is regulated.

To solve this conundrum there are two possible approaches. The first is looking at all the components inside bacteria, understanding the function of each and then inferring how these components interact and change in the different environments. However this approach is extremely complex as it requires understanding of all of the components of the bacterial cell and their function. This was not feasible approach during early biophysical studies of bacteria, due to the lack of genomic, proteomic and metabolomic data, even now genome scale models show several limitations (*28*–*30*). Therefore an alternate way of dealing with the complexity of bacterial growth is using biophysical models. These models attempt to identify state variables that are required for predicting the behaviour of the cells rather than trying to characterize the behaviour of every single system component. The most poignant example that really illuminates the benefits of this approach is the comparison to the ideal gas law (*30*)

$$\rho V = \eta R T. \tag{1.2}$$

The ideal gas law allows prediction of pressure (ρ) from three easily measured variables; temperature (T), number of moles of gas (η) and volume (V), and the gas constant (R) equation (1.2).

This approach is much simpler than trying to model the behaviour of every single gas molecule in a given volume. Furthermore, we understand exactly how any given perturbation will affect the system without having to understand the behaviour of every gas molecule in it. However, it was unclear whether modelling living organisms is even feasible because unlike non-living systems, living systems do not exist in a state of thermodynamic equilibrium. As bacteria are constantly changing it may not be possible to use coarse-grained models to predict their behaviour. Below I will review how quantitative biology was successfully applied to generate models that recapitulate bacterial growth based on knowledge of just a few variables. The most important question for any model is what parameters and variables to include. The best place

to start this investigation is therefore with growth itself.

In the 1940's Monod systematically investigated the lag, exponential and stationary phase of the growth curve. He discovered a Michaelis-Menten type relationship between concentration of sugar in the bacterial growth media and bacterial growth rate during the exponential phase equation (1.3). Monod also noted that the yield of a culture was dependent on the total amount of sugar available (*31*). Monod therefore managed to show that all of the complex biophysical changes and genetic regulation occurring in *E. coli* leading to a reduced growth rate could be recapitulated as

$$\mu = \mu_{Max} \frac{[S]}{K_S + [S]}. \tag{1.3}$$

Where the growth rate (μ) is dependent on the maximal rate of growth (μ_{Max}), the substrate concentration $[S]$, as well as the "half-velocity constant" (K_S), which is the value of $[S]$ when $\mu/\mu_{Max} = 0.5$.

This study was extremely important because it showed that bacterial growth rate is predictable, and bacteria can be brought into a state where modelling reveals clear relationships. The study also demonstrated the importance of the growth rate as a variable resulting from environmental change. It was really Monod's work that led to the realization that exponential growth leads to reproducible experimental conditions. The term used to describe bacteria growing exponentially was balanced growth (*27*), which is mathematically described as bacterial growth matching the following relationship

$$N = N_0 \cdot e^{\lambda t}, \tag{1.4}$$

where the number of bacterial cells N is equal to the initial number of bacteria N_0 multiplied by e to the power of the growth rate λ and time t. Therefore, the time for a bacterial population to double is given by:

$$\text{Doubling Time} = \frac{\ln 2}{\lambda}. \tag{1.5}$$

Therefore, during balanced growth the internal cellular environment must be unchanging as growth itself is the result of cellular processes (*32*). The unchanging cellular environment meant that while the cells were not in thermodynamic equilibrium they were still amenable to modelling during the period of exponential growth, as on aver-

age the conditions within the population are unchanging.

Conversely, cell populations that are not in balanced growth show rapid changes in the biochemical and physical composition of the cell making it difficult to reproduce experimental results as slight variations in sampling time points can lead to drastically different results (*33*). Monods' experiments therefore showed that bacterial populations didn't have a predefined growth cycle but that the growth rate, as well as the population size could be predicted from knowing the environmental conditions. It also made it clear that the reason for the typical growth curve was not that bacteria could grow to some predefined population size but that they ran out of nutrients for growth. Monods' research allowed the development of chemostats in which bacteria are continuously diluted in fresh media allowing for endless exponential growth (*27*).

Based on the observation that the bacterial growth rate is a representation of the physical and chemical processes inside the cell a group of scientists started using an interdisciplinary approach to microbiology, By combining physics, mathematics and, biology they would develop fundamental insights in bacterial physiology and the approach became known as the Copenhagen school of bacterial biophysics. They asked a simple but powerful question: does the growth rate determine important cellular characteristics such as cell size, RNA and DNA content? The answer was a clear yes. Two very different media could yield very similar results as long as the growth rate was the same and two very similar media could have very different results if the growth rates differed (*34*). There is a correlations between the growth rate and these cellular parameters. Based on the correlations they could develop coarse grained models linking various attributes of the cell to the growth rate. As an example consider the relationship between cell size and growth rate equation (1.6)

$$S \propto e^{\gamma\lambda}. \tag{1.6}$$

Here the size S is proportional to the change in size γ, in relation to the growth rate λ (figure 4 plot A). The fact that a complex biophysical phenomena such as cell size could be linked to the growth rate by such a simple equation is a testament to the benefits of using a quantitative model to understand the complex processes governing bacterial cells. Furthermore, the growth rate was proportional to the amount of DNA and RNA present in the cells (figure 4 Plot B and C).

These findings are surprising at first because it suggests that the complex biochemical networks that govern the cell obey simple physical rules. Such simple relationships are unexpected because life is thought to be constantly changing and it was not clear

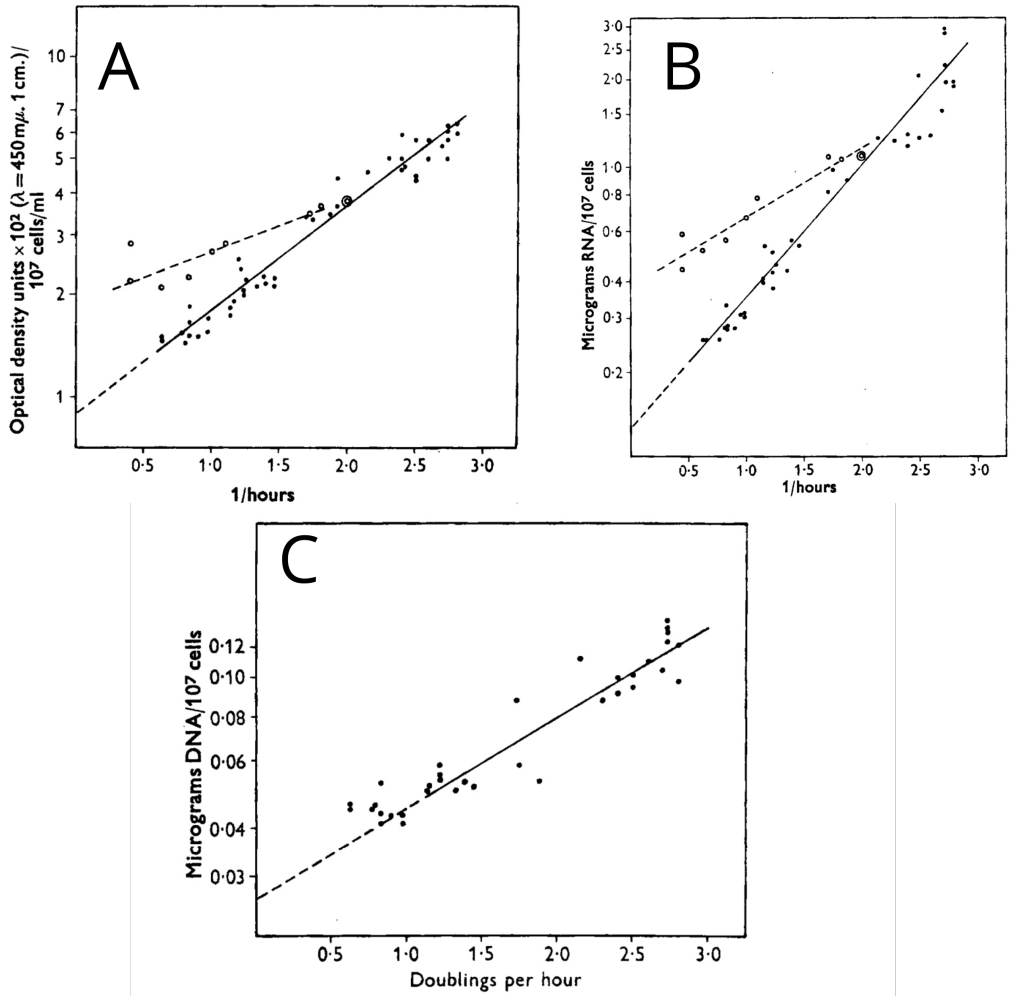

Figure 4: Growth rates exhibit a linear correlation with cell size, RNA and DNA. Original Figures reproduced from (*34*). **A)** Cell size as measured by change in OD for 10^7 cells. **B)** Micrograms of RNA per 10^7 cells. **C)** Micrograms of DNA per 10^7 cells.

that cells would show linear relationships between different variables. However, this makes evolutionary sense as bacterial cells such as *E. coli* must be able to adapt rapidly and grow in a variety of different environments. To ensure that rapid adaptation is possible the networks underlying bacterial growth must be able to sense and respond to changes within the internal environment. Having networks that show proportional regulation is much easier than trying to individually regulate every pathway for every different environmental condition. In fact it is a biological necessity that many of the pathways show linear correlations. Consider if the cell suddenly generated more DNA than cell wall material. As growth progressed more and more DNA is accumulated with insufficient cell wall expansion. The accumulation of DNA could eventually strain the cell wall and lead to rupture and cell death. Causing a disconnect between different growth processes is the mechanism that underlies the effectiveness of antibiotics such as beta-lactams that inhibit cell wall synthesis. These antibiotics are very effective at killing rapidly growing cells but are ineffective against non grow-

ing cells. It is therefore not surprising that most cellular components varied with the growth rate to some extent (*35*).

However, even more coordination between cellular components is required, while many bacterial components were abundant and could be split arbitrarily between the two newly created cells, it is of great importance that exactly one copy of the bacterial chromosome ends up in each of the cells. Having demonstrated the power of biophysical models to understand growth the same principles were now applied to DNA replication.

1.5 Biophysics of DNA Reproduction in Bacterial Cells

Growth is not just addition of biomass but requires actual splitting of cells into two. Without cell division cells would just grow larger and larger which comes with a whole set of physical problems, such as changes in the surface to volume ratio and limits in the rate of diffusion. The observation that cells must balance a variety of complex processes raises the question if the rate of biosynthetic flux is limiting growth rate, or is it a more complex phenomena such as cell division? Growth could be limited by the time it takes to replicate the bacterial chromosome. While abundant cellular components like ribosomes can be roughly split between the two cells, the chromosome is unique with one copy per cell and replication needs to be coupled to cell division. So to grow fast cells need to duplicate their genome quickly.

In eukaryotic cells early studies found that cells paused their growth before division indicating that DNA replication is the limiting factor in growth. These observations led to the discovery of cell cycle checkpoints in eukaryotes (*36*). However, growth is not regulated by cell cycle checkpoints in bacteria as no clear checkpoints could be observed. To compound these problems there was not a good way to study cell division as division synchronization of a culture could not be achieved without shocking the culture (*27*). The inability to synchronize division times was overcome with the invention of the ”baby machine” figure 5. The baby machine consists of a membrane filter through which media is continuously flushed. The dividing cells would get stuck in the membrane only releasing newly born cells. Cooper and coworkers confirmed that only newborn cells were released by size measurements using a Coulter counter (*37*).

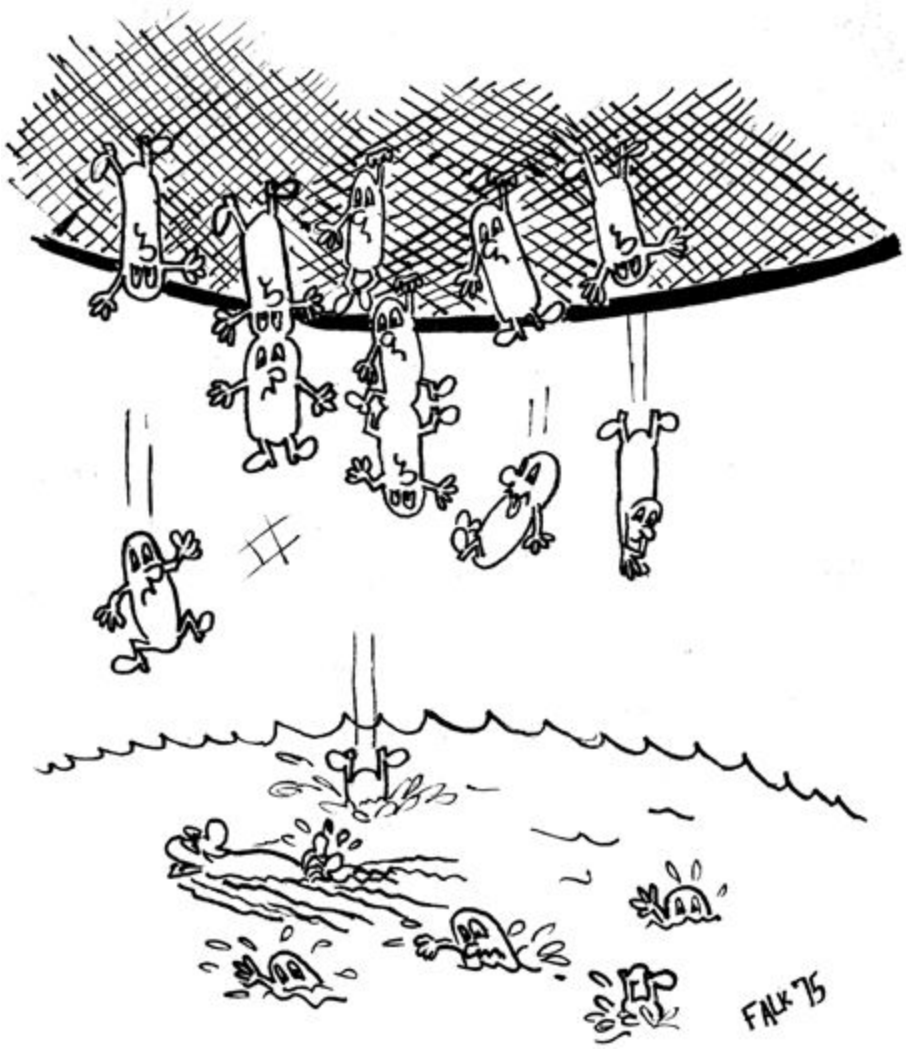

Figure 5: Caricature of baby machine sketched by Avshalom Falk while a student in the laboratory of Eliora Ron at Tel Aviv University. Reproduced under Creative Commons Attribution License from (*38*)

Using these newborn cells Helmstetter and Cooper could now precisely investigate what happened to the nucleoid in bacteria because cells were all at the same stage in the cell cycle. At the time it was already hypothesized that the replication of the *E. coli* chromosome had an origin of replication and a terminus. The time it took for cells to successfully replicate was therefore given by the time taken for replication of DNA (C) and time for division after replication (D). Meaning that the doubling time was equal to C+D (*37*). C was invariant with growth rate and media conditions at a specific temperature (*27*). Therefore, the only way in which *E. coli* could modulate the speed of replication is by changing the time between initiation of replication. Unexpectedly, the time it took for replication, was longer than the doubling time at fast growth rates with chromosome replication taking about forty minutes. Therefore, *E. coli* and other bacteria have to be able to initiate multiple replication forks at the same time (*39*).

The early studies from Monod, Ole Maaløe, Schaechter, Cooper and Helmstetter really underline how the use of mathematical models could explain how complex biological phenomena can arise from simple physical rules. Unlike cells in the human body that experience a tightly controlled environment and die rapidly when the external environment changes, bacteria must be able to survive and adapt to rapid fluctuations in their environment.

However, one mystery that proved resilient to investigation is how bacteria determined the rate at which they grow. So the rate of growth can be seen as the rate of biosynthetic flux which is driven by proteins catalysing reactions. However, there was no clear understanding of how cells regulated their proteins and why growth on two near identical carbon sources such as glucose and mannose varied so drastically. The next section will explore how two very similar sugars can result in different growth rates.

1.6 Bacterial Biophysics of Growth

Growth is the result of substrate flux through the bacterial metabolic networks. *E. coli* and all living things are in essence complex factories of chemical reactions. However, what then determines the maximum rate of metabolic flux through the network and therefore the growth? Schaechter proposed that the growth rate was determined by the ability to generate new proteins as proteins are what catalyze the metabolic flux (*27*). There is a linear relationship between the ribosomal content of the cell and the growth rate (*40*), with the caveat that the relationship between ribosomes and growth rate breaks at slow growth rates due to inactivation of ribosomes (*41*).

The rate of bacterial growth can therefore be described by knowing the number of ribosomes and the speed at which they are making new proteins

$$\lambda = N_R \times k_{ER} \times f_{active}. \tag{1.7}$$

Growth rate can therefore be predicted by multiplying the number of ribosomes N_R by their elongation rate k_{ER} and correcting for the fraction of inactive non translating ribosomes by multiplying by the fraction of actively translating ribosomes f_{active}. The relationship between ribosomes and growth, while important, just pushed the problem further down the road. What limits the number of ribosomes and why do cells in different media make different numbers of ribosomes?

Ribosomes are fascinating molecular machines consisting of both RNA and proteins. They have a special status in the cell translating messenger RNA (mRNA) instructions

transcribed by RNA polymerase into proteins. Ribosome synthesis is so important *E. coli* has seven ribosomal RNA (rRNA) operons (rrnA, rrnB, rrnC, rrnD, rrnE, rrnG, and rrnH) (*42*). The assembled prokaryotic ribosomes sediment as 70S particles. The *E. coli* ribosome is approximately two-thirds RNA and one-third protein. *E. coli* ribosomes consist of two subunits the 50s subunit is composed of the 23s, 5s rRNA, and 33 proteins, while the smaller 30s subunit contains the 16s rRNA, and 21 proteins (*43*).

Ribosomes are considered autocatalytic in the sense that they generate more of themselves. When cells are in balanced growth the rate at which more ribosomes can be made is therefore limited by the number of ribosomes themselves. As ribosomes are metabolically expensive to make, the number of ribosomes is also constrained by the metabolic cost of making ribosomes (*43*). The question how the cell then balances these two opposing constraints for increased protein synthesis and metabolic capacity underlies the growth rate regulation in *E. coli*. Scott and Hwa used a phenomenological approach to reveal the intrinsic constraints that regulates resource allocation to protein synthesis and other cellular functions (*44*).

The proteome is the complete set of proteins expressed by an organism. They note that the total amount of protein does not change between growth conditions. The change in number of ribosomes is determined by a change in proteome composition rather than a change in the total amount of proteins. The proteome composition is determined by what proteins are currently being synthesized.

As ribosomes are autocatalytic the rate at which more ribosomes can be made are determined by two things the translational elongation rate and the amount of ribosomes actively making ribosomal proteins. Scott and Hwa, looked at how translational capacity affected the growth rate. Using various *E. coli* mutants that had different translational elongation rates they show that the number of ribosomes required to achieve a specific growth rate can be described as

$$r = r_0 + \frac{\lambda}{K_t}. \tag{1.8}$$

Here the number of ribosomes (r) is determined by the amount of ribosomes at 0 growth (r_0) and the growth rate (λ) divided by the translational capacity of the cell (K_t). Therefore, at slower translational elongation rates cells need to make more ribosomes to achieve the same growth rate. Applying sub-lethal doses of translational inhibitors would have a similar effect and result in an increase in the number of ribosomes.

As can be seen from figure 6, as concentration of a translational inhibitor increases there is an increase in the number of ribosomes with a decreasing growth rate. The highest number of ribosomes a cell can support is given by the y-intercept of the slope formed by increasing translational inhibition for a given nutrient quality.Resulting in a striking correlation between the maximum number of ribosomes r_{max}, the growth rate λ and the nutritional quality of the media K_n

$$r = r_{max} - \frac{\lambda}{K_n}. \tag{1.9}$$

The equation indicates that there is a maximum r_{max} and minimum r_{min} number of ribosomes the cell can support. Furthermore, the equation shows that decreasing the nutrient quality of the cell results in a reduction in the number of ribosomes despite maintaining the elongation rate. A lower number of ribosomes at a constant elongation rate implies that the are producing less ribosomal proteins. A reduction in production of ribosomal proteins makes sense as reduction in the nutritional quality of the media means that proteins required to make the now missing metabolic components have to be synthesized. The simplest way to describe the observed data would be with a two component model where inducible proteins reduce the amount of ribosomal proteins synthesized. However, the value of r_{max} only accounts for 55% of the proteome meaning that there must be a third sector which is invariant with environmental conditions.

Based on these observations Scott and Hwa proposed a simple but elegant three component model explaining how bacteria regulate their growth. The total protein synthesis capacity of a cell is limited. Therefore cells generate the maximum amount of ribosomes when most ribosomes are making more ribosomal proteins. The maximum amount of ribosomal proteins (R) that can be made is limited by the need for cells to produce a set of proteins (Q) that remain invariant with environmental conditions and non-ribosomal proteins (P) that are generated based on changes in the environment figure 6.

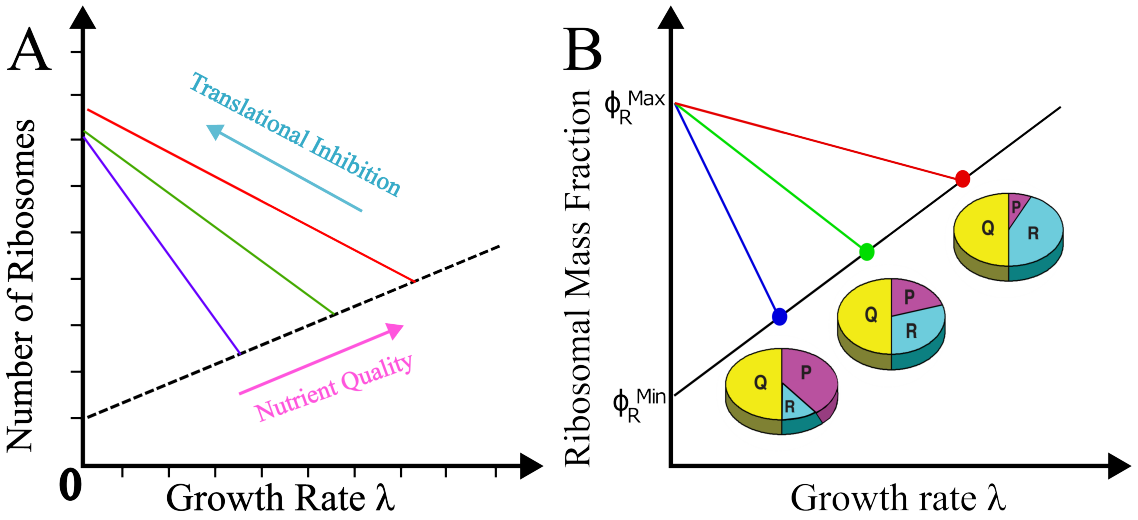

Figure 6: Visual representation of growth laws. **A)** Variation in the number of ribosomes with nutritional quality of the media. Inhibition of translation results in increasing number of ribosomes and slower growth. **B)** As the nutritional quality of the media improves more of the proteome can be allocated to synthesis of ribosomal proteins resulting in faster growth. If the translational capacity of the media is inhibited there is an increase in the number of ribosomes but the translational elongation rate is reduced, resulting in a reduced growth rate. Adapted from (*44*).

The three component model could finally explain how cells regulate their growth rate.

In nutrient rich media the cell dedicates more of its proteome to production of ribosomal proteins allowing for a larger ribosomal pool and faster growth. Conversely, lack of nutrients results in a reduction in the number of ribosomes, as the cell has to generate additional P-sector proteins.

Finally, Scott and Hwa demonstrate that if the translational capacity of the cell is reduced by decreasing the rate of translational elongation there is an increase in the number of ribosomes with a concomitant decrease in the growth rate. To achieve the same protein synthesis rate with a reduced translational elongation rate cells require more ribosomes. The increase in the R-sector necessitates a reduction in the P-sector meaning that generation of substrate for translational elongation is reduced. Therefore, a cell cannot sustain the same growth rate by increasing the number of ribosomes as it places a burden on the P-sector. Similarly, if you inactivate a large proportion of ribosomes by addition of chloramphenicol, the growth rate is again reduced despite having a higher number of ribosomes.

The model could accurately predict how cells behave when the nutritional capacity of the media is altered, as well as why overexpression of a protein not contributing to metabolic flux slows bacterial growth. Using proteomics while changing proteome

allocation allowed for confirmation of this model (*45*–*47*). These groups investigated proteome changes by limiting the carbon metabolism using a titratable glucose transporter glucose-specific PTS enzyme IIBC component (ptsG) strain, amino acid synthesis using glutamine oxoglutarate aminotransferase (GOGAT) titration, or the ribosomal sector using sub-inhibtory concentrations of chloramphenicol. PtsG titration led to an increase in proteins associated with carbon metabolism and was inversely proportional to the reduction in ribosomes. The same phenomena occurred when amino acid synthesis was limited. Inhibition of ribosomes with the translational inhibitor chloramphenicol on the other hand led to an increase in the number of ribosomes while decreasing the amount of metabolic enzymes. It seems that with this powerful new model we could now explain the origin of the growth rate in any given environment.

The biophysics and regulation underling proteome reallocation are also known. When bacteria encounter a shortage of nutrients they induce the stringent response. The stringent response is characterized by a decrease in the levels of guanosine-5'-triphosphate (GTP) and an increase in guanosine-3',5'-bispyrophosphate (ppGpp). PpGpp binds to RNA polymerase and inhibits the transcription of genes involved in growth including the rrn genes resulting in a decrease in the number of ribosomes. The level of ppGpp is controlled by GDP/GTP pyrophosphokinase (relA) that produces ppGpp and bifunctional (p)ppGpp synthase/hydrolase SpoT (spoT) that can act as both a hydrolase or synthetase. Induction of relA occurs by binding of uncharged transfer RNA (tRNA) to the ribosomal a-site (*48*). Ribosomes while complex molecular machines made of both RNA and proteins can be regarded as enzymes catalyzing the elongation of proteins. The rate of reaction of ribosomes is the translational elongation rate which is the speed at which amino acids are added to the nascent polypeptide chain. Ribosomes show Michaelis Menten dependence on their substrate charged tRNA (*49*). ppGpp therefore provides a feedback loop preventing over-consumption of amino acids. The ppGpp feedback loop underlies growth rate regulation as ribosomes sense a lack of amino acids and down regulate their own expression (*50*). Cells therefore sense and modulate their ribosomal content to match the rate of production of charged tRNA finally explaining how cells regulate their growth.

Given that changes in proteome allocation could explain changes in growth rate for nutrient conditions, as well as translational inhibition, it is interesting to investigate whether this applies to reduction of the growth rate in all conditions. Bacteria face a variety of different challenges that affect their ability to grow. Can proteome reallocation explain the reduced growth in all of these conditions?

1.7 How Bacteria Deal with Stress

Microbes are exposed to diverse environments during their growth. *E. coli* and other *Enterobacteriaceae* pass from the mouth, through the stomach and intestines and into whatever external environment the host is living in. During this journey the cells must deal with a wide range of physical stresses which can significantly impact their survival and ability to grow. Here I will discuss some of the specific stresses that *E. coli* encounters and how *E. coli* deals with stress. First it is important to define what is meant by stress. While bacteria are exposed to a variety of rapid changes in their environments, stress in this thesis is used to specifically indicate a prolonged exposure to the encountered shock allowing for adaptation of the bacteria. When investigating the impact of stress on *E. coli* it is the physiology of the bacteria that has adapted to the new environment rather than the rapid and short term changes that bacteria experience when exposed to a sudden but brief change in the environment.

A common stress encountered by all bacteria is nutrient limitation. Bacteria often face scarcity or imbalances of essential nutrients, such as carbon, nitrogen, phosphorus, or magnesium, which can prevent further growth or trigger adaptive responses that slows growth. Bacteria also encounter both low and high temperatures, leading to reduced growth rates or even cell death. Low temperatures slow growth by reducing enzyme activity which is predicted by the Arrhenius equation. Most prominently the translational elongation rate in *E. coli* decreases linearly with temperature between 37℃ and 20 ℃ (*51*). Extreme cold can lead to membrane damage and denature proteins during freeze-thaw cycles. On the other hand high temperatures past the optimal growth range are predicted to increase reaction rates and show faster translational elongation rates. However, growth is still reduced potentially due to protein denaturation, aggregation or excessive synthesis of stress proteins (*51*).

Another common problem *E. coli* face is oxidative stress. Oxidative stress is a natural consequence of aerobic metabolism. To counteract oxidative stress cells sense oxidative stress and a variety of regulators including OxyR, SoxRS, and RpoS are induced (*52*). These regulators control genes important for reduction of oxidative stress. If cells fail to reduce levels of oxidative stress reactive oxygen species can accumulate and damage DNA, proteins and lipids.

The pH of the environments also frequently shifts becoming more acidic or alkaline. Surprisingly, *E. coli* can continue growing between pH 4 and pH 9, a 100,000 fold difference in H^+ concentration. Acid stress can affect protein folding and enzymatic activity, disrupt ion balance, and requires stress protein synthesis to survive and grow in such a wide variety of pH (*53*). Antibiotic exposure is also a frequent problem

that bacteria experience during growth in their natural environment or medical treatment. The type of stress encountered depends very much on the type of antibiotic. Common antibiotics target important molecular machinery such as cell wall synthesis, transcription, translation and, DNA synthesis. *E. coli* and other bacteria can adapt to anti-biotics by synthesizing a protein making them resistant to the antibiotic. These genes are frequently located on plasmids and counter the function of antibiotics by either inactivating them or pumping them out of the cytoplasm. Alternatively, cells exposed to antibiotic also acquire mutations in the gene or pathway targeted by the antibiotic making the antibiotic ineffective.

1.8 The Osmotic Stress Problem

Human cells exposed to small variations of less than 200 miliosmole in osmolarity rapidly die (*54*). *E. coli* on the other hand tolerates several osmole change and can grow nearly 3 osmoles above the optimal osmolarity (*1*). This osmotolerance is very important as *E. coli* are a normal part of the microbiome found inside the intestine of humans and other homeotherms. Here they are exposed to large osmolarity variations as food and liquid passes through the intestine. Even more drastic variations in osmolarity can occur as *E. coli* is excreted from the body. In the exposed environment *E. coli* can encounter extremely arid or hypersaline conditions resulting in a rapid loss of intracellular water, or cells can encounter extremely wet environments where osmolarity is close to 0. Throughout all of this *E. coli* somehow manages to stay alive and even grow. So what happens to bacteria that are exposed to very high osmolarity? Rapid changes in osmolarity disrupt various physical cell properties such as turgor pressure, cell wall strain, and concentrations of intracellular solutes, and it has been known for nearly a century that the osmolarity of the media affects the rate of bacterial growth (*2*). Changes in external osmolarity have drastic effects on *E. coli* as the cytoplasm is bound by the semi-permeable plasma membrane.

The impact osmotic change has on *E. coli* is determined by their physiology. As a gram negative bacteria, *E. coli* have a periplasmic space and a further outer membrane (figure 7).

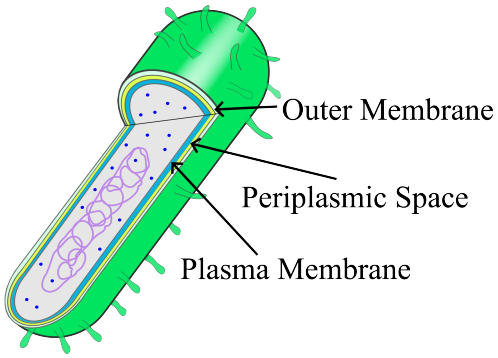

Figure 7: *E. coli* is a gram negative bacteria consisting of a cytoplasmic compartment bound by the cell membrane and a periplasmic compartment bound by the outer membrane

The inner and outer membrane of *E. coli* are phospholipid bilayers with a peptidoglycan cell wall separating them. These membranes are permeable to water while allowing the cell to retain larger molecules such as glucose, amino acids, ribosomes and DNA. This is essential for life as loss of membrane integrity leads to death. As the concentration of solutes inside the cell is higher than outside the cell builds up osmotic pressure 1.1. This pressure inflates the cytoplasmic membrane until the more rigid cell wall constrains further expansion.

During a hyperosmotic shock *E. coli* rapidly loses intracellular water content. While it is unclear why exactly the intracellular water content is important, it is known that *E. coli* makes a significant effort to restore intracellular water (*1*, *55*–*58*). So while there is a temporary efflux of water *E. coli* rapidly imports potassium ions to counteract the change in external osmolarity by K+ transporting P-type ATPase (KdpFABC) or K+ transporter (TrkGH). Glutamate synthesis from GOGAT or glutamate dehydrogenase (GDH) balances the positive charge of potassium and is accumulated in the cytoplasm (*59*). In addition to accumulation of potassium glutamate (KGlu) *E. coli* imports glycine betaine via the high affinity glycine betaine ABC transporter (ProU) transporter or the low affinity osmolyte:H^+ symporter (ProP) transporter. Alternatively the choline:H^+ symporter (BetT) transporter can import choline which is then converted to glycine betaine via the choline dehydrogenase (BetA) betaine aldehyde dehydrogenase (BetB) pathway (*60*). If no suitable osmolytes are present in the environment the cell will start synthesizing trehalose figure 8 (*61*, *62*). After an osmotic shock *E. coli* can restore cell volume and shows slower growth immediately after volume recovery (*57*).

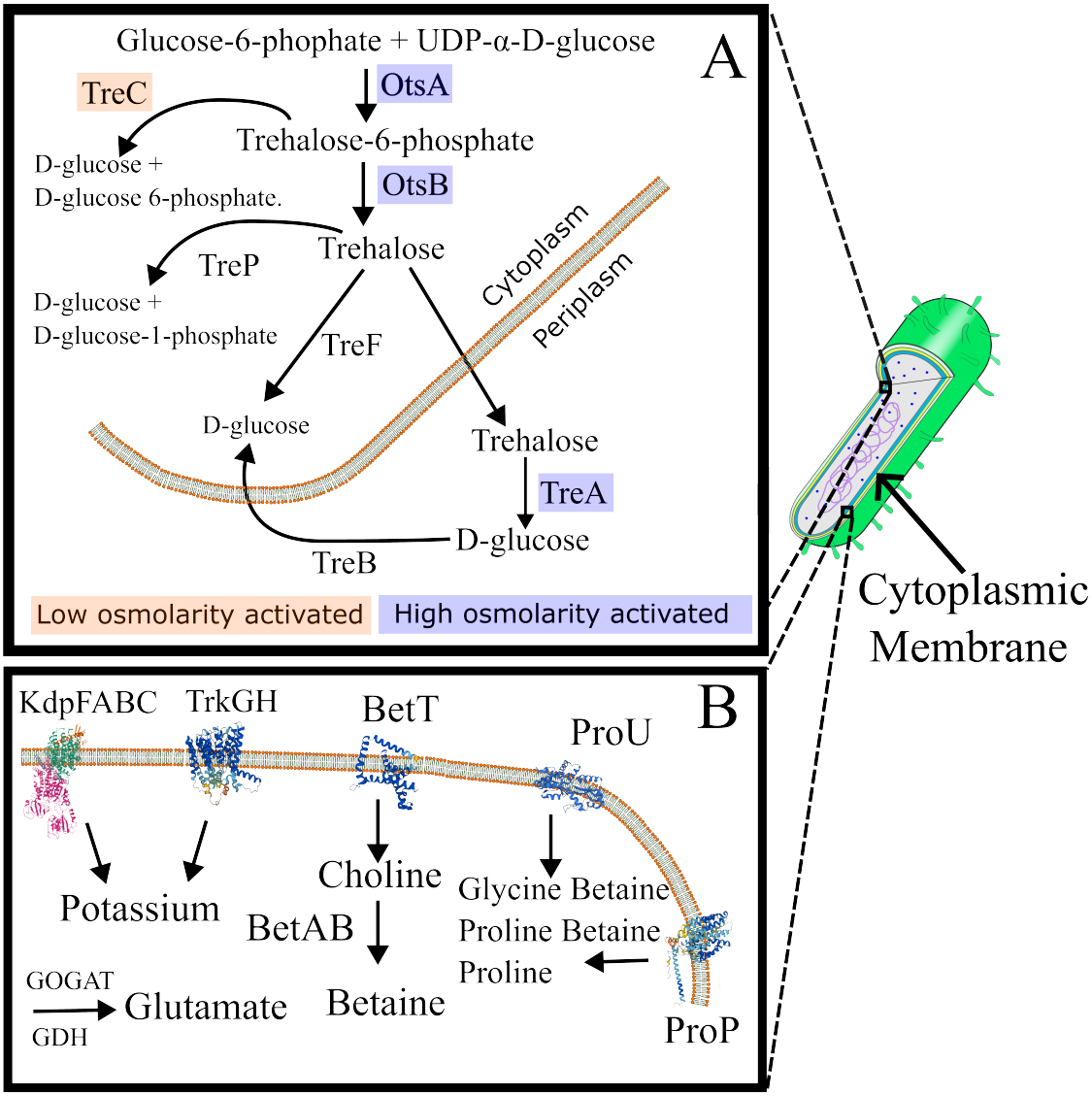

Figure 8: Pathways involved in hyperosmotic stress in *E. coli*. **A) Pathway for trehalose synthesis.** Glucose-6-phosphate and UDP-alpha-glucose are turned into trehalose-6-phosphate by trehalose-6-phosphate synthase (OtsA) which is subsequently turned into trehalose by trehalose-6-phosphate phosphatase (OtsB). In low osmolarity media expression of trehalose-6-phosphate hydrolase (TreC) breaks down trehalose-6-phosphate into glucose preventing accumulation of trehalose in the absence of osmotic stress. Trehalose can also be broken down by trehalose phosphorylase (TreP) or cytoplasmic trehalase (TreF). under osmotic stress there is high amounts of intracellular trehalose . Extracellular trehalose is degraded by periplasmic trehalase (TreA) and taken back up by trehalose-specific PTS enzyme (TreB). **B) Osmolyte specific transporters**. KdpFABC and TrkGH are both potassium transporters allowing for rapid influx of potassium in response to osmotic shock (*63*). ProP is a low-affinity non specific osmolyte transporter. ProU is a high-affinity betaine specific transporter. BetT is a choline transporter, choline is then converted to betaine by the BetAB pathway. 3d crystal structures were made using alphafold with the exception of KdpFABC which was solved using cryo-em (*64*)

So if cells can recover from the osmotic shock by importing osmolytes what exactly limits their potential for growth after the shock under hyperosmotic stress? Various theories have been proposed:

1. Loss of turgor pressure (*2*, *65*, *66*)
2. Accumulation of Potassium (*67*)
3. Destabilisation of proteins (*68*–*71*)
4. Energetic cost of osmolyte import or synthesis
5. Limitation in proteome availability as proposed for nutrient deprivation (*72*)
6. Increased macromolecular crowding (*1*, *49*, *58*, *73*)

Loss of turgor was the first proposed theory by Walter in 1924. Turgor pressure was thought to be essential for expansion of the cell wall. In plants turgor pressure is required to drive outward growth of the cell wall (*74*, *75*). Expansin enzymes weaken the cell wall allowing for insertion of new cell wall material resulting in growth (*76*). A similar mechanism was proposed to occur in bacteria (*77*).

Unfortunately measuring bacterial turgor pressure is very challenging due to their small size (*78*). Nonetheless Rojas and colleagues investigated changes in growth rate in response to hyperosmotic shock. It needs to be noted here again the difference between hyperosmotic shock and hyperosmotic stress. A shock indicates that cells were exposed to high osmolarity and the experiment performed immediately. Therefore, the cells do not have time to induce long term survival strategies such as activating gene expression.

The turgor-growth theory was disproven for *E. coli* as rapidly modulating the turgor pressure within the cell for several seconds over a 10 minute time scale does not reduce the rate of cell wall insertion. Rojas and Huang flushed a hyperosmotic sorbitol solution for around 50 seconds followed by normal media for around 50 seconds. Despite rapid decrease in the cytoplasmic cell volume and therefore the turgor pressure, cells maintained their growth rate. The experiment demonstrated that growth of *E. coli* continues despite absence of turgor pressure. It is important to note that in gram positive bacteria that have much thicker cell walls and higher turgor pressure the growth is slowed down with reducing turgor (*78*).

The accumulation of potassium to balance osmotic stress has been proposed as a potential limiting factor. Either due to the high accumulation of charged ions or the inability to generate enough glutamate as a counterion at higher osmolarities. However, accumulation of potassium fails to address the question of why the cell cannot generate more trehalose or when presented with an excess supply of betaine what exactly stops it from accumulating whatever amount is needed to equalize the osmotic pres-

sure without potassium. Cells replace the initially accumulated potassium with other osmolytes such as trehalose or betaine (*61*). Therefore accumulation of potassium as the origin of the growth slow down can be dismissed as it does not account for the fact that the cell can counteract osmotic stress without having to import excessive potassium.

Destabilization of proteins in a crowded environments can potentially explain the observed slowdown in growth. However, trying to investigate how osmolarity affects protein stability is difficult. Molecular crowding is predicted to have a stabilizing effect on most proteins making it difficult to predict the effect on enzyme activity (*79*–*82*). Furthermore, the fact that *in-vivo* measurements of enzyme kinetics are difficult to obtain make investigation of osmotic stress on enzyme activity challenging. In a single experiment looking at the 7-kDa N-terminal SH3 domain of Drosophila signal transduction protein drk (SH3), Stadmiller observed protein destabilization during osmotic stress using NMR-spectroscopy (*83*). Furthermore, addition of betaine (betaine in this work will be used to refer exclusively to glycine betaine) resulted in improved folding of the protein. Furthermore, uptake or synthesis of very high concentrations of trehalose could impose an energetic cost on the cell that may slow growth.

Another potential way to explain why increased osmolarity slows growth is the the model developed by Hwa and colleagues. As osmotic stress increases more and more of the proteome needs to be allocated to import or synthesis of osmolytes and therefore there is a reduction in the level of ribosomal proteins as figure 6.

Osmotic stress could also induce substantial molecular crowding experienced by bacteria as the cell accumulates osmolytes to counteract loss of turgor pressure (*49*, *55*). The increased crowding could slow diffusion of large molecular complexes such as the ternary complexes (TC). The TC consists of tRNA, GTP, and elongation initiation factor 2 and acts as the substrate for ribosomes during translational elongation. Measurements show that there is a rapid decrease in the translational elongation rate during osmotic stress just as predicted (*73*). Furthermore, a general crowding model shows that intracellular crowding negatively affects growth (*84*). Alric et al. induce crowding by physically limiting the space yeast *Saccharomyces cerevisiae* can grow in. They demonstrate that there is a reduction in diffusion, especially of larger particles. Furthermore, they show a reduction in the rate of protein production consistent with a reduction in the growth rate. It therefore seems like molecular crowding resulting in a reduction of diffusion leading to slower growth. However, as mentioned by Dai the rapid slow down in translational elongation rate elicits only a modest increase in ribosomes (*85*). While overexpression of less efficient ribosomes can cause a proteome burden the small increase seen during osmotic stress is unlikely to be the major

cause of the growth slow down encountered.

To summarize, bacteria experience a wide variety of stresses during growth. Understanding how these stresses limit the rate of bacterial growth is important for a variety of applications ranging from increasing bacterial growth for biotechnology and agricultural uses, to reducing bacterial growth during disease. However, despite intensive research there is still no definitive answer as to why growth slows down as the osmolarity of the growth media increases.

1.9 Thesis Aim

The primary objective of this doctoral thesis is therefore to comprehensively investigate the influence of osmolarity on bacterial growth dynamics. Specifically, I will focus on deciphering the intricate mechanisms employed by *E. coli* to regulate its growth under hyperosmotic stress. I hope to provide valuable insights regarding the adaptive responses and physiological adaptations that enable bacterial cells to thrive under high osmolarity environments.

Building upon the knowledge acquired from investigating growth under elevated osmolarity, the subsequent aim is to apply these findings to improve industrial *Lactobacillus animalis* (*L. animalis*) culture. I hope to devise strategies and interventions that can effectively enhance the growth performance of *L. animalis* strains, thereby optimizing their growth and yield during industrial batch culture. By using the insights gained from studying *E. coli* under hyperosmotic conditions, novel approaches can be developed to create improved growth kinetics and enhance productivity in *L. animalis* cultures.

Overall, this comprehensive investigation seeks to deepen our understanding of the impact of osmolarity on bacterial growth, unravel the regulatory mechanisms employed by *E. coli* during hyperosmotic stress, and leverage the obtained knowledge to augment growth optimization strategies in industrial *L. animalis* cultures.

2. Method & Materials

2.1 Strains and Culture Conditions

Throughout this work a variety of different *E. coli* strains are used. To facilitate easy identification they are summarised here. All strains used were K-12 derivatives (*86*)

Table 1: Strains used in this thesis

Strain	Description	Reference
MG1655	*E. coli* K-12 MG1655	(*87*)
MZ1	*E. coli* K-12 MG1655 OtsB::sfGFP	This Study
MZ3	*E. coli* K-12 MG1655 $\Delta OtsA\ \Delta OtsB$	This Study
NCM3722	*E. coli* K-12 NCM3722	(*88*)
HE647	*E. coli* K-12 NCM3722 chs::phi(Ptet:otsBA) chs::Ptet:tetr x 1	(*89*)
HE650	*E. coli* K-12 NCM3722 chs::Ptet:tetr x 3 & pZA31-Ptet-otsBA	(*89*)
NQ1468	*E. coli* K-12 NCM3722 lacZ α	(*41*)
HE902	*E. coli* K-12 NCM3722 kan:T:PlacIq:betBA & pZE-PLlac-betT	Hwa Lab
HE936	*E. coli* K-12 NCM3722 1R chs km:T:Ptet-proVWX proP-	Hwa Lab

2.1.1 Media and Growth Conditions

These studies utilise M63, MOPS, and Luria-Bertani liquid medium (LB). The following media represent the base media used and any modification for experiments are noted in the relevant sections. **M63:** 100mM KH_2PO_4 1.4µM $FeSO_4.7H_{20}$, 20mM $(NH_4)_2SO_4$, 1.4µ M Thiamine−HCl. pH was adjusted to 7 using KOH, 20mM glucose unless another carbon source is explicitly stated. **MOPS:** 40 mM morpholinepropanesulfonic acid (MOPS), 4 mM Tricine, 0.1 mM $FeSO_4$, 0.276 mM Na_2SO_4, 0.5 µM $CaCl_2$, 0.523

mM $MgCl_2$, and various micronutrients fully detailed by Cayley et al., (*58*). 10 mM Ammonium Sulphate and 10 mM carbon source. **LB:** 10g of Tryptone, 10g of NaCl, 5g of Yeast extract per litre. **Complex Media (complex media):** Media is made using industrial raw glucose, yeast extract, Polysorbate 80 and various minerals provided by Chr. Hansen (Hørsholm, Denmark). The media is similar to De Man–Rogosa–Sharpe (MRS). **Ammonia:** 24% weight / weight.

2.1.2 MZ1 Construction

Strain MZ1 is modified from parent strain MG1655 by replacing the otsB gene with super-folder green fluorescent protein (sfGFP) by homologous recombination using the protocol describe by Merlin and coworkers (*90*). In brief, I generated a donor plasmid using Gibson assembly to insert sfGFP flanked by two 400 base pair homologous regions onto a pTOF24 backbone figure S1. The assembly of the homologous region was done by Dario Miroli and I used his construct for Gibson assembly into a new plasmid backbone with intact SacB. *E. coli* MG1655 were transformed with the assembled plasmid and grown overnight at 30 ℃ on a chloramphenicol plate. A single colony was selected and grown at 30 ℃ in chloramphenicol containing media overnight. The media was diluted 10^4 and streaked on a chloramphenicol plate then incubated at 42 ℃ overnight. pTOF24 has a temperature sensitive origin of replication meaning that the plasmid is lost from the bacteria. Bacteria that survive overnight culture have integrated the plasmid into the nucleoid. The overnight culture at 42 ℃ is repeated to ensure that the plasmid is lost. Single cultures are picked and cultured at 30 ℃ allowing for homologous recombination of the integrated plasmid and the overlapping DNA sequence. The bacteria are cultured on 5% sucrose plates and cultured overnight at 37 ℃. The pTOF24 backbone contains the SacB gene encoding levansucrase. Levansucrase causes bacteria to die in the presence of sucrose. Therefore bacteria that have inserted the entire plasmid rather than just the homologous sequence face negative selection pressure. However, frequent mutations in the levansucrase gene can result in the retention of gene insertion without homologous recombination. Therefore, correct integration of the construct was confirmed by Sanger sequencing.

2.1.3 MZ3 Construction

MZ3 is a trehalose deficient strain in which both the OtsA and OtsB gene are deleted using P1 phage knockout. For each donor strain, two tubes were prepared, one serving as the negative control. The overnight culture was diluted 1:100 in 15 ml LB medium supplemented with 10 mM $CaCl_2$ and grown until the OD_{600} (OD_{600}) reached between 0.15 and 0.25. 50 μL of P1 lysate was added to 5 ml of donor culture. The

culture was incubated with vigorous shaking at 37℃ for 2-4 hours until the medium appeared clear. The culture was passed through a syringe/0.22 μm filter assembly to remove cellular debris. The lysate was transferred to a labeled tube and stored in the dark at 4 ℃. An overnight culture of the recipient strain was then set up in LB medium. The overnight culture of the recipient strain was diluted 1:100 in 10 ml LB medium supplemented with 2.5 mM $CaCl_2$ and grown until the OD reached 0.8. 900 μL of the culture was transferred to a 15 ml centrifuge tube, and 100 μL of the P1 lysate from the appropriate donor strain was added. 'Phage only' and 'no phage' controls were also set up. The culture and P1 lysate mix were allowed to stand for 30 minutes at 37℃ without shaking. The mixtures were diluted in 5 ml fresh LB medium supplemented with 5 mM sodium citrate. The mixture was incubated at 37 ℃ without shaking for 1 hour. Finally the transformed recipient bacteria were plated onto LB agar plates supplemented with 5 mM sodium citrate and antibiotics. The plates were incubated overnight at 42 ℃ to destroy any remaining p1 phage. The plates were restreaked and incubated again overnight at 42 ℃ to minimize secondary infection.

2.1.4 Growth of *E. coli*

Frozen aliquots of bacterial strains were prepared by mixing 50 µl of overnight bacterial culture grown in LB with 50 µl 50% glycerol and flash frozen in liquid nitrogen. For growth the frozen stock was diluted 10^5 in growth media. For growth on mannose I noted residual growth on trace glycerol in the culture. I therefore added another initial culture on mannose containing media and used confluent cells from the culture for growth so the initial frozen media was diluted by a factor of 10^{10}. Flask growth was done in a hot room at 37 ℃ using a flask shaker. Growth in bioreactors was set up in a similar way the reactors being placed inside the hot room. 15 ml incubator tubes were inoculated by diluting frozen culture 10^5. Stirring speed was kept at maximum for growth of *E. coli*.

2.1.5 Growth of *L. animalis*

Frozen aliquots of *L. animalis* were received from Chr. Hansen. Cells were inoculate by diluting them 10^{-5} in the growth media and grown at 37 ℃ in complex media media. Growth was done inside a bioreactor. 15 ml of MRS media was added to each reactor tube. The headspace of the reactor was filled with gaseous N_2. Cells were gently agitated by setting bioreactor to lowest stirring setting while still preventing cell sedimentation.

2.2 Plate Reader Methods and Analysis

2.2.1 Plate Reader Setup

For analysis of growth and fluorescence data I utilised the Tecan infinite 200M Pro plate reader. Corning 96 well plate TC-treated flat bottom with lid plates were used (Scientific Laboratory supply: 3596). Outer edges were always filled with sterile water to counteract evaporation effects figure 9. The lid was attached to the plate using standard laboratory tape to prevent excessive micro-plastic production from friction during plate shaking. Cells were either diluted 10^{-5} from frozen stock or pre-cultured in LB and then diluted 10^{-5}.

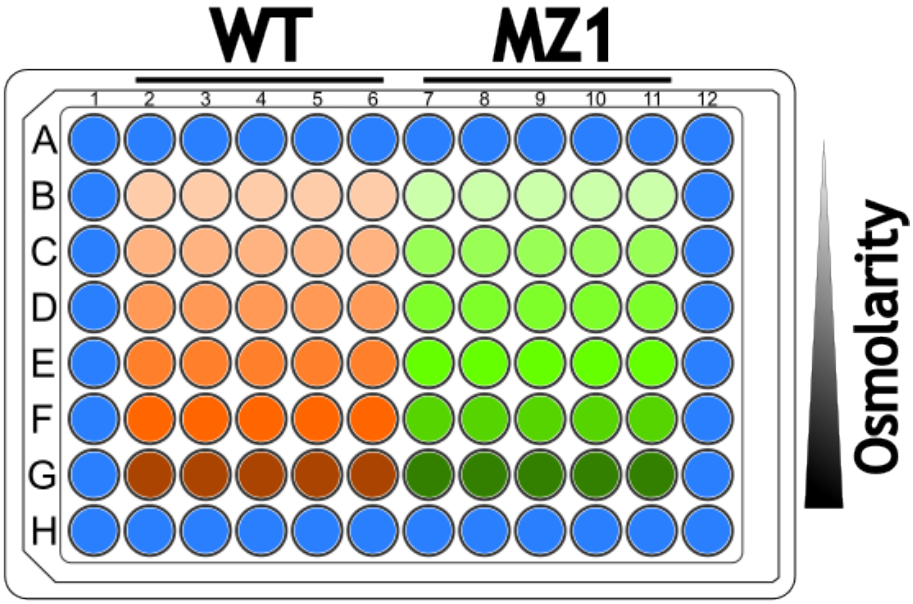

Figure 9: Standard plate layout for osmolarity study. Edge wells were filled with water. Half the plate was filled with Wild-Type (WT) cells and half with MZ1 or MZ3 cells. Osmolarity was varied throughout the plate.

2.2.2 Growth and Measurement Conditions

Experiments were done at 37℃ except when noted. The reader was set up for 5 minutes of orbital shaking at 300 RPM to achieve optimal aeration. Experimental duration was varied based on growth rate. OD_{600} was measured averaging 25 flashes. sfGFP fluorescence intensity was measured using an of excitation filter 485 nm and emission filter of 525 nm, using bottom reading and keeping the gain constant. A standard plate layout consisted of five repeats of each condition.

Edge wells were filled with water to mitigate evaporation effects. Each plate contained five replicates of each condition allowing for testing of six different osmolarities for both

the experiment strain and the WT strain. Analysis was done using a custom coded analysis program.

2.2.3 Custom Plate Reader Analysis Program

Using a plate reader allows for generation of large data sets with each experiment resulting in around 60 different experimental conditions up to 2000 data points for each well. In total the final analysis encompasses over 5.8 million individual data points. To aid analysis of the large amount of data I developed a custom analysis program available at Plate reader analysis GitHub. The program functions as following. First the data from the excel generated by Tecan is extracted and annotated so that each well now corresponds to a column in a Pandas data frame. The name of each column contains the strain, the osmolarity of the media and the number of repeats. The program starts by giving a graph displaying OD_{600} versus time allowing inclusion or exclusion of wells and data was manually screened for irregular growth or errors in measurements. Wells that show clear growth anomalies or incomplete growth not reaching the end of exponential phase are excluded and not analysed. For each included well the background value is calculated by averaging of the first 10 recorded time points. Due to the high dilution of the bacterial cultured far below the limit of detection I can accurately estimate the average background value of just the media in the well. The background is then subtracted to give an accurate estimation of the OD_{600} value of each well. Next the natural logarithm of the OD_{600} is calculated. To estimate accurate growth rates a running window is used to calculate the instantaneous growth rate by taking 8 time points corresponding to about one hour of growth. By default the growth rate is taken as the linear regression of $ln(OD)$ between OD_{600} 0.01 and 0.1. A plot is generated showing the change in OD_{600}, $ln(OD)$ and instantaneous growth rate over time and the suitability of the default OD_{600} window is evaluated by seeing whether cells show exponential growth in that range of OD_{600} figure S2. For calculation of fluorescence auto-fluorescence from cells must be subtracted to give an accurate prediction of sfGFP at a given time-point. To accurately calculate sfGFP fluorescence I compare the $sfGFP \times OD^{-1}$ in the WT strain compared to the mutant strain expressing sfGFP. The $sfGFP \times OD^{-1}$ value is then used as a measure of gene induction.

$$sfGFP \cdot OD^{-1} = \frac{MZ1_{sfGFP}}{MZ1_{OD}} - \frac{MG1655_{sfGFP}}{MG1655_{OD}} \tag{2.1}$$

Finally, the program attaches relevant labels such as growth conditions, temperature and date to the generated data frame and exports all of the experiments as a

comma-separated value file. The outputs give the growth rate for both WT and mutant strain. The program also computes the average sfGFP fluorescence during exponential growth. The maximum yield is determined by detecting entry into stationary phase when growth rate is less than 0.001 h^{-1} and then calculates the average of the next 10 OD_{600} values.

2.3 Determination of Translational Elongation Rate

Translation elongation rates were measured by using the lacZ induction assay (*41*). The translational elongation rate assay measures the time taken to create one complete LacZ protein after isopropyl-β-d-thiogalactopyranoside (IPTG) induction. Cells were grown in various growth media. 5 mM of IPTG was added at OD_{600} 0.4. 400 µL were then taken every 10 or 20 seconds for up to 4 minutes and elongation was stopped by dropping cells into prepared Eppendorf tubes containing 5 µL $34mg/l$ chloramphenicol on ice. Closed tubes were immediately thrown into liquid nitrogen. LacZ activity was measured for each sample by diluting sample 1:5 in lacZ activity buffer: 0.06 M Na_2HPO_4, 0.04 M NaH_2PO_4, 0.01 M KCL, 0.001 M $MgSO_4$. 50 µL of 2 mg/ml 4-Methylumbelliferyl-β-D-galactopyranoside (4-MUG) is added and samples were incubated for 30 minutes at 37℃. LacZ cleavage results in conversion of 4-MUG from non-fluorescent to fluorescent. The reaction was stopped by addition of 250 µL 1 M Na_2CO_3. Fluorescence was measured in a Tecan infinite 200M Pro plate reader (excitation:365 nm, emission: 450 nm).

To calculate time needed for IPTG induction strain NQ1468 was used which has a shortened active lacZ protein of only 90 amino acids compared to the WT length of 1024 amino acids. To predict the translational elongation rate I generated Schleif plot of the lacZ induction curve. The plots were generated by taking the square root of the lacZ enzyme activity and plotting it versus the time since induction as described (*41*). The time to produce 1 lacZ protein is then equal to the x-intercept. The Elongation rate k can be calculated as follows:

$$k = \frac{\text{length of protein}}{(\text{x-intercept} - \text{induction time})} \tag{2.2}$$

To calculate the induction time of IPTG, I make the assumption that the elongation rate is constant whether using MG1655 or NQ1486. The induction time can be solved as follows

$$\frac{1024}{\text{x-intercept} - \text{induction time}} = \frac{90}{\text{x-intercept} - \text{induction time}}. \tag{2.3}$$

2.4 Estimating RNA / Protein Ratio

The RNA / Protein ratio is proportional to the ribosomal mass fraction and thus the number of ribosomes present inside the cell (*44*). The RNA / Protein ratio was shown to also be a good indicator of total amount of ribosomal proteins during osmotic stress (*73*).

2.4.1 Total RNA content

To estimate ribosomal content I performed total RNA and protein quantification. Total RNA extraction was done as described in (*73*). 1.5 ml of cells grown to OD_{600} 0.4 were centrifuged at 15000 g and pellets were washed with ice cold 0.7 M perchloric acid $HCLO_4$. Cells were centrifuged again and the resulting pellet was digested using 0.3 ml of 0.3 M KOH at 37 ℃ for 60 minutes while continuously mixing on an automated shaker. Digestion was stopped by addition of 0.1 ml of 3 M $HCLO_4$ and 0.4 ml of supernatant was collected after centrifugation. To ensure complete collection of all RNA the pellet was suspended in 0.55 ml of 0.5 M $HCLO_4$ centrifuged and the process was repeated one more time. Finally the 1.5 ml of supernatant was centrifuged at 15000 g for 10 minutes to remove any remaining particles and transferred to a UV-cuvette. Absorbance was measured at 260 nm. The total RNA content per OD was calculated

$$RNA/ml/OD = \frac{A_{260}X31}{OD_{600}}. \tag{2.4}$$

2.4.2 Total Protein Content

Total protein was determined using the Biuret method. 1.5 ml of bacteria grown into exponential phase (OD_{600} 0.4), were collected by centrifugation. The supernatant is collected and OD_{600} was recorded to estimate cell loss. The pellet was re-suspended in phosphate buffered saline to wash away any extracellular protein. Cells are centrifuged and again the supernatant is collected to measure cell loss. The pellet is suspended in 200 µl of water. The sample was digested by addition of 0.1 ml 3 M NaOH heated to 100 ℃ for 5 minutes. Samples were cooled for 5 minutes and 0.1 ml of 1.6% $CuSO_4$ is added. Samples were briefly vortexed and incubated at room temperature for 5 minutes. Tubes are centrifuged at 15000 g for 3 minutes and super-

natant is transferred to 96 well plate and absorbance measured at 555 nm. A Bovine Serum Albumin standard curve is used to infer total protein content of the sample. Total protein is then inferred by calculating protein/ml/OD. Finally RP ratio was calculated as follows:

$$RP\,ratio = \frac{RNA/ml/OD}{protein/ml/OD} \tag{2.5}$$

2.5 Determination of Lactic Acid Content, CFU, and Yield

Frozen aliquots of *L. animalis* were received from Chr. Hansen. Cells were inoculated by diluting them 10^{-5} in complex media media received from Chr. Hansen and cultured at 37 ℃ overnight for 16 hours as described previously. Lactic acid content of the media was determined using a lactic acid assay kit and both L and D lactic acid were determined by addition of lactate dehydrogenase converting lactic acid into pyruvate converting Nicotinamide adenine dinucleotide (NAD) to Nicotinamide adenine dinucleotide H (NADH). Pyruvate was converted to D-Alanine and 2-Oxoglutarate by glutamate pyruvate transaminase. OD_{340} of the sample was measured using a spectrophotometer, which measures amount of NADH. Total NADH produced is calculated:

$$c = \frac{V \times MW}{\varepsilon \times d \times v} \times \Delta A_{\text{D-lactic acid}}. \tag{2.6}$$

Here, V is the final volume, MW is the molecular weight of D-lactic acid (g/mol), ε is the extinction coefficient of NADH at 340 nm, d is the light path in cm, v is the sample volume, $\Delta A_{\text{D-lactic acid}}$ is the change in absorbance.

Yield was determined by measurement of final OD_{600} of cells grown overnight in a spectrophotometer, cells were diluted in fresh media to ensure that readings were in the linear range. Colony forming units (CFU) after freeze drying were counted as follows: Grown cells were centrifuged at 8000 g at 4℃ for 5 minutes. Supernatant was discarded and cell pellets were suspended in 1 ml cryo-buffer (200 g/L sucrose, 9 g/L sodium chloride and 5 g/L sodium ascorbate) and dropped into liquid nitrogen. Lyophylization was performed using a Mini Lablyo lyophilizer. Lyophilization was allowed to proceed for 24 hours and dried product was immediately rehydrated using a peptide broth. Serial 10-fold dilution was performed for colony counting. MRS agar was prepared by melting in the microwave followed by cooling until it is warm to the touch. Cells were added to liquefied agar and dispersed by an 8-shape motion. Once

solidified cells were placed in an anoxic jar using anaerogen to replace any oxygen with carbon dioxide (Thermo Fisher, AN0025). Plates were incubated in warm room at 37 ° overnight. Plates were imaged using a Biorad geldock using the bright-field mode.

2.6 Development of an Automated CFU Counter

Counting CFU has been a standard microbiological technique since its development over 100 years ago (*91*). The main aim of the CFU assay is to count the number of viable bacteria. Unlike microscopy this assay is selective to only bacteria that are viable as they rely on growth of single bacteria. During large scale industrial culture CFU counting is the gold standard for output as it measures the number of viable bacteria and is correlated with metrics important to industrial food production such as acidification rate. The assay theory is simple: The liquid culture is serially 10-fold diluted and spread on an agar plate. The plate is then incubated anaerobically at 37℃. Many of the plates prepared will be completely overgrown with bacteria or not contain colonies. However, at the right dilution plates will show clearly visible single colonies. These colonies represent growth from a single bacteria and are then counted and multiplied by the dilution factor to estimate number of viable bacteria in the original media. One of the most time intensive processes and a source of variability is the manual counting of the cell numbers on the agar plate. Systematic investigations revealed significant differences in the number of CFU for the same sample as it varied depending on the counter (*92*). To resolve this issue I developed an automatic colony counter based on the spline dist neural network (*93*).

Image segmentation has been a fundamental problem in biology. Various early approaches relied on whole cell or partial thresholding. Images are typically 8-bit giving each pixel an intensity value between 0 and 255. Thresholding relies on the fact that areas of interest are brighter than the background, therefore setting a cut off value allows you to segment the foreground from the background. However, these approaches suffered from various problems. First the intensity of illumination could vary between each image changing the optimal value for thresholding. Mathematical derivation of a threshold value from the image is a potential solution (*94*). However, many challenges still remain. Uneven illumination results in incorrect segmentation. Also thresholding methods cannot distinguish between bright objects of interest and unrelated bright objects. Furthermore, these techniques fail to distinguish between two separate objects that are in close proximity of each other. Other image analysis algorithms were developed to account for some of these problems such as watershed segmentation. A full review of historical image segmentation is outside the scope of

this thesis but can be found here (*95*).

Like many fields, current automatic image detection and segmentation was revolutionized by the advent of artificial intelligence and machine learning. Specifically neural networks have had tremendous success in image segmentation and classification and a full review of the field can be found here (*96*). I decided to use the spline dist neural network as it was ideally suited to my task of identifying many small adjacent objects. The splinedist network allows for identification of spline convex polygons and can separate objects in close proximity (*93*). It is based on a U-net architecture (*97*).

Training and validation data sets were generated by manually annotating 16 different images, with 8 images containing plates in which dilution was $10^{-}6$ and 8 plates that contained cells with $10^{-}7$ dilution. The network was trained on 12 images with four withheld for quality control. Training was done using google colab and a Nvidia Tesla P100 GPU. The image dimensions of the input image are 1694, 2267, 3 and the network used a patch size of 512, 512 with a batch size of four and a mean absolute error loss function. The training used the zerocostdl4mic implementation of the splinedist network, allowing for reproducible results when training neural networks with the code available at (*98*). No data augmentation was used. The network was trained for a total of 30 epochs and the initial learning rate was set to 0.0003.

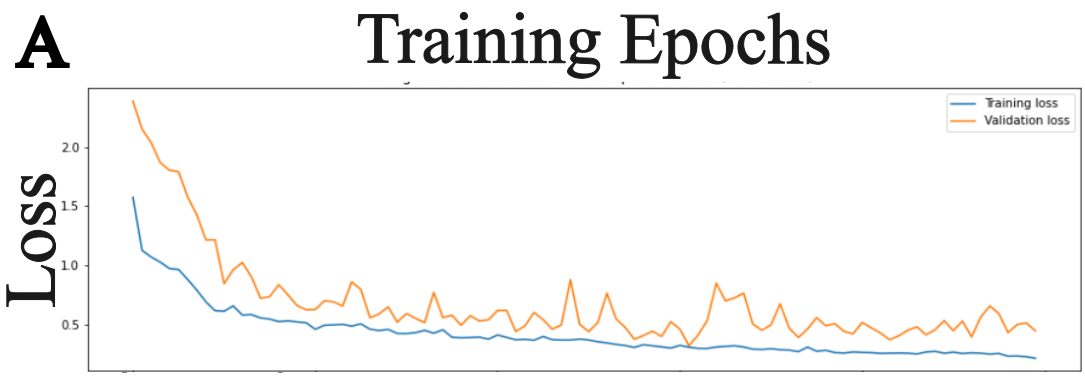

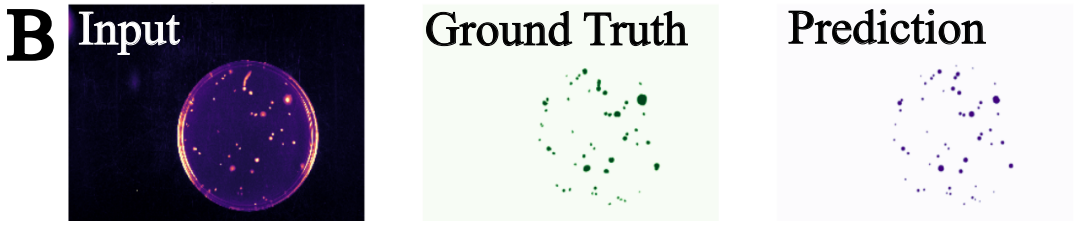

image #	IoU	false positive	true positive	false negative	Precision	recall	Accuracy	f1 score
1	0.649	6	48	9	0.889	0.842	0.762	0.865
2	0.787	8	370	35	0.979	0.914	0.896	0.945
3	0.792	7	31	6	0.816	0.838	0.705	0.827
4	0.803	10	348	51	0.972	0.872	0.851	0.919

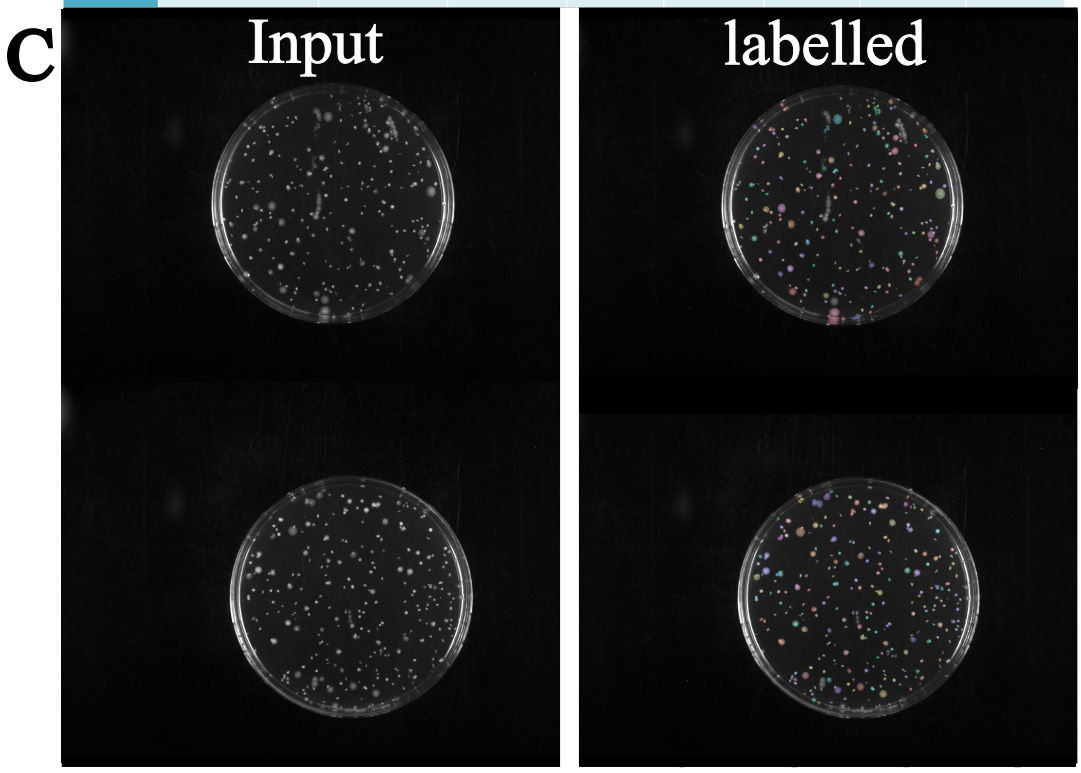

Figure 10: Splinedist network trained on 12 manually labelled images. **A)** Network loss during training for 30 epochs. Training loss is shown as the blue line, validation loss is shown in orange. **B)** comparison of ground truth vs predicted labelling on a quality control plate. Summary of quality control metrics for four quality control plates. **C)** Example of two sample plates. On the left the input image and on the right the predicted mask is overlaid onto the image.

Plot A shows both training data loss (blue line) and validation data loss (orange line) (figure 10). Training data loss represents how much of the training data is accurately identified by the model, while validation data loss represents how much of the quality control data not used by the model to train is correctly identified by the model in each epoch.

Various quality control metrics were calculated to assess performance of the network. Intersection over union (IoU) shows the % overlap between network labelled pixels and manually annotated pixels. The IoU measure is important to determine exact location of the colony and is an important indicator for how accurate tasks such as colony size estimation are. However, as I am interested only in correctly identifying colonies a metric to quantify correct identification is accuracy which can be defined as:

$$Accuracy = \frac{TN + TP}{TN + FP + TP + FN} \tag{2.7}$$

Here TP is a true positive, TN is true negative, FP is a false positive and FN is a flase negative. Accuracy therefore identifies how many true positives (TP) and true negatives (TN) are identified as a fraction of all cases. A true positive is an accurately identified colony. However, using accuracy raises a problem as with image based colony counting we cannot define true negatives, as it is just the absence of a colony. Therefore, accuracy may underestimate how good the network is. Instead I could use precision:

$$Precision = \frac{TP}{TP + FP} \tag{2.8}$$

Precision only considers positive identification, however, precision again is incomplete for our example as it does not consider the impact of false negatives. Recall can be used to account for false negatives.

$$Recall = \frac{TP}{TP + FN} \tag{2.9}$$

Finally, the F1-score incorporates both precision and recall. Specifically it is the harmonic mean of recall and precision allowing for an estimate of the correct identification of true positives in relation to false positives and false negatives.

$$F1score = 2 \times \frac{Precision \times Recall}{Precision + Recall} \tag{2.10}$$

The F1-score of my network ranged between 0.827 and 0.945. As the number of colonies on the plate increased so did the F1-score. Therefore, for all CFU counting a lower dilution of $10^{-}6$ was used yielding 300-400 colonies per plate. This demonstrates that using a neural network to accurately identify and count colonies, as well as provide accurate results allowing for rapid determination of colony counts. To further confirm the accuracy of the network 16 plates were manually counted and compared to the colony counts from the splinedist network. Manual validation showed a 3% coefficient of variation between the counted values and the predicted values. Automated colony counting shows a large improvement on the coefficient of variation compared to manual CFU counting that has a coefficient of variation around 36% (*92*).

Here I demonstrate that using a neural network capable of object segmentation is useful for rapidly and accurately counting colonies. Furthermore, counting colonies is an extremely labour intensive process having to focus and mark every cell for dozens or even hundreds of plates. Imaging the plates on the other hand is very easy and running the network takes only a couple of seconds per plate with GPU acceleration cutting down the manual labour required for cell counting from hours to just being limited by the camera speed. While I manually collected all images and ran them through an image analysis pipeline it would be simple to automatically start analysis as soon as the image was taken allowing for near instant colony counting which is reproducible regardless of the counter.

2.7 Measuring Bacterial Cell Size After Osmotic Shock

In addition to understanding how osmolarity affects viability during growth, cells are exposed to various changes in osmolarity during the freeze-drying process. The solution in which cells are freeze dried has a big impact on survival after rehydration. Addition of high concentrations of polyols among other compounds has been proven to protect cells during the freezing process (*99*). One of the potential ways in which high concentrations of polyols can protect cells is by causing loss of cytoplasmic water. Cytoplasmic water may therefore have an impact on survival after freeze-drying as ice-crystal formation during the freezing process can negatively impact cell physiology. Specifically, Ice crystal formation is a major source of cryoinjury and is unavoidable during the freezing process (*100*).

However, the amount of ice formation should be related to the water content inside

the bacterial cell. I therefore wanted to determine the relationship between intracellular water and survival after freeze-drying. Measuring intracellular water directly is extremely challenging (*58*). Instead, loss of water can be determined by reduction in cell size.

To determine cell size, cells were attached to a tunnel slide constructed as described by Barboza-Perez and colleagues (*101*). Briefly two strips of double sided sticky tape are placed vertically approximately 4 mm apart on a microscope slide. The edges are trimmed using a razor blade. A rectangular cover slip is placed on top of the slide. The slide is then flushed with water. Cell-Tak (Corning, 354240) is prepared by addition of 19 µl of 0.1 M Sodium Bicarbonate to 1 µl of Cell-Tak. One µm polystyrene beads are prepared by dilution of 7.5 µl of beads in water. Beads are washed twice in water by centrifugation. Prepared Cell-tak is flushed into the tunnel slide and the slide is incubated for 15 minutes at room temperature. The slide is washed with 100 µl of water twice. 50 µl of beads are flushed in and slide is incubated for 5 minutes. The beads are washed out with 200 µl of depleted growth media. 50 µl of *L. animalis* cells grown to stationary phase as described previously are flushed in and left to incubate for 10 minutes at room temperature. Non attached cells are flushed away using 200 µl of depleted growth media. Cells were imaged using 100X objective and using back-focal-plane interferometry to stabilize image slide as described previously (*102*). Effect of addition of different freeze dry-buffers was investigated by flushing depleted media with different osmolarity water solutions containing 0-5 Osmole sucrose or NaCl.

2.7.1 Development of a Custom Size Analysis Program

To analyze cell size changes I developed a custom code that uses cellpose, a neural network to identify and segment the cells based on bright-field microscopy. I used an iterative training approach segmenting the cells using the general user interface provided (*103*). Once the trained network could accurately segment cells I developed a user interface that loads microscopy images. The user selects a directory containing *.tif images, the program will then calculate the cell masks using the cellpose network and overlay them onto the microscopy images. Note that depending on your GPU capabilities processing time varies from a few seconds per image to several minutes without a GPU. The program allows for the drawing of bounding boxes and determines the area of the largest cell located inside the bounding box over a series of microscopy images (figure 11).

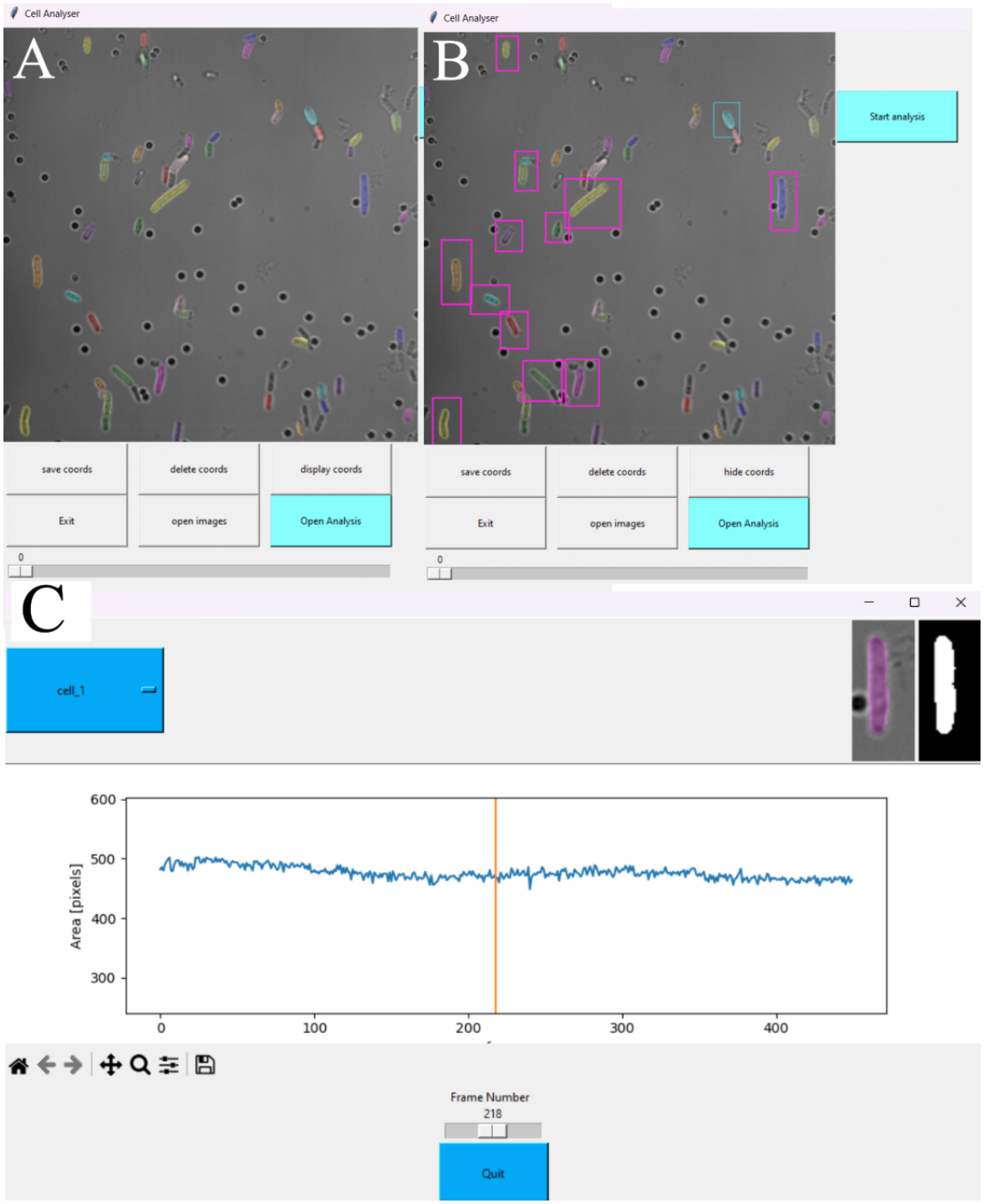

Figure 11: General user interface program utilizing the cellpose neural network to determine cell size changes. **A)** Image displayed once you open your microscopy images. **B)** By dragging the mouse and clicking ”add coordinates” the user can select regions containing cells for analysis. By using the scroll bar at the bottom of the program the user can scroll through all microscopy images and check that the cell of interest remains within the field of view. Once all desired cells have been marked the user can click ”start analysis”. **C)** The analysis window showing a trace of cell size over a number of frames. The overlaid mask image and the cell mask are located in the top right to see any issues with cell segmentation during the experiment.

The program generates various outputs in the folder containing the initial microscopy images. The ”coords” directory contains the X, Y coordinates of the bounding boxes drawn by the user for the generated image. Furthermore, a base display is generated and stored to initialize the canvas before the cellpose network has had time to generate masks. The ”heatmap” directory contains the overlaid microscopy images generated by the cellpose network that are loaded into the user interface. The ”masks” directory contains the cellpose calculated masks. Finally after selecting cells and running the analysis a directory is created for each region of interest containing all data associated with that ROI. The main output of the program is the CSV file named ”01_final_df.csv” after running the analysis function. This CSV file contains the frame number, Area, Length of Cell, Width of Cell and orientation compared to the x-axis of all of the cells inside the ROI bounding boxes. Note that to calculate the time passing the frame number needs to be multiplied by the time between images. The full code is available at Github Cell Size Analyser.

3. The Impact of Increasing Media Osmolarity on Bacterial Growth

3.1 Introduction to Bacterial Stress

As mentioned in the main introduction bacteria encounter various stresses during growth. These include but are not limited to temperature fluctuations, pH changes, oxidative stress, antibiotic exposure and nutrient limitation. Here, stress refers to the burden imposed on the bacteria both by the environment and by the adaptation to the environment. Therefore, stress not only considers the physical challenges bacteria endure in a new environment but also the adaptations cells made to survive the new adverse physical conditions. Stress is therefore not a condition encountered during short term exposure but requires time for cells to react. It is also important to note that stress is relative. Some halophiles grow optimally in media where NaCl concentration exceeds 6 osmole (*104*), while most organisms are unable to grow under these conditions. Stress is therefore not determined by the physical environment itself, but rather by the environment in relation to the organisms optimal environment. Furthermore, stress happens on a continuous scale with small changes not noticeably affecting bacterial growth and extreme changes leading to cessation of growth and even cell death.

Here, I focus specifically on the impact of osmotic stress on bacterial growth. As *Enterobacteriaceae*, *E. coli* has an optimal osmolarity that matches mammalian blood plasma osmolarity ranging between 270-310 milliosmoles (mOsm) (*58*, *105*). However, *E. coli* can grow at ten times its optimal osmolarity in environments where external osmolarity is 3 Osmole (*1*). An osmotic shock by transfer from normal growth media to a hyperosmotic media leads to immediate growth cessation. Cells then adapt to the shock and restore growth but at a slower rate (*57*). The term osmotic stress therefore refers to the state where *E. coli* has adapted to the new high osmolarity environment but grows at a slower rate in the new adapted state.

The link between growth rate and osmolarity of the media has so far been enigmatic, and will be the specific focus of this chapter. Bacteria grow best in media at around 0.3 osmole and show a linear reduction in their growth rate as media osmolarity increases. So what physical phenomena could be responsible for the reduced growth at high osmolarity? *E. coli* wants to maintain osmotic pressure and there is evidence that *E. coli* must restore osmotic pressure at least partially before continuing growth (*57*). To maintain osmotic pressure *E. coli* accumulates or synthesizes osmolytes, small organic molecules, often referred to as compatible solutes, that do not interfere with cellular reactions. Importing or synthesizing osmolytes is an energy intensive as cells need to expend Adenosine triphosphate (ATP) or proton-motive force to pump or synthesize these osmolytes. The energy cost of driving these reactions could be related to the reduction in growth rate. The number of ATP required for synthesis of osmolytes in halophiles can outweigh the energy requirements for synthesis of proteins and DNA (*106*).

Alternatively, it has been proposed that cells cannot restore their osmotic pressure fully resulting in water loss from the cytoplasm (*1*). The loss in cytoplasmic water volume together with accumulation of osmolytes increases crowding in an already crowded cytoplasm, potentially leading to a slowing of diffusive processes (*1*).

The existing proteome reallocation model of Scott and Hwa can potentially also explain the reduced growth at elevated osmolarity. The growth laws have become a widely accepted way of understanding limits to bacterial growth (*44*). To briefly summarize, Scott and Hwa were interested in understanding why a small change in the nutrient quality of the media makes such a large difference to the growth rate. For example in minimal media *E. coli* grows twice as fast on glucose as it does on mannose. However, the structure of the two sugars is nearly identical. So why would such a small change have such a large effect on the growth rate? The answer is in the proportion of the proteome that can be allocated to production of ribosomal proteins. As described in equation (1.7) the growth is limited by the number of actively translating ribosomes and their elongation rate. It was known that the ribosomal content varied with quality of the growth media (*40*), explaining the reduced growth. However, there was no explanation linking the change in nutritional quality of the media to the reduction in ribosomal content. Various studies managed to elucidate the relationship between an accumulation of uncharged tRNA and number of ribosomes (*48*, *107*–*110*). These authors showed that the ribosomal content of the cell varies linearly with ppGpp, ppGpp increases as a result of uncharged tRNA binding to the ribosome. However, the authors did not have a constraint based model and could not explain why cells maintained certain ppGpp levels in a given condition (*108*, *110*). If ppGpp was the source of growth rate control in bacteria then abolishing ppGpp in minimal media

should cause a rapid acceleration in growth. However, the growth rate drops from 1.2 h^{-1} to 0.63 h^{-1} in minimal media with glucose after relA / spoT deletion (*110*). Scott manages to explain why an artificial reduction in ppGpp does not increase growth rate despite increasing number of ribosomes.

Scott and Hwa proposed that the bacterial proteome is inherently limited, as the cellular resources available for protein synthesis and maintenance are finite, imposing constraints on the total amount of proteins that can be produced in a given time. Limitation of the proteome necessitates a careful allocation of resources to different cellular processes. Interestingly, allocation can be analyzed through the lens of economic principles. Just like economic systems aim to optimize the allocation of scarce resources to maximize overall benefit, cells face a similar challenge. The cells must balance the rate at which they generate substrates for growth with the rate of growth itself. Furthermore, they have to account for essential proteins required for growth, survival, and adaptation (*41*, *44*, *50*, *111*, *112*). The result is an automatically balancing system where production and consumption must be equal to prevent waste of resources.

Monod showed that there is a Michaelis Menten relationship between growth rate and glucose concentration in the growth media (*31*). Even if substrates for bacterial growth are present in abundance in the growth media the growth rate is limited. Therefore, the growth limitation must arise through a limitation of the metabolic flux inside cells. Therefore a rate-limiting metabolic reaction or exists inside the cells in any given nutrient condition. However, the rate of metabolic flux through that pathway can still be increased by increasing the amount of proteins involved in the rate limiting reaction. As bacterial growth rate does not approach infinity there must be some limit to how much a pathway can be up-regulated. Scott and colleagues show that increasing a limiting pathway comes at a cost. Ribosomes are autocatalytic and produce ribosomal proteins required to make more ribosomes. If another pathway is up regulated the limited ribosomal output now produces less ribosomal proteins leading to an overall reduction in the total number of ribosomes during steady state growth. Increased P-protein production at the cost of ribosomes, explains the striking linear relationship between number of ribosomes and growth rate observed by Ecker 60 years ago (*40*). As ribosomes can sense the abundance of charged TC, they are also auto-regulatory. If the amino acid pool is being depleted faster than it is produced it will lead to an increased binding of uncharged TC to the elongating ribosome. Binding of uncharged TC causes production of ppGpp by activation of RelA (*48*). An increase in ppGpp causes a reduction in the number of ribosomes slowing growth (*50*).

Returning to our example of switching the carbon source from glucose to mannose.

The rate at which mannose can be processed is slower meaning that cells up-regulate enzymes involved in the catalytic processing of mannose which results in reduced production of ribosomal proteins causing a reduction in the number of ribosomes. Proteome reallocation explains growth when varying the nutritional quality of the media and can be used to explain Monod's observations. In fact Monod's equation can be reformulated to explain growth as the result of nutrient availability and translational capacity equation (1.3) (*111*)

$$\lambda = \lambda_{Max} \frac{K_n}{K_n + K_t}. \tag{3.1}$$

Here λ is the growth rate and λ_{Max} is the maximum growth rate. K_n is the nutritional capacity and K_t is the translational capacity as described in (*44*).

The theory underpinning the growth laws was validated experimentally using quantitative proteomics (*46*). Cells were exposed to either limiting amounts of glucose by using a titratable ptsG strain, limiting amounts of amino acids using a titratable GOGAT strain or limiting translational capacity by using subinhibitory concentrations of chloramphenicol. Using this approach convincingly shows that the decrease in ribosomal mass fraction was directly correlated to the upregulation of the bottleneck pathway. The slowdown in growth under nutrient limitation is therefore attributable to proteome reallocation as the cell balances metabolite production with metabolite consumption for growth.

So having a new powerful theoretical framework explaining growth, the question is can proteome reallocation be used to explain growth under various stress conditions? Potentially, as bacteria facing osmotic stress are known to upregulate a variety of different proteins to restore osmotic pressure. Therefore, the growth rate slows more and more with increasing osmolarity as cells try to match the change in osmolarity by producing more stress proteins that increase the number of osmolytes.

Another way by which osmotic stress could cause a proteome burden is by macromolecular crowding. As cells are under osmotic stress they become more crowded by accumulation of osmolytes as well as loss of cytoplasmic water (*1*). The increased crowding leads to a reduction in diffusion (*113*). The reduced diffusion would disproportionately affect larger molecules, therefore it may slow down the rate of translational elongation, as diffusion of large ternary complexes is slowed (*49*). The reduction in translational elongation rate leads to a proteome burden as cells increase the number of ribosomes to compensate for the reduced elongation rate. The relationship between osmolarity and translational elongation rate has already been investigated

and will be discussed in more detail in the following section (*73*). Based on these known observations, I will discuss three testable hypotheses that can explain growth slowdown at elevated osmolarity.

1. Increased energy burden due to synthesis and transport of osmolytes.
2. Proteome reallocation as cells attempt to deal with osmotic stress.
3. Inability to restore cytoplasmic water content leading to macromolecular crowding.

I will start by looking at the energy burden associated with transport and synthesis of osmolytes. Measuring the energy cost of osmolyte synthesis or import is easy. The energy cost can be calculated by looking at how many bacteria as measured by OD_{600} are made on a fixed amount of carbon. By growing cells on various carbon sources at various osmolarities I will be able to estimated how much of the the total available energy is spent on dealing with osmotic stress. Next, I want to understand whether expression of proteins in response to osmotic stress places a burden on the proteome and explains the growth rate reduction. Finally, Cayley and coworkers suggest that the reduction in growth during osmotic stress is caused by the cells inability to restore cytoplasmic water content (*1*). They propose that failure to restore cytoplasmic water causes macromolecular crowding leading to a reduction in diffusion explaining the reduction in growth rate.

3.2 Understanding the Effect of Osmolarity on Fixed Carbon Yield

3.2.1 Development of High-Throughput Determination of Growth Rate and Yield

I started my investigation by looking at how increasing media osmolarity affects energy consumption in bacteria. I wanted to test a wide range of growth conditions, I developed and validated a high-throughput plate reader growth protocol allowing for calculation of both yield and growth rates of *E. coli* under osmotic stress.

To ensure that experimental protocols are reproducible across various conditions, I measured growth rates manually using a spectrophotometer, a plate reader and a custom built bioreactor. Cells were grown in M63 media with glucose and casamino acids (CAA) at 37 ℃.

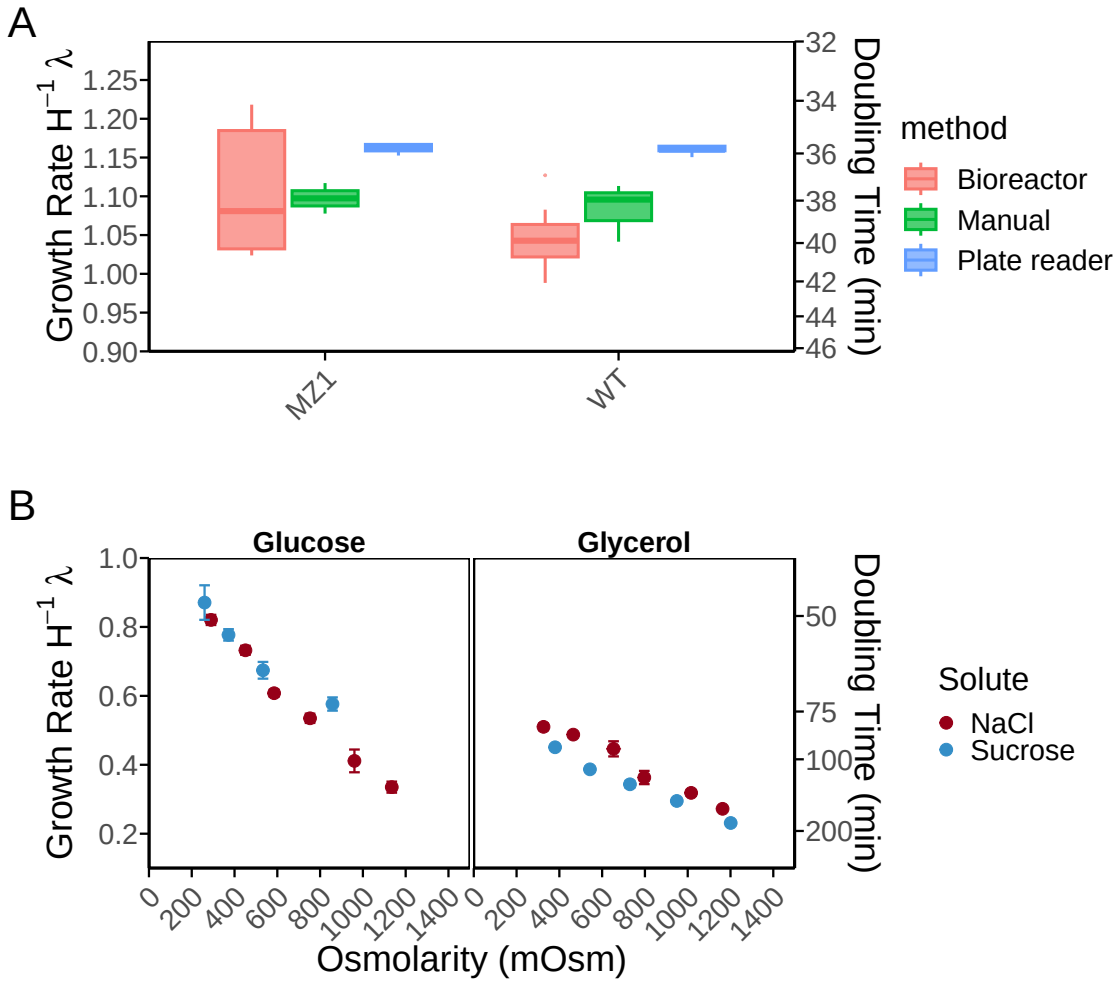

Figure 12: **A)** Growth rates were determined using a plate reader, a bioreactor or manually using a spectrophotometer. **B)** Change in growth rate using either sucrose or NaCl as the solute to change osmolarity for cells grown in M63 minimal media using either glucose or glycerol as the carbon source.

I observed slightly faster growth in the plate reader compared to manual measurements or in the bioreactor with doubling time being approximately 2 minutes faster in the plate reader. The growth rate of 1.1 h^{-1} is comparable to previous experiments using M63 media with CAA (*30*, *44*, *114*). Furthermore, I determined that the impact of osmolarity is solute independent by adding varying concentrations of either sucrose or NaCl to cells grown in M63 media with glucose or glycerol as the carbon source (figure 12 B). The decrease in growth being solute independent is consistent with previous observations (*72*, *115*).

Yield is a measure of how many cells can be generated by a fixed amount of resources (*116*). If importing osmolytes imposes an energy cost on the cell the energy cost could explain the reduction in growth. To measure yield I used the maximum OD_{600} value

that cells grow to on a fixed amount of carbon. While, use of sucrose and NaCl both had the same effect on growth rate I noticed a large reduction in yield with increasing sucrose concentration. However, use of sucrose changes the refractive index of the media making yield estimates using OD_{600} unreliable appendix A.2.3. As growth rates were constant irrespective of solute I used only NaCl to change the osmolarity of my media for the following experiments.

Another potential issue is that cell size changes can affect OD_{600} readings (*114*). However, osmolarity does not affect cell size of *E. coli* in stationary phase in M63 media with CAA (*30*). Therefore using OD_{600} readings as an estimate of cell number is justified. I predicted that due to the cost of synthesizing or importing osmolytes, *E. coli* grown at elevated osmolarity would show reduced yield. In minimal media *E. coli* generates trehalose as the main osmolyte. To estimate the relative amount of osmotic stress induction, I used the MZ1 strain that has sfGFP linked to the trehalose synthesizing promoter to understand how yield and trehalose expression correlate. Yield was obtained for WT cells with 20 mM of a given carbon source in the media.

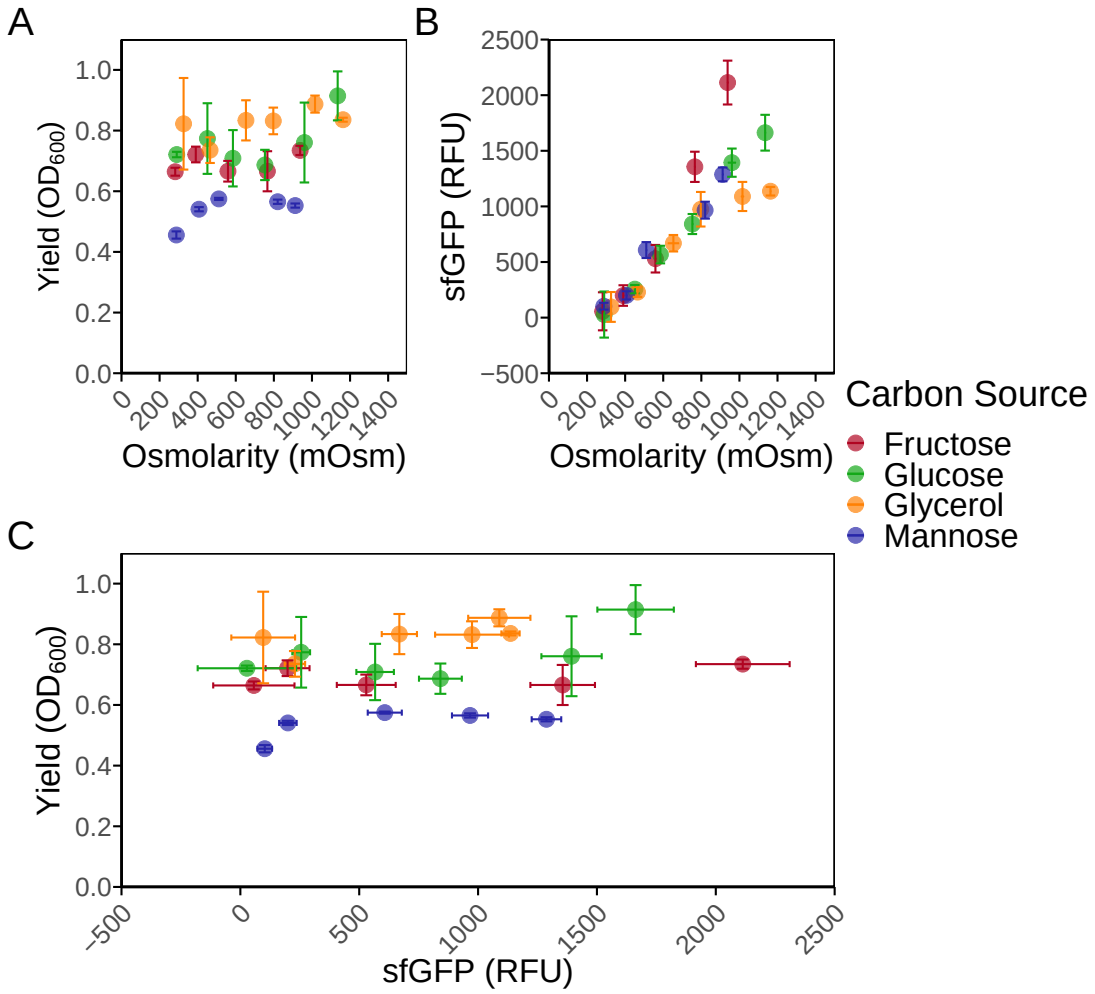

Figure 13: Change in yield and trehalose expression with increasing osmolarity. **A)** Yield for growth on a fixed amount of four different carbon sources. **B)** Relative change in sfGFP expression measured by Relative Fluorescence Units (RFU). **C)** Change in yield compared to change in sfGFP expression.

Surprisingly, there was no yield reduction with increasing osmolarity (figure 13 A). However, there is a strong correlation between osmolarity of the media and induction of trehalose synthesis as measured by sfGFP. The observation that yield does not decrease with osmolarity is counter-intuitive as synthesis of trehalose should consume a large amount of ATP appendix A.11. I therefore verified that I was not saturating the OD_{600} detection limit of the plate reader figure S5, and was not. I next made sure that the maintenance in yield was not an artefact from the plate reader and grew cells manually and again found no difference in yield figure S6.

Another potential problem was that the amount of carbon source used was too high and that bacterial growth was limited by another factor such as accumulation of a waste product in the media. I decided to characterize yield when specifically limiting

either the bacterial nitrogen or carbon source. I employed carbon limitation with 1 mM glucose or nitrogen limitation with 1 mM ammonia, while maintaining 10 mM of the other. This ensured that growth stops due to depletion of carbon or nitrogen. Additionally, I examined the hypothesis that knocking out the trehalose synthesis pathway could increase yield production, as cells might utilize the more energetically favorable potassium glutamate as an osmolyte instead.

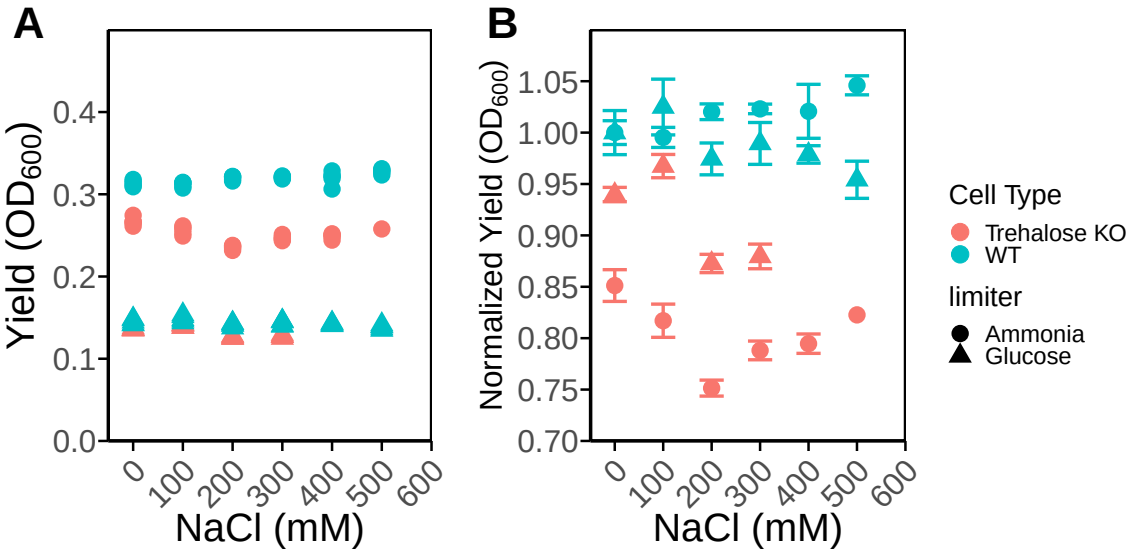

Figure 14: WT cells do not show a reduction in yield with increasing osmolarity. However, when MZ3 cells are grown in M63 media under nitrogen limitation, a decrease in yield is observed. **A)** Yield of WT and MZ3 cells grown in M63 media and limited by either ammonia or glucose. **B)** Normalized Yield of previous plot with yield normalized to the mean of the WT condition at 0 mM NaCl.

WT cells under nitrogen limitation grew to an OD_{600} of 0.3 and 0.15 when limited by carbon. Again they show no decrease in yield with increasing osmolarity, suggesting that the absence of yield loss is not due to accumulation of toxic product in the media. I also tested yield generated by a trehalose KO cell line (MZ3). Under carbon limitation a small decrease in yield was observed for MZ3 cells. Under nitrogen-limited conditions, a decline in growth rate is noticeable even at regular osmolarity, and the decline continues with increasing osmolarity up to 200 mM, after which it starts to increase again. The cause for the reduction in yield is unknown but may suggest an increased burden on amino acid synthesis as glutamate generation is up regulated in trehalose deficient cells (*61*). Alternatively, increased overflow metabolism can lead to a reduction in yield. I investigated overflow metabolism by quantifying acetate excretion at increasing osmolarity. The acetate excretion is increased relative to the growth rate but cannot explain the reduced yield in MZ3 cells figure S7.

Based on these measurements, it can be inferred that increasing osmolarity does

not seem to place a significant energetic burden on the cell, as the yield remains constant. However, I noted that there is large induction of the OtsA OtsB trehalose synthesis pathway as measured by sfGFP expression. Extra expression of protein can place a burden on the proteome and can cause a reduction in the number of ribosomes, therefore explaining the growth rate reduction. So next I want to explore what impact, if any osmolarity has on the proteome.

3.3 Activation of Osmotic Stress Response Correlates with Growth Rate Decrease

If the reduced growth is not due to an energy burden placed on the cell, the impact of media osmolarity on growth could potentially be explained by the induction of osmotic stress genes. To investigate whether expression of stress genes can explain the reduction in growth, both WT and MZ1 *E. coli* strains were cultured simultaneously under varying osmolarity conditions. Measurements of OD_{600} and fluorescence were taken in the cells as detailed appendix A.3. The expression of sfGFP serves as an indicator of osmotically-induced stress response. The measurement of sfGFP expression was corrected for both changes in OD_{600} and autofluorescence (see section A.2 for details).

I verified the methodology by growing cells in M63 media with glucose as a carbon source with either casamino acids and ammonia as a nitrogen source or just ammonia. Notably, two distinct trends emerged depending on the media condition. In M63 media without CAA, a clear upregulation of OtsB expression was observed at higher osmolarities during exponential growth. Conversely, when cultured with CAA, no OtsB expression was detected in the exponential phase (see figure S8), I reasoned that in CAA supplemented media cells would inhibit trehalose synthesis for preferred uptake of proline and showed that this was the case figure S10.

These findings demonstrate the suitability of the plate reader for simultaneous measurements of bacterial growth and activation of the osmotic stress response. Having established a precise and consistent quantification method for bacterial growth and OtsB gene induction by osmolarity, the subsequent aim was to investigate the effects of osmolarity and various nutrient conditions on gene expression.

In order to explore the variations in the activation of osmotic stress response under different nutrient conditions, I conducted experiments using M63 media with various carbon sources, and ammonia as the sole nitrogen source. M63 media is well-suited for studying the osmotic stress response in *E. coli* since it does not contain any os-

molytes that can be utilized by the bacteria. **M63** media primarily contains essential components for growth, including Carbon, Nitrogen, and Magnesium, with only small additions of thiamine and iron in micromolar quantities.

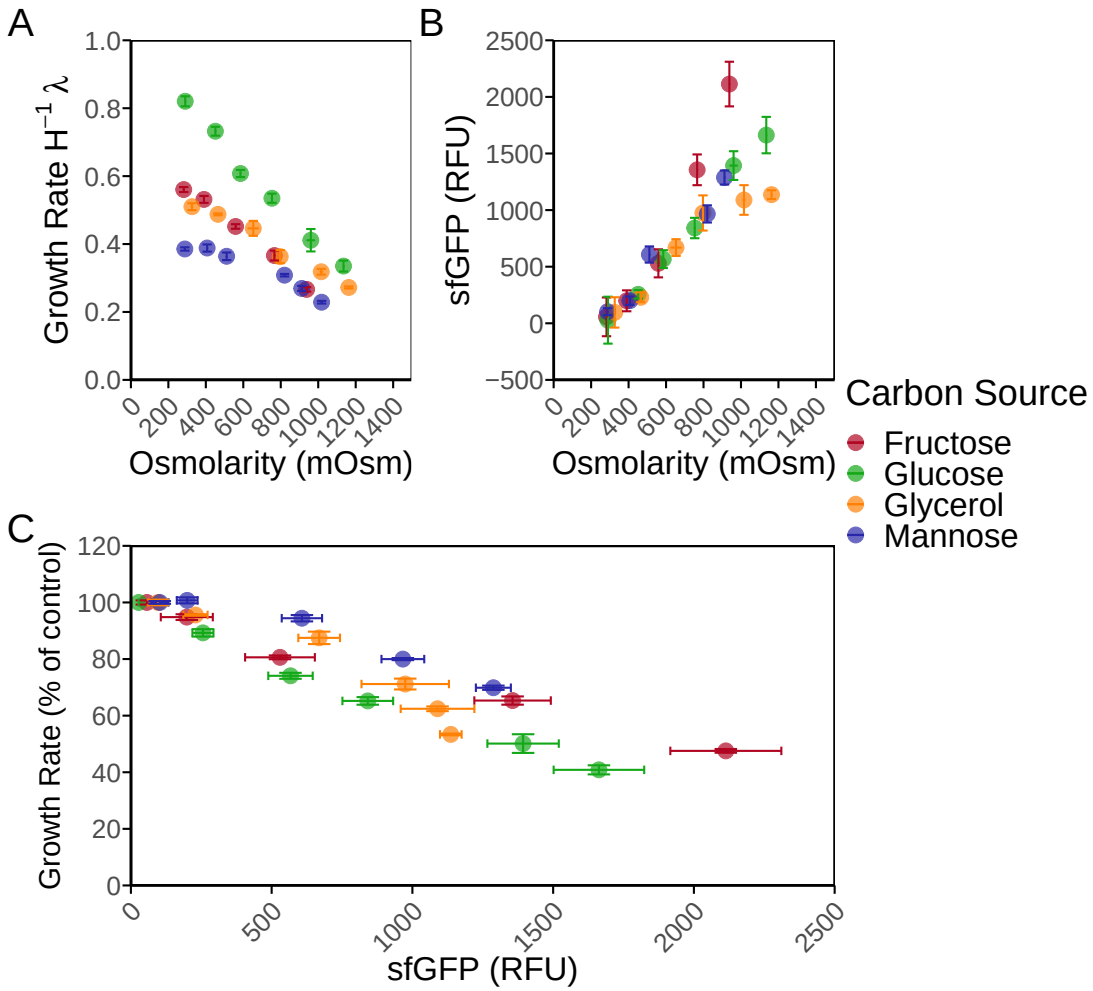

Figure 15: Cells grown in M63 minimal media on different carbon sources. Media osmolarity was modified by addition of varying levels of NaCl. **A)** Change in growth rate by osmolarity. **B)** Change in sfGFP expression as a function of osmolarity. **C)** Change in Growth rate as a function of sfGFP expression.

Glucose, fructose, glycerol and, mannose result in very different growth rates at normal osmolarity, which is about 280 mOsm for M63 media. *E. coli* using mannose show about half the initial growth rate of glucose. As expected there is a linear decrease in growth rate with increasing osmolarity, however, the growth rate slowdown is different for each carbon source. *E. coli* grown on glucose show a decrease of 0.4 h^{-1} in their growth, as media osmolarity is increased from 280 mOsm to 1000 mOsm. However, cells cultivated with mannose as the carbon source, starting with an initial growth rate of 0.4, continue to exhibit substantial growth at approximately 0.2 h^{-1} even at 1000

mOsm. The data suggests that the effect of osmolarity on growth rate is not absolute but rather can be expressed as a % change, with growth in 1000 mOsm media causing about a 50% reduction in the growth rate.

In parallel with growth rate measurements, I recorded the expression level of OtsB Induction by change showing increased activation of sfGFP. Cells showed a linear activation of trehalose synthesis with osmolarity $r^2 = 0.696$, regardless of carbon source (figure 15 B). Furthermore the expression of sfGFP is linearly correlated with growth rate reduction (figure 15 C). Therefore, the induction of osmotic stress genes could place a burden on the proteome.

The converging growth rates at higher osmolarities was unexpected (figure 15 A). Previous research by Dai observed a nearly parallel decline in growth rate for cells grown on fructose and glucose (*73*). When extrapolating the trend in my growth rates using a linear fit mannose and glycerol surprisingly show a higher predicted x-intercept indicating that slower growing cells are less affected by high osmolarity compared to fast growing cells figure S9. Further investigation revealed that the converging nature of the growth rates at high osmolarity were dependent on an intact trehalose pathway as in trehalose deficient cells glucose, fructose and mannose showed the expected parallel behaviour figure S9. Dai utilizes the NCM3722 strain in which there is an amber mutation in the RpoS gene, specifically the 33Am variant from EMG2 (*88*). The mutation most likely results in deficient trehalose synthesis and thus potentially explains the observation of parallel growth curves by Dai.

Another explanation is that mannose and glycerol can be protective during growth at high osmolarities. Glycerol is an osmolyte used by many halophiles as well as *Saccharomyces cerevisiae*, raising the possibility that it may possess similar properties in *E. coli*. However, mannose, which is not considered an osmolyte, also shows better than expected growth at higher osmolarity.

These findings provide confirmation of a growth rate slowdown as osmolarity increases. Moreover, there is a noticeable induction of the trehalose synthesis pathway, which correlates with the growth rate slowdown. The expression of osmotic stress genes could potentially place a burden on the proteome explaining the growth rate reduction.

Fortunately, extensive investigation of proteome reallocation was published recently that included data on osmolarity (*47*). Here, Mori and coworkers used the previously established approach of limiting carbon (C-lim) by titrating expression of ptsG, limiting amino acid synthesis by titrating GOGAT (A-lim) or limiting translational capacity by addition of chloramphenicol (R-lim). They provide data for cells grown in both normal

osmolarity MOPS media (*58*) and MOPS media supplemented with 500 mM NaCl. Here I use their data to estimate the proteome burden for different limitations. Mori detects 2335 proteins of which 1821 can be clearly assigned to a protein sectors. which protein sector a protein belongs to depends on the proteins response during carbon, nitrogen, and translational limitation. For example a protein that is up-regulated under carbon limitation but down-regulated during nitrogen and translational limitation would be assigned to the C-sector. For a full classification of all sectors see (*47*). I defined the proteome burden as the sum of all increases in mass fraction across the A, C, S, O, U and, R sectors of the proteome from the reference condition (*47*).

The proteome burden is therefore defined as any increase in protein expression compared to the reference condition. For example during titration of ptsG, there is an increase in proteins in the C-sector as well as the A and O sector. The percentage change increase in all of these sectors would then be equal to the proteome burden.

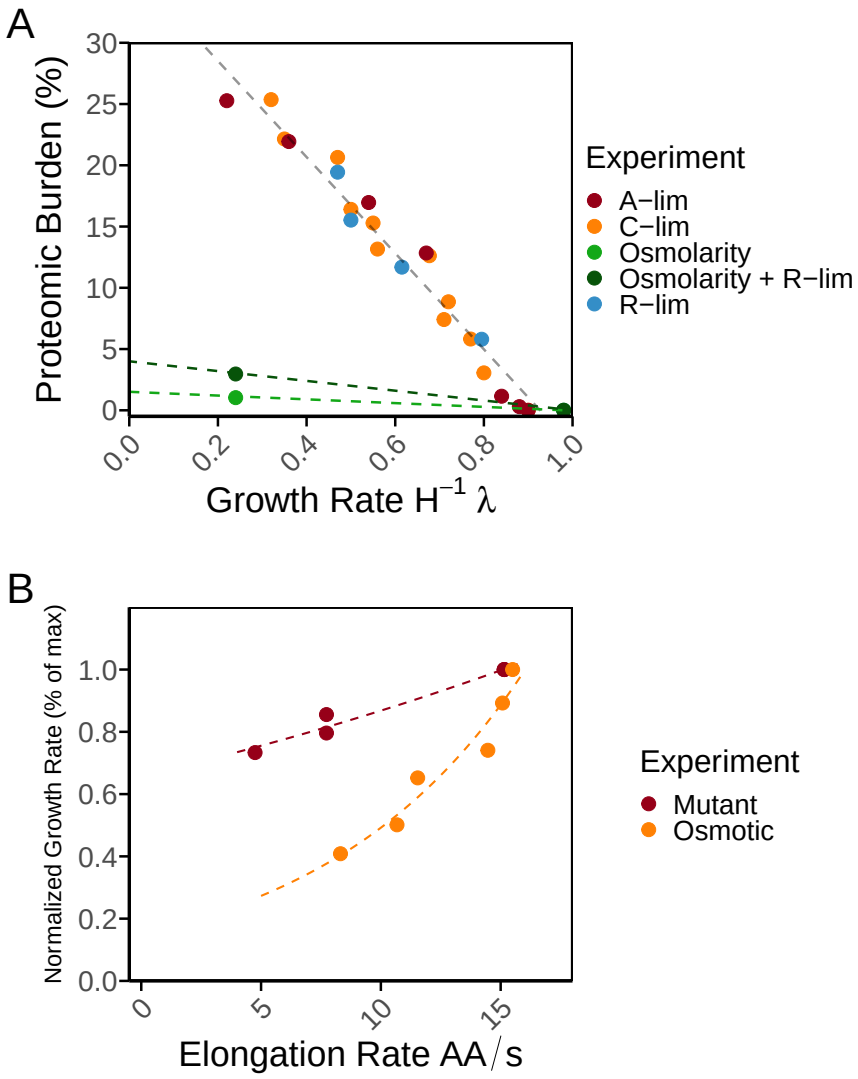

Figure 16: **A)** Mori and coworkers investigated changes in the proteome under a variety of different limitations. They show that there is a burden placed on the proteome by limitation of carbon uptake (C-lim), amino acid synthesis (A-lim) or translational capacity (R-lim). The proteome burden during osmotic stress comes from upregulation of rpoS controlled genes such as otsA and otsB (Osmolarity) (*47*). Cells grown under osmotic stress compensate for a lower translational elongation rate by increasing the number of ribosomes. Increasing number of ribosomes also places a burden on the proteome. Data from Dai was used to estimate the proteome burden caused by ribosome upregulation and added as the line osmolarity + R-lim (*73*). **B)** The change in translational elongation rate is not sufficient by itself to explain the reduction in growth rate observed at high osmolarity. Data was taken from Dai (*73*) and Scott (*44*) on translational elongation rate and growth rate under osmotic stress or in a group of translational mutants showing reduced ribosomal function.

As expected the growth rate decreases as A-lim, C-lim and, R-lim place a burden on the proteome. However, osmotic stress resulted in a negligible proteome burden as only a small number of rpoS controlled genes are up regulated (figure 16 **A** light

green).

Cayley suggests that the reduced growth rate is caused by loss of cytoplasmic water resulting in macromolecular crowding within osmotically stressed cells (*1*). Crowding results in a significant reduction in diffusion (*113*). Reduced diffusion will disproportionately affect larger particles as described by the Stokes-Einstein equation equation (3.6). Therefore, an interesting hypothesis is that the substrates for translational elongation TC are the cause of the reduced growth rate (*49*). Dai investigated the impact of osmolarity on translational elongation and found a reduction in translational elongation rate (*73*).

It is tempting to attribute the growth slowdown on the remarkable slowdown of the translational elongation rate during osmotic stress (*73*). However, slowdown in translational elongation generally places a burden on the proteome as cells upregulate ribosomal protein synthesis (*41*, *44*, *47*) increasing the number of ribosomes to counteract the slower elongation rate. However, the modest increase in ribosomal proteins observed during osmotic stress cannot account for the large reduction in growth rate observed even when summed with the upregulation in rpoS (figure 16 **A**, Dark green).

I also highlight the fact that the reduced translational elongation rate alone cannot explain the large reduction in growth encountered under osmotic stress by comparing data from Scott (*44*), who used a family of mutants showing greatly reduced translational elongation rate. I compare translational slowdown from mutant stains to the translational slowdown observed by Dai (*73*). I show that the reduction in translational elongation rate should not lead to such a drastic reduction in the growth rate. When elongation rate is reduced to 5 amino acids per second, growth rate only drops 20% in translational mutants compared to a 60% drop under osmotic stress (figure 16 **B**). The drop in growth rates for translational mutants is smaller for a given reduction in translation because translational mutants show a large increase in the ribosomal fraction to compensate for the reduced translational elongation rate. Under osmotic stress however, cells only show a small increase in the ribosomal fraction for a given growth rate (*73*). Mori and colleagues therefore rightfully conclude that the growth rate at high osmolarity is not due to a protein allocation bottleneck.

3.4 Understanding Growth Limitation In the Absence of Proteome Reallocation

The growth slowdown at higher osmolarity cannot be attributed to the energy cost of synthesizing or importing osmolytes, nor is it caused by a proteome burden resulting

from osmotic stress. Furthermore, the reduced translational elongation rate by itself cannot explain the growth rate reduction.

These results were unexpected, as the growth rate was decreasing but no burden was placed on the proteome. As the proteome burden placed on the cell at high osmolarity is very small, I concluded that something else was limiting growth. Growth is determined by the rate of flux through the metabolic network. To understand growth at high osmolarity we therefore need to look at how the flux is changed under osmotic stress. Dai shows that under osmotic stress there is a reduction in the translational elongation rate (*73*). The reduction in elongation rate means that the rate of amino acid consumption is drastically slowed. If reduction in translational elongation rate was the source of growth slowdown then it would result in upregulation of ribosomes via ppGpp, thus increasing the rate of consumption and once again balancing consumption and production of amino acids (*50*). However, during osmotic stress we observe the opposite as there is also a decrease in the number of ribosomes (*73*). The absence of an increase in ribosomes indicates that not only the rate of amino acid consumption is slowed. Imagine if metabolic processes within the cell continued at their normal rate, while translation is slowed down, then metabolites serving as precursors for growth, such as amino acids, would be generated far quicker than they are used.

Overproduction of amino acids compared to consumption would indicate that the slowdown at higher osmolarities is caused by inefficient resource allocation. If production surpasses consumption for a sufficiently long period of time, amino acids would accumulate within the cell and eventually start leaking out into the media. Yet growth curves generated did not show growth after the exponential phase and there was no reduction in the yield of cells indicating that there is no loss of metabolites to the surroundings.

The absence of these predicted signs allows us to speculate that not only translational elongation is slowed at increased osmolarity, but that there is an overall slowdown of the metabolic activity within the cell, and the reduction is directly proportional to the external osmolarity. What could be the source of global metabolic slowdown?

Enzymes that catalyse metabolic reactions are surrounded by water and loss of water results in loss of enzymatic activity (*117*). Cayley and coworkers show that there is a large reduction in cytoplasmic water in osmotically stressed cells and that the reduction in intracellular water directly correlates with a reduction in the growth rate. To restore cytoplasmic water cells can accumulate osmolytes and addition of osmolytes to the media causes an increase in cytoplasmic water as well as growth rate (*1*).

Therefore, could the reduction be caused by lack of cytoplasmic water causing a loss of enzymatic activity?

The main question arising from the relationship between cytoplasmic water and growth rate is why can cells not simply restore cytoplasmic water by importing more osmolytes? I wanted to understand how various osmolytes affect bacterial growth. While trehalose is the only osmolyte *E. coli* can synthesize *de-novo*, cells can use proline, choline, and betaine as osmolytes when they are provided in the media (*55*).

3.5 Impact of Various Osmolytes on the Growth Rate of *E. coli*

My initial focus was on proline, that has been shown to be an osmolyte and accumulated in the *E. coli* cytoplasm in response to osmotic stress (*118*–*120*). Interestingly, I found during validation of my sfGFP reporter strain that proline suppressed expression of trehalose synthesis appendix A.5.

My aim was to explore the impact of proline supplementation on growth under osmotic stress. However, supplementation of a single amino acids can have deleterious consequences (*121*). To control for any spurious effect of adding a single amino acid, I also used CAA, a mix of all amino acids obtained from acid hydrolysis of casein. I supplemented M63 media using glucose as a carbon source with either 0.2% CAA or 0.5 mM proline.

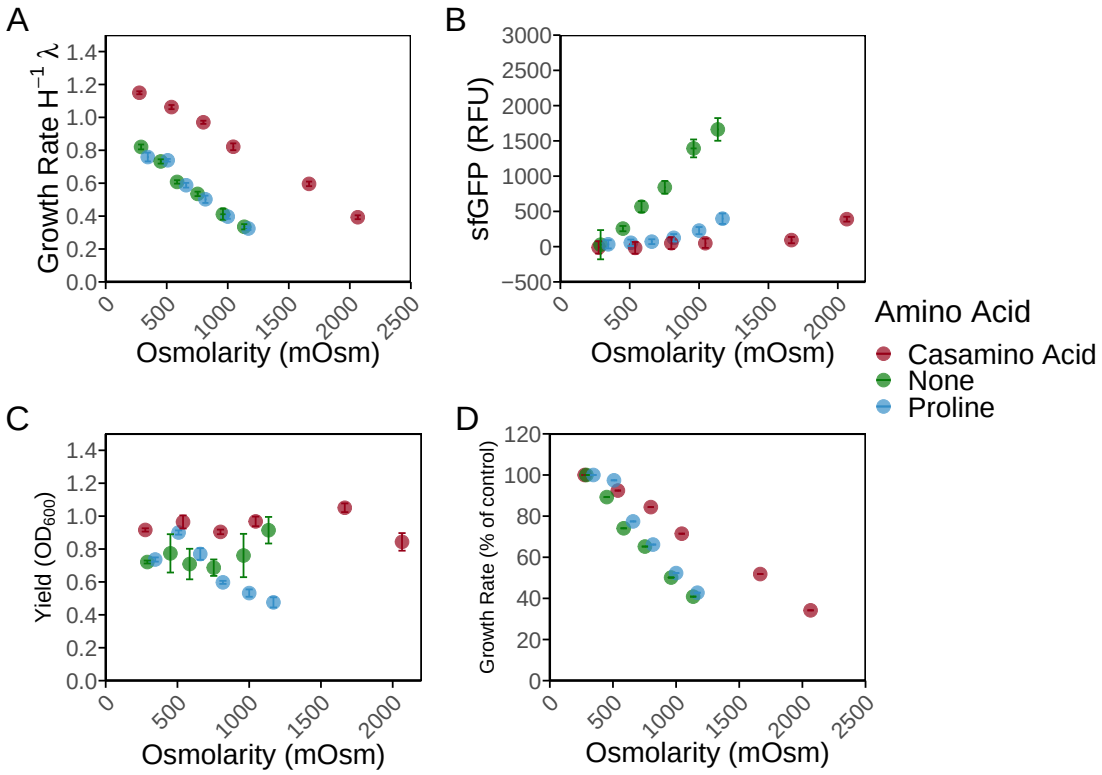

Figure 17: Addition of CAA or proline to media changes induction of OtsB as measured by sfGFP. **A)** Change in growth rate with increasing osmolarity, **B)** Change in sfGFP expression with increasing osmolarity, **C)** Change in Yield with increasing osmolarity, **D)** % change in growth rate compared to osmolarity.

The addition of CAA led to a 50% increase in growth rate at normal osmolarity, as expected due to change in proteome allocation (*44*). However, the growth rate decrease in CAA-supplemented media was comparable to that of the base media, resulting in remarkably higher tolerance to NaCl compared to the base media with growth being observable at over 2000 mOsm in media containing CAA. If we consider the % change in growth rate we can see that CAA cells grow better for a given osmolarity (figure 17 D). Proline on the other hand does not improve the growth rate or increase tolerance to osmolarity. If we look at the effect of proline and CAA on the expression of sfGFP we can conclude that proline replaces trehalose and inhibits expression of trehalose producing genes. My data is consistent with previous observations that proline is used instead of trehalose (*61*). However, it is important to note that the exact protective nature of CAA can be questioned as there may be betaine or other osmolytes present in CAA media, as casein used for production of CAA can contain betaines (*122*, *123*). Surprisingly, addition of just proline has no noticeable impact on the growth rate. Unlike previous studies (*120*), my observations do not indicate any protective effect from the addition of proline. Another intriguing finding is that the final yield decreases when proline is used as an osmolyte. The decrease in yield is particularly surprising since

proline can be picked up for only the cost of transport from the media, while trehalose synthesis incurs a substantial ATP cost. Potential causes of reduced yield are further discussed figure 14.

In conclusion, my findings demonstrate that regardless of whether the cell synthesizes trehalose or imports proline, the growth rate reduction remains identical. My data also indicates that cells do not generate trehalose while importing proline. The observation that cells choose a single osmolyte is consistent with previous research (*61*). However, it is hard to explain why cells do not accumulate multiple osmolytes. Increased accumulation under osmotic stress should increase cytoplasmic water and therefore prevent a reduction in the growth rate (*1*).

To further investigate whether an increase in cytoplasmic water can counteract decrease in growth rate during osmotic stress, I investigated the addition of choline and betaine. Choline is taken up by the BetT transporter and converted to betaine by the BetAB pathway. Betaine is a zwitterionic molecule, it has a positively charged quaternary ammonium group and a negatively charged carboxylate group. Its structure consists of three methyl groups attached to a central carbon atom, which is also connected to a glycine moiety. Betaine is accumulated and utilized as an osmolyte by a wide variety of different organisms (*55*, *71*). Some bacteria have the ability to synthesize betaine directly but *E. coli* is not one of them. The inability to synthesize betaine may be due to the metabolic expense of the three methyl groups required for synthesis. In these experiments, I grew cells in M63 media with glucose as the carbon source and supplemented the media with 1 mM of choline or betaine.

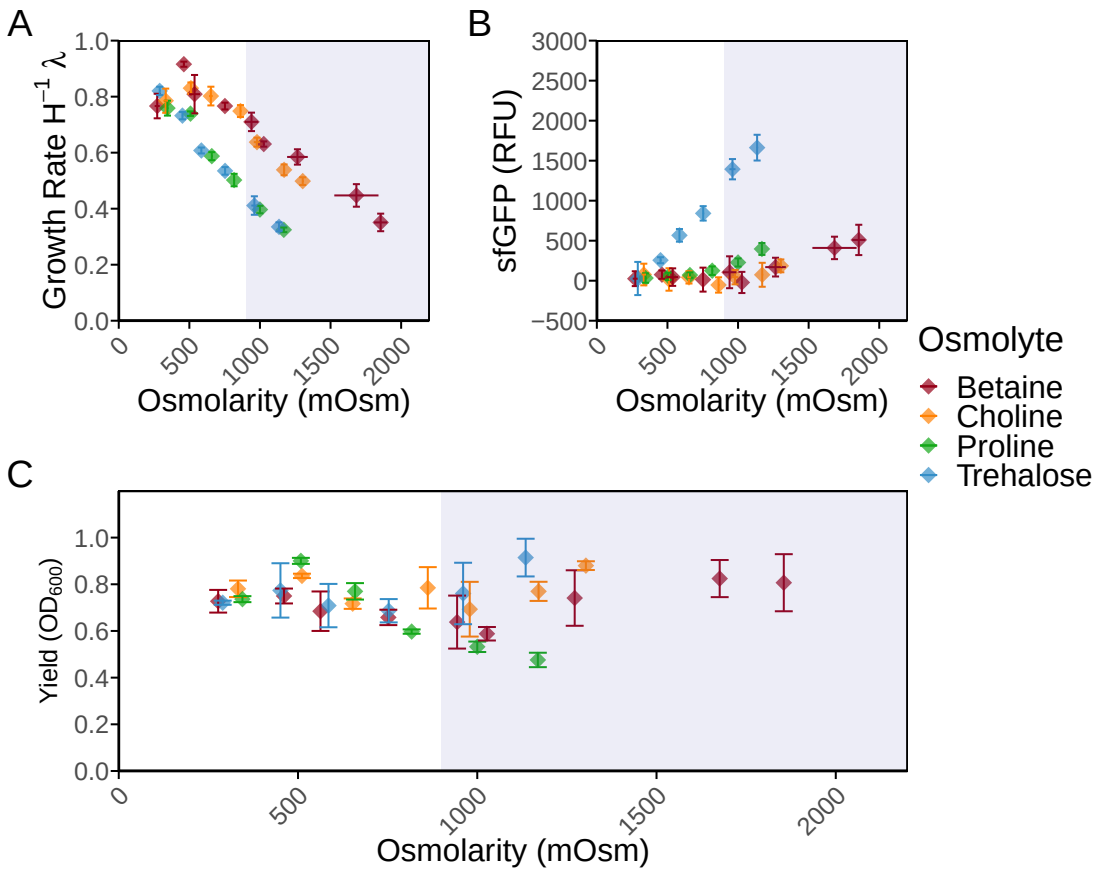

Figure 18: Cells grown in M63 minimal media were supplemented with choline, betaine or proline. Light blue shading is used to indicate osmolarity at which OtsB expression as measure by GFP is detected. **A)** Change in growth rate with increasing osmolarity. **B)** Change in sfGFP expression with changing osmolarity. **C)** Change in yield as osmolarity increases.

Addition of choline or betaine improved the growth rate of *E. coli* initially. However the rate of growth decrease was nearly identical compared to growth without osmolytes but shifted by about 0.5 osmole. The collected data is consistent with previous observations from Cayley that choline and betaine delay the decrease in growth rate but then show near identical decrease in growth rate (*120*). Originally, I assumed that the reduction in growth rate coincides with induction of trehalose synthesis. The region during which trehalose synthesis is detected was shaded blue and starts at about 0.9 osmole. However, there is a reduction in the growth rate before the induction of sfGFP starts (figure 18 A & B). There is also no relation between the level of growth rate reduction and the level of sfGFP.

These data further support the conclusion that the problem with elevated osmolarity is not a lack of potential osmolytes. The cell seems to only accumulate one osmolyte at a time with the preference being betaine. Furthermore, different osmolytes seem to

have different impacts on the growth rate. Cells only accumulating a single osmolyte at a time suggests that reduction in growth rate is not solely caused by an inability to restore cytoplasmic water content. The amount of cytoplasmic water content is determined by the difference in concentration of solutes inside the cytoplasm compared to solutes outside the cytoplasm. Therefore, cells could increase cytoplasmic water content by accumulating more osmolytes. I reasoned that maybe cells may still be limited by rate of osmolyte uptake. Therefore, I attempted to force cells to accumulate more osmolytes by over-expressing transporters responsible for choline or betaine uptake.

3.6 Over-expression of Osmolyte Transporters Does Not Improve Growth at High Osmolarity

Based on the absence of a proteome burden it seemed that cells should be able to accumulate more osmolytes by up-regulating the transporter and synthesis pathways. Additionally, the absence of simultaneous accumulation of osmolytes suggests that the cause of the growth slowdown is not solely due to the inability to accumulate sufficient osmolytes. To confirm that further osmolyte uptake does not restore growth during osmotic stress, I used strain HE902 which is an NCM3722 derived strain. HE902 has an IPTG inducible BetT gene on a high copy number plasmid showing strong overexpression of the target gene (*89*). As well as constitutive over expression of BetA / BetB pathway. HE936 is another NCM derived strain titratable high-affinity betaine transporter ProU using Chlorotetracycline (CTC) and a ProP deletion (table 1). Finally, a strain with CTC inducible low-affinity osmolyte transporter ProP with intact ProU transporter was also generated. As I am switching strains I characterized their response to osmolarity making sure the two strains were comparable figure S11. NCM3722 cells have an initial higher growth rate of around 1 compared to 0.8 h^{-1} of MG1655 in minimal media on glucose. As osmolarity increases there is a convergence of growth rates as growth rates move towards 0 h^{-1}. Therefore, NCM3722 is comparable to results collected in MG1655.

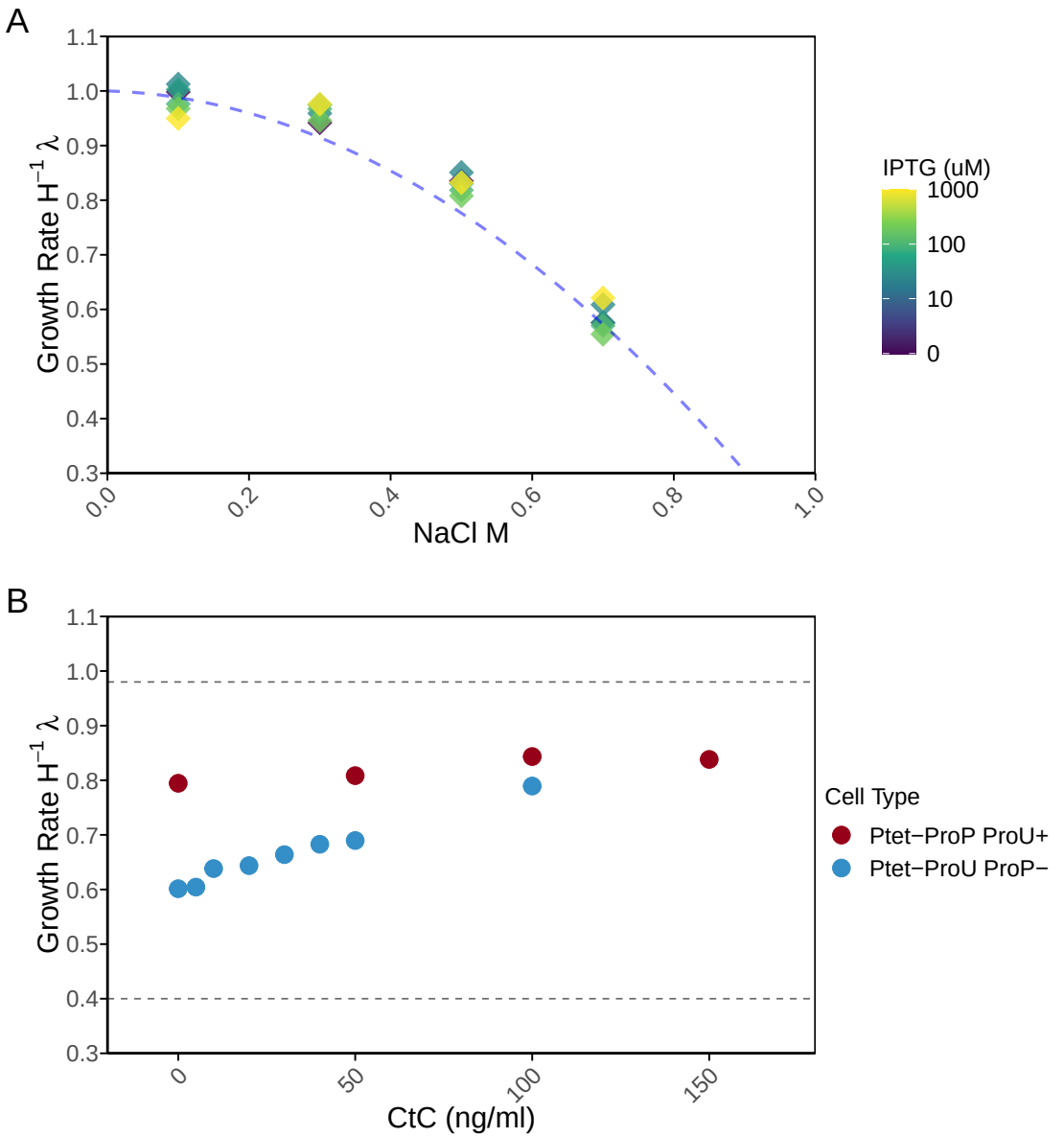

Figure 19: HE902 and HE936 cells were grown in MOPS media and the ability resist osmolarity induced growth slow down was assessed. **A)** HE902 was grown in MOPS containing 0.5 mM Choline and BetT was induced by addition of 0-1 mM IPTG. Osmolarity was varied by addition of NaCl. Previously measure growth rates in WT NCM cells were plotted as the dashed blue line. **B)** Cells were grown in 0.5 M NaCl MOPS containing 0.5 mM Betaine. To induce ProU or ProP, I varied the concentration of CTC. The dashed grey line at 0.98 h^{-1} represents the growth rate under normal osmolarity conditions, and the dashed grey line at 0.4 h^{-1} represents the growth rate of WT cells with no betaine in the media.

Over-expression of the BetT transporter did not result in noticeably improved growth with increasing osmolarity (figure 19 **A**). The expected growth rate determined in the WT parent strain is drawn as the dashed blue line again showing that overexpression of osmolyte transporters does not lead to better growth with increasing osmolarity.

Furthermore, overexpression at normal osmolarity did not lead to reduced growth as would be expected from the metabolic sum rule proposed by Taylor (*89*), and High-Performance Liquid Chromatography (HPLC) analysis did not detect any intracellular betaine at normal osmolarity indicating that the uptake of choline is tightly regulated (data not shown).

ProU is a high affinity transport system for betaine and is the dominant betaine uptake system showing a K_M of 1.3 µM in *Salmonella typhimurium* (*124*). ProP is a secondary betaine transporter that shows a lower affinity for betaine. In ProU+ NCM cells titration of ProP had little effect on the growth rate (figure 19 **B** red circles) suggesting that ProU by itself is sufficient to import betaine at 500 mM NaCl.

Deletion of ProP with titration of ProU shows that there is a correlation between CTC concentration and growth rate with near maximal betaine up take achieved at around 100 ng/ml (figure 19) **B** Blue). Interestingly, Ptet-ProU ProP- cells grow faster than in media without betaine (0.6 vs 0.4 h^{-1}), suggesting either the presence of another unidentified betaine transporter, or a leakiness of the construct. Due to the high affinity and fast kinetics even a small amount of ProU expression could explain the improved growth rate.

So overexpression of ProU, ProP or BetT did not allow for protection of the growth rate. It seems like these pumps are tightly regulated and a mechanism for regulation has been suggested (*55*, *125*). ProU has been reconstituted in artificial liposomes and showed activity in the absence of any osmotic gradient *in-vitro* (*126*). However, my data indicates that *in-vivo* these channels are tightly regulated and it is not possible to import more osmolyte than what cells import under normal conditions. A potential way to force increased import of these osmolytes is mutation of the regulatory C-terminal domain (*125*). The tight regulation of osmolyte transporters supports the notion that the growth slowdown encountered by cells is not caused by lack of ability to import osmolytes.

To further, confirm that cells do not benefit from increased osmolyte accumulation, I attempted to overexpress trehalose while supplementing cells with betaine appendix A.8, overexpression of trehalose negated the protective effect of betaine at higher osmolarities and reduced the growth rate. Cells are therefore being very stubborn and resisting considerable effort to load them with osmolytes and increase their cytoplasmic water content. The data also show that if trehalose is over-expressed cells will grow at the same rate with or without betaine. The most likely explanation for the data is that overexpression of trehalose results in inactivation of betaine transporters, preventing betaine from being accumulated. Therefore, cells do not accumulate betaine

if trehalose is induced even if betaine is present in the media. However, absence of betaine in cells over-expressing trehalose should be confirmed using HPLC as another potential explanation could be that trehalose somehow negates the protective effect of betaine while still allowing for intracellular accumulation.

In conclusion, these data indicate that the growth rate slowdown is not caused solely by a lack of cytoplasmic water. Instead, the cells tightly regulate the amount of accumulated osmolyte within the cell. Careful regulation of osmolyte accumulation suggests that the growth rate slow down may not be caused by the osmotic stress itself but a result of the accumulated osmolytes. Cells seem to know exactly what level of osmolyte accumulation is good for them and when using trehalose overexpression to force increased intracellular osmolyte concentration it reduces the growth rate. Therefore, the growth rate under osmotic stress must balance at least two negative effects. First, increased media osmolarity and loss of cytoplasmic water must be detrimental to the cell as otherwise cells would not waste effort synthesizing and importing osmolytes. Second, the high intracellular concentration of osmolytes must also become detrimental to the cell as otherwise the cell would just keep importing more and more osmolytes to balance the loss in cytoplasmic water.

3.6.1 The Question of Cytoplasmic Water

Cayley and coworkers show that cells restore cytoplasmic water concentration by synthesis of trehalose or import of proline, choline or, betaine (*120*). In their paper they claim that they observe an approximately 25% lower cytoplasmic free water volume in cells accumulating trehalose compared to betaine containing cells. They then show that the growth rate varies with cytoplasmic water content (*1*).

However, they critically fail to show how cytoplasmic water content varies with the growth rate independently of osmotic stress. Taylor and coworkers demonstrate a variation in cytoplasmic water by just changing the carbon source from glucose to mannose (*89*) figure S12. Additionally, the link between reduced cytoplasmic water and growth rate is still unclear. They proposed that loss of cytoplasmic water leads to macromolecular crowding (*1*). However, attempts to link macromolecular crowding with reduced growth have not been successful (*73*). Therefore, the link between cytoplasmic water and bacterial growth rate in my opinion remains unresolved. My data argues that the loss of intracellular water is not the origin of the observed growth rate slowdown. Osmolyte transporters show careful regulation suggesting that inability to take up enough osmolytes during osmotic stress cannot explain the reduction in growth rate. Furthermore, attempting to increase intracellular solute concentration in betaine supplemented media via trehalose overexpression results in reduced growth

by preventing betaine accumulation. The accumulation of osmolytes therefore seems to have a negative impact on the growth rate itself. Therefore, two opposing mechanisms weighing on the growth rate are at play. Osmolytes are accumulated during osmotic stress. In the absence of osmolytes *E. coli* grow worse than in their presence so we can conclude that osmolytes help mitigate osmotic stress. However, the osmolytes themselves potentially also have a negative impact on growth. Therefore, the reduction in growth rate is uniquely dependent on the properties of the osmolyte used.

3.7 The Varied Effects of Osmolytes on Growth Rate

I propose that the growth slowdown experienced by the cells must be due to the import of osmolytes and accumulation to a high level within the cytosol. I therefore wanted to understand how different osmolytes affect the growth rate of *E. coli*. I investigated five different ways in which *E. coli* can restore its osmotic pressure.

1. WT *E. coli* cells mainly use trehalose to balance osmotic pressure (*61*).
2. The only osmolyte that is known to accumulate in trehalose deficient cells is K^+ and Glutamate as the major counterion.
3. If proline is present in the media cells will preferentially accumulate it over trehalose (*61*).
4. Choline is transported into the cell by BetT and is converted to betaine via the BetAB pathway.
5. Betaine can be taken up directly by the ProP or ProU transporter.

Cells were grown in M63 media with glucose as the carbon source and were supplemented with 1 mM betaine, choline, or proline. Additionally growth rates and yield of MZ3 trehalose deficient cells were collected, the major osmolyte within these cells is suspected to be potassium glutamate, but contents of cells was not confirmed in the current study. Growth rates and the yield of each condition was determined by plate reader.

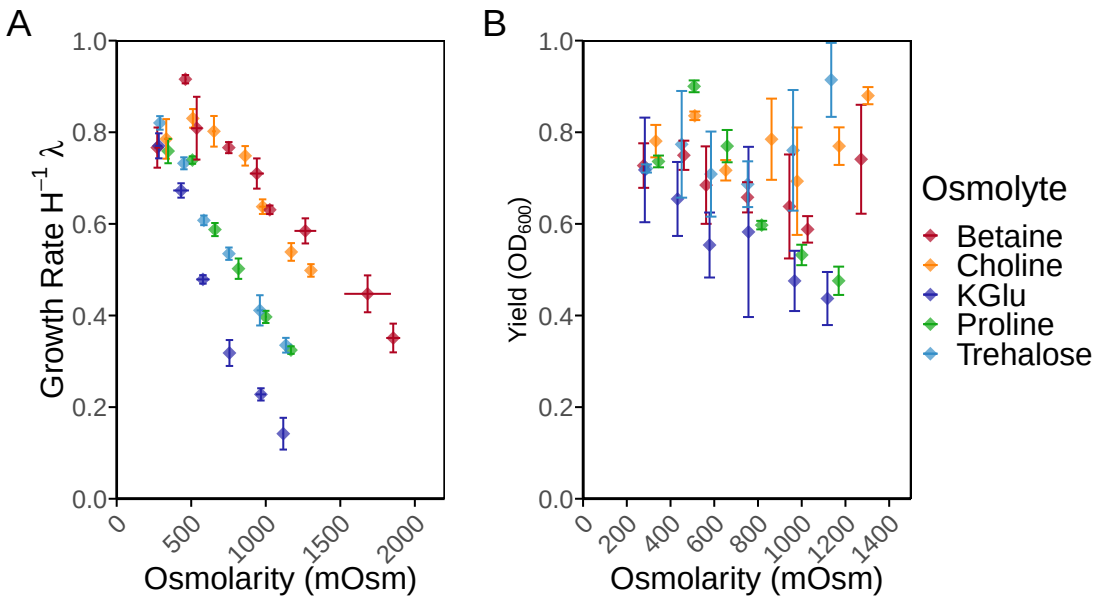

Figure 20: WT or MZ3 cells grown in m63 minimal media supplemented with choline, betaine or proline. MZ3 cells that are unable to make trehalose are labelled as KGlu. **A)** Change in growth rate with osmolarity. **B)** Change in normalized yield with osmolarity.

There are three distinct effects on growth with osmolarity, formed by the MZ3 trehalose deficient cells, WT cells accumulating trehalose or proline, and finally WT cells accumulating betaine or choline figure 20. Interestingly, trehalose deficient cells can still grow at surprisingly high osmolarity and the correlation between growth and osmolarity holds. The ability of cells to grow in the absence of any organic osmolyte may be explained by the fact that cells can restore water initially by an influx of potassium (*67*). Furthermore, the cell produces glutamate to balance the positive charge of K^+ ions. However, the potassium is quickly replaced by compatible solutes when available (*61*). If no compatible solutes are present in the media and protein synthesis is blocked by addition of chloramphenicol, K^+ concentration inside the cell remains high (*61*). It is surprising how well cells grow under osmotic stress even in the absence of any known organic osmolyte. It is unclear whether the growth rate decrease in MZ3 cells is caused by the same mechanisms as those accumulating organic osmolytes. Alternatively MZ3 cells could accumulate another compatible solute that is still unknown.

Interestingly, trehalose deficient cells along with the proline supplemented cells show a decrease in yield with increasing osmolarity. The cause for the yield decrease is unclear but it is not related to altered overflow metabolism figure S7. Furthermore, it is not due to an elevated energy burden on the cell as the limitation is created by ammonia not glucose figure 14. Trehalose deficient cells may have to accumulate more

glutamate to neutralize the higher concentration of K^+ which is a potential explanation for the increased ammonia demand. Alternatively, the high concentration of K^+ may have a negative impact on cell metabolism (*67*).

Given the varying growth rates exhibited by *E. coli* when supplementing different osmolytes, it prompted the question of whether the growth slowdown mechanism is similar to that observed in minimal media. Previous publications have shown that there is a small decrease in the ribosomal proteome fraction and a reduction in the translational elongation rate for WT cells (*73*). However, the authors did not look at the different effects trehalose, proline, choline and betaine had on the ribosomal mass fraction and the translational elongation rate.

3.8 Estimation of Ribosomal Mass Fraction and Translational Elongation Rate under Osmotic Stress

Growth can be determined by knowing the translational elongation rate and number of actively translating ribosomes equation (1.7). So to understand how different osmolytes affect growth I wanted to determine the ribosomal mass fraction as determined by Scott (*44*), as well as the rate of translational elongation (*41*). Determining the relationship between total cellular RNA and protein is an easy way to determine the ribosomal mass fraction. Translational elongation rate was calculated by inferring the time it takes to generate one LacZ protein as described (*41*).

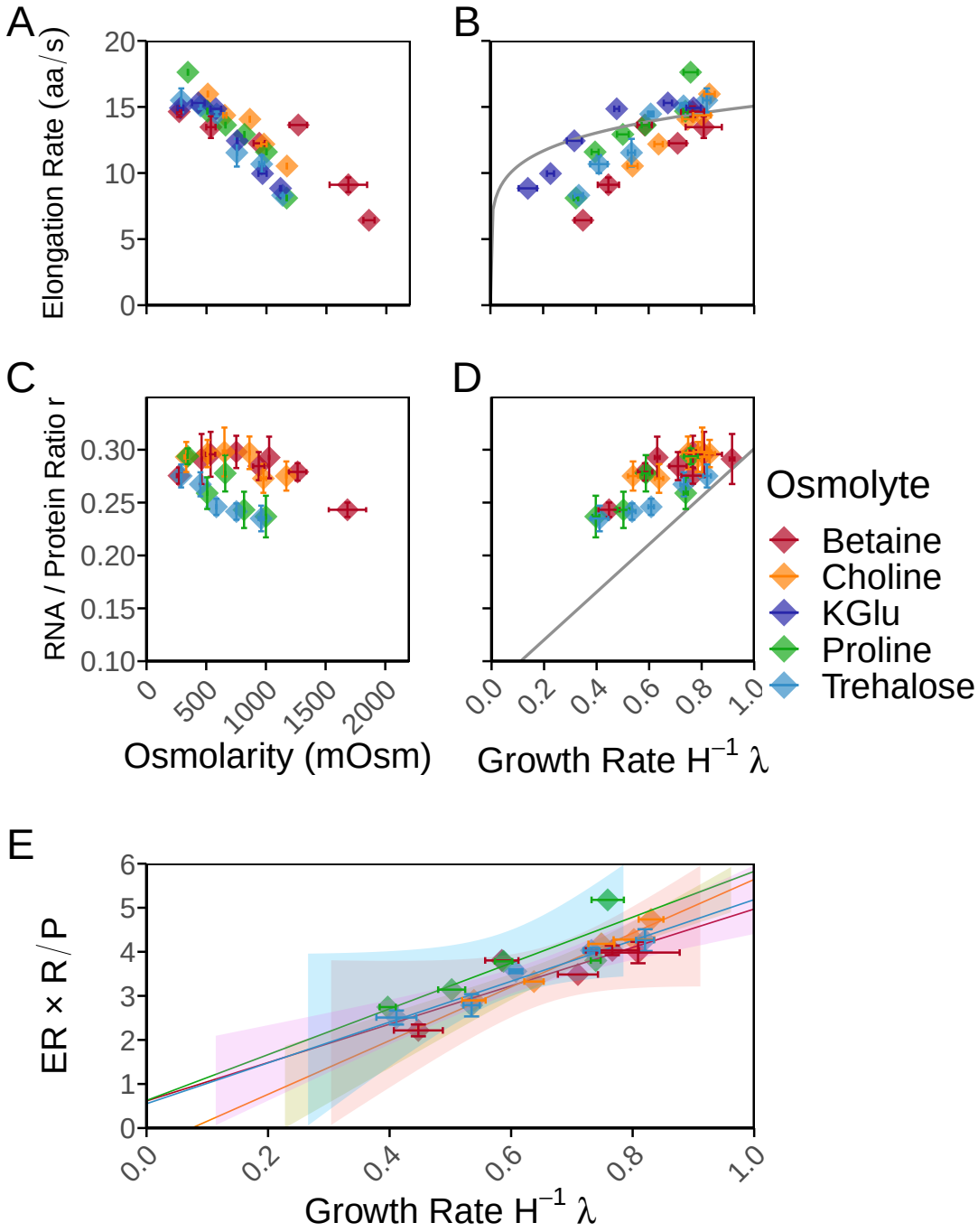

Figure 21: WT or MZ3 cells were grown in M63 media supplemented with choline, betaine or proline. **A)** Change in elongation rate with osmolarity. **B)** Change in elongation rate compared to the growth rate. The gray line is a line of best fit obtained from fitting the change in elongation rate vs. the change in growth rate in various nutrient media (*41*) **c)** Change in RNA / Protein ratio (R/P) with Osmolarity. **D)** Change in R/P compared to the growth rate. The gray line indicates the result of fitting a least squares regression on change in R / P compated to the change in growth rate in various nutrient media (*41*). **E)** Change in growth rate as a result of change in number of ribosomes and translational elongation rate.

The ribosomal content and translational elongation rate roughly mimic what is observed with growth rates, as there is a linear decrease in WT cells ($R^2 = 0.902$) for RNA Protein ration and $R^2 = 0.915$ for translational elongation rate. Analysis of linear regression is reported in full for change in ribosome content with change in growth rate. As well as change in $R/P \times ER$ with growth rate appendix A.10.

Cells containing betaine or choline sustain a higher level of ribosomes for a given osmolarity (figure 21 A, C). In general I show that the reduction in translational elongation rate and R/P ratio is similar compared to the change in growth rate regardless of osmolyte used, with the exception of KGlu (figure 21 B, D). Panel E confirms the accuracy of the measurements as the elongation rate multiplied by R/P varies linearly with the growth rate and suggests that ribosomal inactivation is not important at growth rates larger than 0.4 h^{-1} as observed by Dai (*73*). The one osmolyte that really stood out was KGlu as cells showed a much higher elongation rate for a given growth rate. For example at a growth rate of 0.3 h^{-1} MZ3 cells show an elongation rate of around 12.5 aa/s. Compared to 8 for trehalose cells and 6 aa/s in betaine supplemented cells. The variation in translational elongation rate suggests that the slowdown in MZ3 cells is fundamentally different from the other osmolytes.

I have previously mentioned that a slowdown in translational elongation without an increase in the ribosomal mass fraction suggests that there is a global metabolic slowdown. Here I show a decrease in translational elongation rate regardless of osmolyte used.

It is important to be aware of the relative effects of R/P changes and elongation rate changes as variations in these two metrics may point towards the origin of the osmotic induced slowdown. Here I demonstrate that growth rate is maintained not by increasing the number of ribosomes as is observed during translational slowdown in mutant strains (*44*). Instead addition of betaine and choline seem to counteract the slowdown in metabolic function protecting both the R/P ratio and the elongation rate. Understanding the effect of osmolarity on translational elongation rate may shed light on the source of the slowdown, and it has been studied previously. (*73*). Under nutrient or translational stress induced with chloramphenicol, there is a Michaelis-Menten relationship between the number of ribosomes and the elongation rate that arises from co-regulation between rRNA, tRNA and EF-Tu as previously described (*49*, *50*, *73*).

$$[TC_{\text{eff}}] = C \times \left(\frac{R}{P}\right) \tag{3.2}$$

where C is the proportionality constant that arises from co-regulation between rRNA, tRNA and Elongation Factor thermo unstable (EF-Tu). The proportionality constant holds at higher osmolarity, instead the decrease in translational elongation appears to arise from a reduction in the k_{on} implying worse binding of ternary complexes to ribosomes as described by equation (3.3) (*73*).

$$\frac{1}{k} = \frac{1}{k_{\text{on}} \times [TC_{\text{eff}}]} + \frac{1}{k_{\text{elong}}} \tag{3.3}$$

Dai shows that under chloramphenicol inhibition there is no change in the maximal elongation rate k_{elong} at high osmolarity and the concentration of $[TC_{eff}]$ is unchanged, the only potential source of the reduced elongation rate at high osmolarity must be a reduced k_{on}. The question is what could drive reduction in TC binding?

So to recapitulate, we know that the source of the growth slowdown is not related to energy, nor is it caused by a proteome burden. I also show that attempts to further increase osmotic pressure by forcing cells to accumulate additional osmolytes is unsuccessful. It therefore seems that the accumulation of osmolytes themselves is what is driving the reduced growth. The variation in growth rate compared to the osmolarity when different osmolytes are accumulated imply that different osmolytes have different effects on metabolic flux with cells accumulating betaine fairing a lot better than those accumulating trehalose or proline. Future experiments should investigate the metabolome of cells under osmotic stress and precisely quantify total metabolite concentrations inside cells to determine the effect on growth of each osmolyte, as it is unclear if osmolytes accumulate in equal concentrations.

If the growth rate slowdown is caused by osmolyte accumulation, then the reduction in growth is independent of osmotic stress. Instead the growth rate slowdown would come from the accumulation of high quantities of osmolytes. Accumulation of osmolytes causing the growth slowdown is consistent with all the data so far. It would explain why there is no proteome reallocation in osmolarity as upregulation of one pathway or another would not benefit the cell. It explains why cells do not benefit from increased uptake or production of osmolytes because the issue is not the loss of osmotic pressure. Instead increased accumulation of osmolytes have a negative effect of osmolytes on growth. It would also explain why cells choose to accumulate trehalose and betaine when available as these substances somehow have a less negative effect than whatever else could be accumulated.

To establish whether accumulation of osmolytes could be the source of the growth rate slowdown, I set out to find solutes that would fulfil two criteria. First the solute

had to be inert and act as a ”compatible solute” to *E. coli* cells in high concentrations and second the solute would pass through the cell membrane. By using solutes that pass the cell membrane I would attempt to mimic what happens inside the cells that are osmotically stressed but instead of accumulating or synthesizing osmolytes the cells would accumulate the solute present in the surrounding environment.

3.9 Using Membrane Permeable Solutes to Investigate the Impact of High Intracellular Osmolyte Concentrations

If the osmolyte accumulation theory is correct it has two main implications. First, the main cause of the growth slowdown and the problem faced by bacteria during osmotic stress is not caused by a change in osmotic pressure or loss of cytoplasmic water but rather the high concentration of osmolyte in the cell. The second implication is that high concentration of intracellular osmolytes can slow metabolic activity by reducing enzymatic velocity.

To demonstrate the potential ability of osmolytes to reduce growth, I identified two solutes that I believed would be membrane permeable and act as compatible solutes, Ethylene Glycol (EG) and glycerol. Glycerol, was shown to equilibrate across the cell membrane in a matter of seconds meaning that any osmotic gradient formed would be temporary (*127*). Furthermore, EG was predicted to cross the cell membrane and be non-toxic in *E. coli* (*128*, *129*), and was chosen as an extremely small non-polar molecule with a molar mass of 62. I confirmed that these molecules equilibrate across the cell membrane by monitoring cell size changes in response to molar concentrations of glycerol or ethylene glycol figure S14.

To see the effect of high intracellular solute concentration in the absence of osmotic stress I grow cells in M63 media with glucose. I vary the osmolarity of the media with NaCl or with EG nor glycerol. Cells are labelled with the suspected intracellular solute so for cells grown with NaCl but no betaine the main intracellular osmolyte is suspected to be trehalose. For cells grown with NaCl and betaine in the media the main intracellular osmolyte is thought to be betaine. For cells grown in high glycerol and EG media the main intracellular solute is thought to be the glycerol and EG respectively.

I determined the growth rate, induction of trehalose synthesis genes, elongation rate and R/P ratio for cells grown in molar concentrations of glycerol or EG. I compare the cells to cells grown in M63 media that are under osmotic stress.

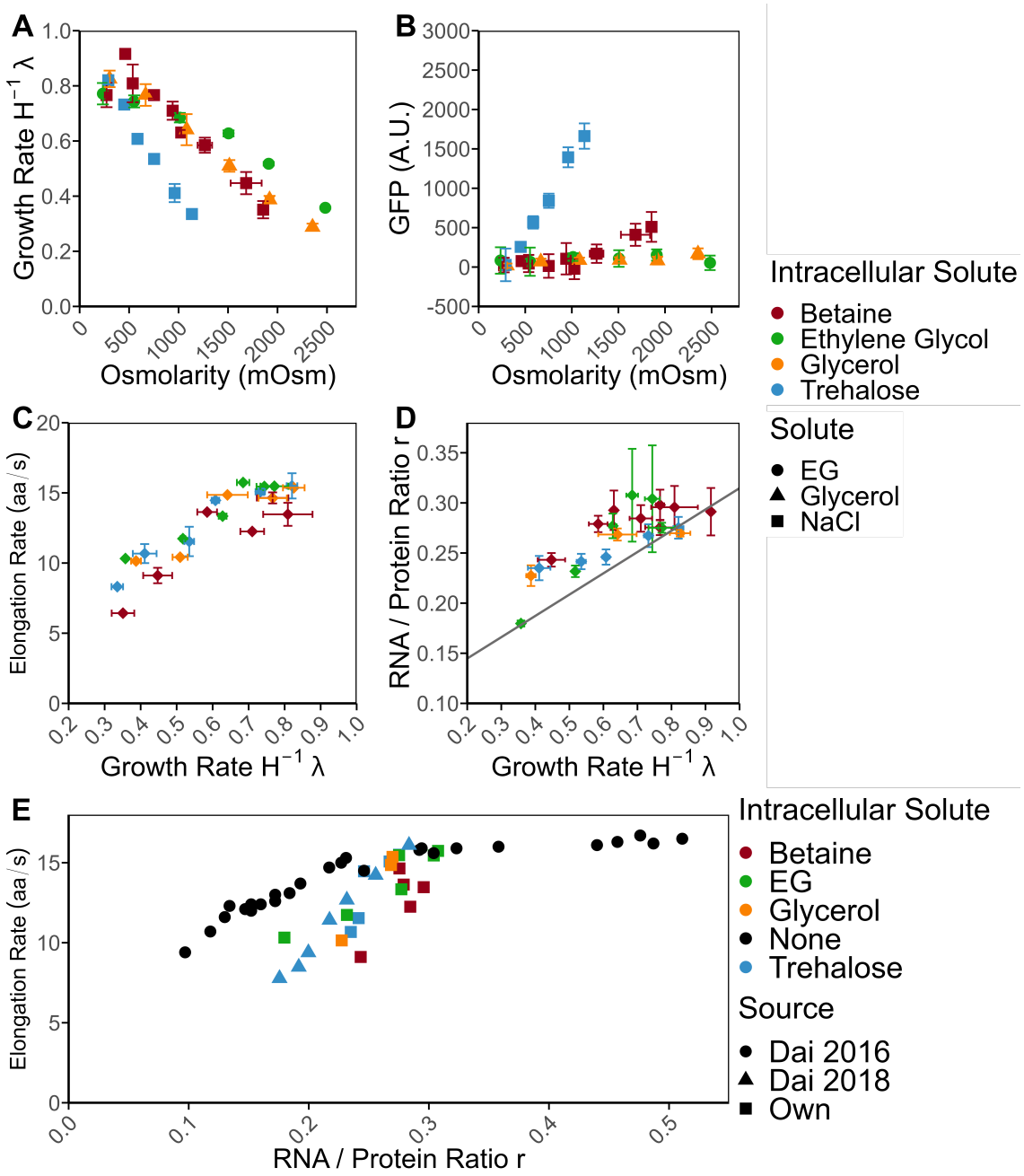

Figure 22: Addition of glycerol or EG causes a reduction in growth rate that is comparable to growth rate slowdown seen with betaine. **A)** Change in growth rate with increasing external osmolarity. **B)** Expression of trehalose synthesis with increasing external osmolarity. **C)** Change in Elongation rate compared to growth rate. **D)** Change in R/P ratio compared to growth rate with nutrient stress line from (*44*) in gray. **E)** Comparison of elongation rate with RNA / Protein ratio.

Cells tolerated addition of molar quantities of both ethylene glycol and glycerol to the media. Surprisingly, the growth rate slowdown observed for cells supplemented with glycerol closely mimicked that of cells growing in the presence of betaine. Addition of EG seems to have the smallest impact on growth rates with cells showing about half their maximal growth after addition of 2 M of EG.

Neither EG or glycerol induced activation of the Ots pathway. While the exact cause of Ots gene expression is unknown the current theory is that activation is related to a change in osmotic pressure. The assumption thats Ots gene expression is activated by changes in osmotic pressure, is supported by the results that trehalose synthesis is activated only when there is a shift that cannot be equalized by another osmolyte like proline, betaine or choline. Additionally, I confirmed that these compounds do not cause osmotic stress by looking at cell size changes figure S14, confirming that they cross the bacterial membrane freely.

It is interesting to note that the Elongation rate and R/P fraction behave very similar to what is observed during osmotic stress, with a rapid decrease in elongation rate and an increased R/P ratio. During nutrient stress or chloramphenicol inhibition the elongation rate and R/P ratio are linked due to a correlation between $[TC_{eff}]$ and R/P as described in equation (3.2). However, with both EG and glycerol we observe the same pattern as observed with osmotic stress where there is a faster than expected decrease in the translational elongation rate (figure 22 C, D, E). The fact that elongation rate decreases faster than expected by the Michaelis-Menten relationship observed by Dai (*41*), suggests that the problem faced by cells with high intracellular EG and glycerol concentration is identical to that faced by cells under osmotic stress.

Taken together these data suggest that the growth rate slowdown under osmotic stress is not related to the osmotic stress itself. Instead the problem is related to the internal concentration of solutes rather than the difference between internal and external solute concentration. While only two compounds have been demonstrated here, in theory a lot of membrane permeable compounds exist that could be used to further test whether high solute concentration slows growth. (*127*, *130*). If osmolytes accumulation is the source of the growth slowdown at higher osmolarity, then what is the mechanisms that could underlie such a slowdown? Osmolytes accumulated by *E. coli* and other species are highly conserved among various domains of life. The level of conservation led to the suggestion that these solutes are accumulated because they do not interact with macromolecules in detrimental ways. So why would accumulation of a high amount slow down the growth of *E. coli*?

3.10 Understanding the Osmolarity Problem

Based on the data I have shown in this chapter it becomes clear that current theories on osmotic stress are inadequate to explain the observed growth rate slowdown. To understand what is going on at the end, let us return to the beginning. Walter in 1924 proposed that a major cause for growth slowdown at higher osmolarity is the loss

of turgor pressure experienced by cells, and loss of turgor pressure as the cause of growth slowdown has been proposed as early as 1837. Theoretically, turgor could regulate growth by preventing expansion of the cell wall, as turgor is required for insertion of new cell wall material in plants. Rojas and colleagues showed that turgor over a short period does not affect the rate of cell wall expansion in *E. coli*. Therefore, cell wall expansion can continue regardless of osmotic pressure (*78*).

So if turgor is not the cause of growth slowdown then it could be related to energetic cost of synthesizing or importing osmolytes. However, my data indicates that osmotic stress does not place an energy burden on the cell as yield on a fixed amount of carbon is constant irrespective of media osmolarity. The absence of a yield reduction is surprising as trehalose consists of two glucose molecules and is therefore energetically expensive. Nonetheless the lost energy does not seem to result in a yield reduction. Moreover, providing osmolytes such as proline, choline, or betaine in the media, which should be much more cost-effective to accumulate compared to generating trehalose, also does not affect the yield.

I initially noted a direct correlation between the amount of OtsB induction and the % reduction in the growth rate (figure 15 plot D). I hypothesized that the extra protein expression due to osmotic stress was placing a burden on the proteome and causing a reduction in the growth rate. Data from other publications however show that the growth rate slowdown could not be explained by a proteome burden (figure 16 plot A (*47*, *73*)).

The absence of a proteome burden under osmotic stress was unexpected. Cayley and colleagues showed that cytoplasmic water content is reduced under osmotic stress and can be restored by addition of osmolytes to the media. They demonstrate a near linear relationship between cytoplasmic water and growth rate. The unaffected proteome is surprising because if the reason for reduced growth was a decrease in cytoplasmic water, I would have expected a large proportion of the proteome to be dedicated to restoring cytoplasmic water. According to the Morse equation equation (1.1) water can be restored by increasing the content of intracellular solutes. Therefore, if loss of cytoplasmic water is the cause of reduced growth all the cell can restore cytoplasmic water by continued import of osmolytes. I investigated how addition of proline, choline and betaine affect the growth rate. I found that cells supplemented with betaine or choline grow much better. Addition of betaine protected the translational elongation rate and ribosomal mass fraction. However, these cells did not synthesize trehalose which is consistent with measurements of intracellular trehalose showing that cells supplemented with betaine do not accumulate trehalose (*120*). Surely, if the problem with growth at high osmolarity was a loss of cytoplasmic water

then cells would just keep increasing osmolyte concentration until the desired level of cytoplasmic water has been restored. I show that even when trying to over-import choline or betaine using mutant over-expressing strains I was unable to change the growth rate. Inducing trehalose expression in high osmolarity media in the presence of betaine greatly reduced the growth rate appendix A.8.

E. coli shows careful regulation of osmolyte accumulation, suggesting that further accumulation of osmolytes is harmful rather than helpful. In fact it seems like the growth rate reduction is not coming from osmotic stress at all but from accumulation of osmolytes themselves. To test the impact of osmolytes in the absence of osmotic stress I used two membrane permeant solutes EG and glycerol. I show that these two molecules do not induce any osmotic stress. However, just as with osmotic stress they show a rapid decrease in their translational elongation rate as well as R/P ratio. I would therefore argue that the mechanism of growth rate slowdown is the same for loading of these membrane permeant solutes and osmotic stress. The growth rate slowdown in high osmolarity media is therefore not caused by osmotic stress at all. Instead it is caused by accumulation of osmolytes during osmotic stress.

The cell must have a good reason for osmolyte accumulation and another interesting avenue for investigation will be what happens to cells in the absence of osmolytes. Further, investigation of the MZ3 trehalose deficient strain should be conducted to discover what metabolites if any are accumulated during osmotic stress. Theoretically, then there should be a dual effect of osmotic stress on growth. First, there is a negative impact of cells not able to accumulate osmolytes. However, there is also a negative effect of the osmolytes themselves as can be seen from the decreasing growth rate with increasing osmolarity.

So to summarize there is no energy burden placed on the cell from synthesizing or importing osmolytes. The overexpression of osmotic stress genes does not place a proteome burden on the cells, and the proteome otherwise is unchanged (*47*). Cells do not face a lack of intracellular osmolytes. Finally, I demonstrate that cells presented with membrane permeant solutes show a similar reduction in growth without experiencing osmotic stress.

Based on these observations I propose that the the accumulation of osmolytes themselves are the cause for the reduced growth rate at elevated osmolarity. How could osmolytes effectuate such a growth slow down? Growth can be understood as the rate of metabolic flux, an active process combining the metabolome and proteome present inside the cell (*131*). If the rate of growth slows but the proteome is unchanged then the activity of the proteome must be slowed. Therefore, the solution to the growth

puzzle seems to be that all metabolic reactions within the cell are slowed. Meaning that the flux of substrates through the bacterial network decreases. Furthermore, it decreases approximately proportionally for all enzymatic reactions. Additionally, metabolic flux slowdown can be achieved in the absence of osmotic stress using just EG or glycerol. In the final section I propose potential solutions to how accumulation of osmolytes could result in reduced enzymatic velocity.

3.11 Potential Mechanisms for Osmolyte Induced Reduction in Growth Rate

Based on these studies we can deduce that the most likely reason for the growth slowdown is therefore related to the increasing osmolyte concentration within the cells. Ideally, we would be able to accumulate trehalose or betaine within the cell and observe their impact on growth. However, accumulation of these osmolytes at normal osmolarity also negatively impacts the metabolite pool (*89*). Due to the inability to freely change the intracellular content, studying the impact of membrane permeable solutes may be one of the most promising approaches to further study how high solute concentrations affect enzymatic activity. So the question becomes why does accumulation of high concentrations of osmolytes result in metabolic slowdown? Here I will advocate that the solution is based on inhibition of protein motion due to increased media viscosity.

High concentration of osmolytes lead to an increased viscosity of the solution. Viscosity has already been proposed to affect the rate of diffusion within the solution. As viscosity is important let us precisely define it. Viscosity is a measure of a fluid's resistance to flow. The resistance is created by a frictional force between adjacent layers of fluid. This can be defined mathematically as:

$$\tau = \eta \times \left(\frac{\partial v}{\partial y}\right). \tag{3.4}$$

Here η is the dynamic viscosity of the fluid, τ is the shear stress experienced by the fluid, in relation to the velocity gradient in a fluid, the shear rate is ∂v referring to the change in velocity with respect to change ∂y in distance between adjacent layers of moving liquid. More simply viscosity can be imagined as the resistance of a liquid to displacement, which can be conceptualized by dropping a sphere into a liquid. In viscous liquids the velocity of the ball will be slowed rapidly and can be calculated as follows:

$$\eta = \frac{2ga^2\Delta\rho}{9v}. \tag{3.5}$$

Here $\Delta\rho$ is the density difference between the sphere and the fluid, a is the radius of the sphere, g is the acceleration due to gravity and v is the velocity of the sphere. The velocity of a particle in a fluid will be reduced with increasing viscosity. Accurate determination of viscosity in gases can be done using elementary kinetic theory (*132*). However, estimating viscosity of complex liquids is complicated and empirical determination is the most accurate way to measure viscosity (*133*).

High viscosity will impact diffusion and can be understood via the Stokes Einstein equation equation (3.6), where the diffusion coefficient D of a sphere in a solution is related to the Boltzmann constant k_B, the temperature T, the dynamic viscosity of the media η and the radius of the sphere

$$D = \frac{k_B T}{6\pi\eta r}. \tag{3.6}$$

A slowdown in diffusion has already been proposed as the source of the growth rate slowdown (*1*). However, reduced diffusion alone cannot explain the growth rate slowdown as it would selectively inhibit rates of enzymes that use large substrates. Leading to a selective inhibition of enzymes using large substrates resulting in proteome reallocation. Instead what is observed is a global slowdown in metabolic activity. While, change in diffusion is insufficient to understand growth slowdown at high osmolarity it gives us an important insight into the change in intracellular viscosity.

Kramers' seminal 1940 paper explores the importance of viscosity in the context of chemical reactions (*134*). Transition state theory (TST) at that time had been the dominant way of understanding how any chemical reaction occurs. It posits that for a reaction to occur the products must come together simultaneously. If these molecules collide at the correct orientation with sufficient energy to overcome the activation energy barrier they will form an activated high energy complex. The activated complex can then either proceed to products or revert back to substrates. Arrhenius showed that the rate constant k is dependent on the pre-exponential factor A which includes information on the orientation and frequency of collision. Whether the reaction occurs after collision depends on the required activation energy of the reaction E_a as well as the gas constant R and temperature T equation (3.7)

$$k = A \cdot exp^{-E_a/RT}. \tag{3.7}$$

The pre-exponential factor can be derived either experimentally or numerically for gases using TST(*135*). However, TST is best suited for calculations of molecules in gaseous phase, as number, angle and energy of collisions can be calculated from knowing, Gibbs free energy, enthalpy and entropy. However, these calculations are not well suited for estimating reaction rates in liquid as Brownian motion plays a major role in particle motion. Kramers instead used the Langevin equation to predict the impact of Brownian motion on reaction kinetics in solution (*134*).

So how does Kramers' rate theory impact metabolic rate? Reactions in living organisms are accelerated by enzymes. Enzymes are 10^6 times more efficient than corresponding synthetic catalysts (*136*). Enzymes achieve this amazing feat by lowering the activation energy required for a reaction to proceed. However, as pointed out by Kramers the viscosity of the surrounding media negatively impacts the reaction rate. As enzymes catalyse reactions they are impacted by the viscosity of the media (*137*). However, the slowdown of the enzymatic reaction is not due to substrate diffusion itself. Instead, viscosity negatively impacts the ability of enzymes to catalyse reactions. Enzymes do not exist as rigid structures but occupy a large number of conformational substates (*138*, *139*).

The energy landscape of a protein can therefore be imagined as a series of valleys and mountains. The valleys in an energy landscape diagram represent stable conformational substates and the mountains the energy barriers required for converting between the substates. Enzymes naturally interconvert between conformational substates due to random interactions with the solution pushing an enzyme over the energy barrier required for change into another conformation. As the temperature of the solution is reduced it will trap enzymes in a given substate (*140*). Studies on the enzyme folding process itself have shown that the folding rate varies with viscosity of the solution (*141*). Therefore viscosity affects not just the diffusion of substrates within the media but also the rate of conformational change of enzymes. Kramers' calculations can be used to infer that an increase in viscosity will oppose the ability to switch between conformational substates. An increase in viscosity therefore negatively affects the rate of conformational change required for catalysis of a reaction.

Ansari and colleagues provide experimental data showing that Kramers' theory can explain the effect of solvent viscosity on unimolecular rate processes. They calculate that for a reaction to proceed the rate is inversely proportional to the friction encountered by an enzyme during catalysis. The friction proteins experience is a direct result of the viscosity of the media. In their model proteins experience two types of friction. First the protein atoms in contact with the solution experience friction slowing the motion of the protein surface. Furthermore, proteins experience internal friction

which slows the motion of protein atoms relative to each other. Under the assumption that friction is additive, Kramers' equation for the rate constant in the high-friction limit experienced by proteins becomes:

$$k = \frac{B}{\alpha\xi_P + (1-\alpha)\xi_S} \exp^{-E_0/RT} \tag{3.8}$$

Here R is the gas constant, T is the temperature, E_0 is the average height of the potential energy barrier separating the two protein conformations. They introduce the parameter B as a viscosity and temperature independent parameter dependent on the shape of the protein surface. The xi_P represents the friction constant for motion inside the protein and xi_S is the friction constant for motion in the solvent and is proportional to viscosity. As the relative frictional contribution from the protein and solvent differ α estimates the relevant contribution of the protein atoms and solvent. Various measurements of cytoplasmic viscosity have been done and vary from 1.1-3.6 cP, with *E. coli* cytoplasm thought to be around 2.82 cP. The intracellular viscosity is therefore in the region where solvent viscosity would become important for determining rate reactions. They support their calculations with experiments using Nano second lasers to measure conformational change within myoglobin and observe a slowdown in conformational change with increasing viscosity as predicted by their theory. The slowdown in conformational change results in slowed reaction kinetics (*142*).

The effect of viscosity is further explored showing that as solution viscosity increases the rate at which proteins fold and unfold changes (*143*). The folding and unfolding kinetics of the cold shock protein CspB were studied. The unfolding and refolding rate of the protein were both affected by solvent viscosity as described by:

$$k = \tau_{sx}^{-1} \exp^{-\Delta U/RT} \tag{3.9}$$

Here the rate constant k denotes the reaction of substrates (s) into products via the intermediate complex x, where τ_{sx} is the time constant of the reaction in the absence of an energy barrier. ΔU is the energy barrier or activation energy required for the reaction to proceed and RT are the gas constant and temperature. As solute viscosity increased so did τ_{sx}. The rate of enzyme activity seems to be directly tied to the ability of enzymes to sample through conformational substates (*139*, *140*). As viscosity slows the rate at which enzymes change conformation it is natural to expect a slowdown in reaction rates at increased viscosity. Puchkov points out that the time constant τ_{sx} in solution directly corresponds to the friction coefficient suggesting that as viscosity increases so does time for a reaction to proceed (*144*).

So, there is now a clear link between solvent viscosity and enzymatic activity explained by the increase in friction experienced by enzymes *in-vitro*. Furthermore, there is various indirect data that media viscosity can have a significant impact on enzyme activity *in-vivo*. Data studying the impact of organic osmolyte accumulation in renal kidney cells shows accumulation changes viscosity sufficiently to impact enzyme activity (*145*). Demenchenko and colleagues investigated the impact of solution viscosity on reaction rates of lactate dehydrogenase and found that as fluid viscosity increases the maximal enzyme velocity decreases. Furthermore, the decrease in activity cannot be explained by decrease in diffusion within the solution as the substrate is in excess (*146*).

H^+-ATPase from *Kluyveromyces lactis* and lactate dehydrogenase from rabbit muscle also show linear correlation between maximum enzyme velocity and the viscosity of external media (*147*, *148*). Addition of 2.5 M glycine betaine also resulted in a large decrease of oxaloacetate and isocitrate activity *in-vitro* in *E. coli*, the same enzymes in a halophilic bacterium *Schmidingerothrix salinarum*, are more resilient to high concentration of glycine betaine (*149*). Suggesting that enzymes can be adapted to be more efficient in media containing high amounts of compatible solutes.

Therefore, the relationship between the viscosity and the reaction rate must be enzyme dependent as the amount of friction experienced in the solution is unique for each enzyme. To account for the unique friction of each enzyme an enzyme specific parameter can be introduced as proposed by Sitnitsky (*150*). Further studies looked at how a variety of different enzymes respond to viscosity, a test of five different glycolytic enzymes in yeast was done and that there is indeed a varied response in enzyme activity compared to the viscosity of the solution *in-vitro*. glyceraldehyde-3-phosphate dehydrogenase (GAPDH), hexokinase and, glucose 6-phosphate dehydrogenase (G6PDH) showed a decrease in activity with increasing trehalose concentration. Aldolase and phosphoglycerate kinase (PGK) on the other hand showed no correlation between viscosity and enzymatic activity (*151*).

Based on these assumptions I conclude that a global metabolic slowdown could potentially be explained by the effect of viscosity on enzyme activity. As proteins in cells are surrounded by water, it is not surprising that the water dynamics of the protein hydration shell also affect the enzymatic activity. Trehalose seems to be preferentially excluded from the protein hydration shell allowing the proteins to stay hydrated but resulting in dynamic coupling between trehalose and the hydration shell (*152*).

To demonstrate that the growth rate at high osmolarity is slowed by change in solute viscosity I noted that the Monod equation has the same form as the Michaelis-Menten

equation. Therefore, I was curious as to whether growth rate in response to increasing osmolarity would show the same behaviour as *in-vitro* enzyme modelling in response to increase in solute viscosity. Monod showed a hyperbolic relationship between the growth rate of *E. coli* and the concentration of glucose (*31*). The relationship can be explained by the bacterial growth laws (*111*). As glucose concentration drops cells must devote more of the proteome to increasing carbon flux placing a burden on the proteome. Here, I systematically varied the glucose levels in the growth media within the range of 0.1 to 20 mM, while concurrently changing the osmolarity using NaCl. I compare the growth rate to the changes in *in-vitro* enzyme activity observed when varying trehalose concentrations.

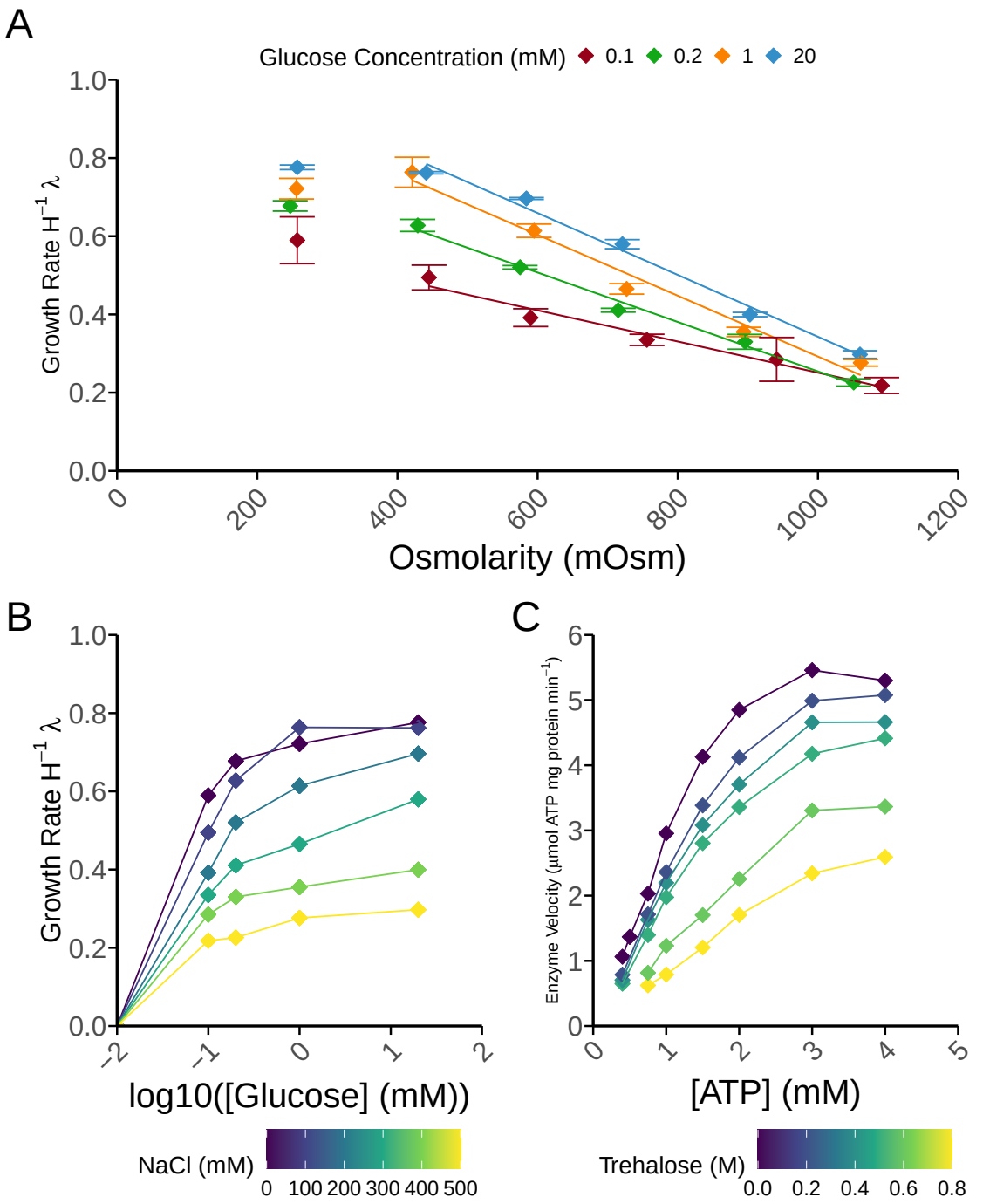

Figure 23: Cells grown in M63 minimal media while changing the concentration of glucose. **A)** Convergence of growth rate at higher osmolarities irrespective of starting growth rate. **B)** Michaelis-Menten dynamics of cells grown with varying glucose concentrations. **C)** Michaelis-Menten dynamics of H^+-ATPase from *Kluyveromyces lactis*, with varying trehalose concentrations (*147*).

I observe a growth rate convergence occurring as predicted (figure 23). Strikingly, the growth rate of *E. coli* behaves similar to the enzyme velocity plot generated by Sampedro (*147*), using increasing trehalose concentrations. These data provide ini-

tial evidence that the growth rate slowdown at higher osmolarities could be mediated by increased cytoplasmic viscosity. However, one of the challenges during this experiment was reducing glucose to lower than 0.1 mM to obtain data for lower values of λ. However, measuring OD_{600} changes accurately becomes technically challenging as the cells deplete glucose nearly instantly. An alternative approach to solve the problem of short growth would be to use a carbon source that displays less efficient Michaelis-Menten kinetics such as mannose.

However, another way to verify whether viscosity potentially affects enzymatic activity is to look at the effect of temperature. Reaction rates vary with temperature, and under heat stress yeast as well as *E. coli* accumulate trehalose, potentially due to its protein stabilizing effects. However, if trehalose removal after a heat shock is inhibited by knocking out all functional trehalases then yeast cells show worse survival after temperature is restored to normal (*153*). Furthermore, data from Sampedro indicate that viscosity causes a relative decrease in enzyme efficiency regardless of the temperature. Therefore, even when the initial catalytic efficiency is low enzymes continue to function at high viscosity.

I therefore wanted to see if varying both temperature and viscosity could explain the growth rate decrease observed in *E. coli* when osmolarity and growth temperature were varied. Here I compared enzyme efficiency measurements from the H^+-ATPase of *Kluyveromyces lactis* showing that change in enzymatic activity due to changes in viscosity and temperature closely mirrors the changes observed in growth of *E. coli*. Enzyme data was taken from Sampedro et al (*147*) and growth data for *E. coli* was obtained from Medvedova et al. (*154*).

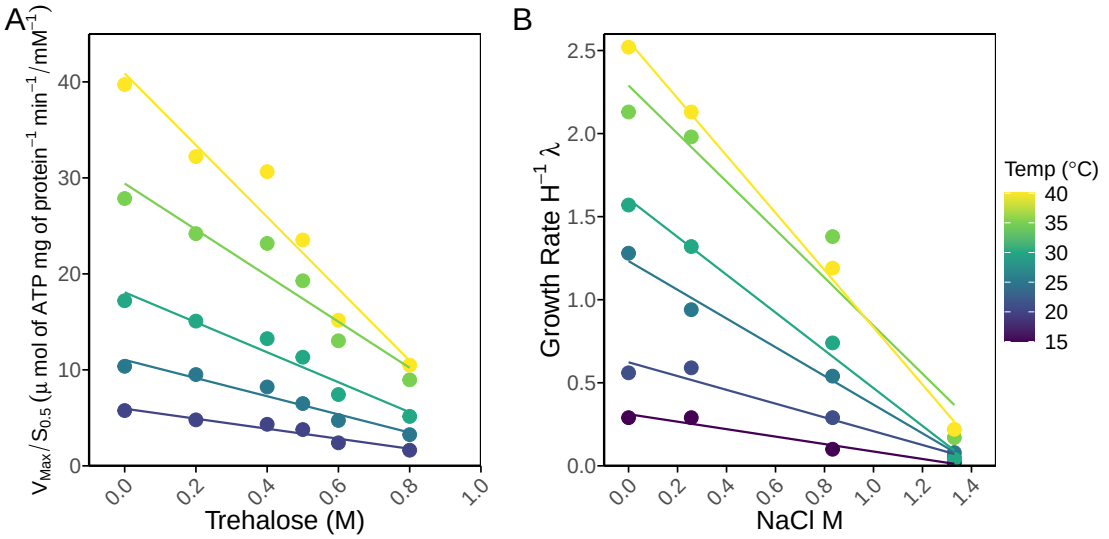

Figure 24: Interestingly changing osmolarity and temperature affects growth in the same way as changing viscosity and temperature affects enzyme efficiency. Data on the H^+-ATPase from *Kluyveromyces lactis* is compared to the growth rate of an *E. coli* strain isolated from foodstuffs. **A)** maximal enzyme activity V_{Max} divided by the substrate concentration at which velocity is 0.5 $\times$ V_{Max}. Showing how a change in temperature is affecting the rate of the enzyme. **B)** Growth rate of *E. coli* showing a very similar behaviour as would be expected from viscosity induced metabolic inhibition.

Sampedro demonstrated that for temperatures between 20 and 35 ℃, there is a linear correlation between change in V_{Max} and change in η (*147*). They show that varying viscosity and temperature results in a linear decrease in catalytic efficiency as described by $V_{Max}/S_{[0.5]}$ as observed (figure 24 A). The growth rate of *E. coli* closely mimics the reduction in enzyme catalytic efficiency. The decrease in catalytic activity raises the interesting possibility that the enzymatic reaction rate and the resulting bacterial growth rate is a function controlled by temperature and viscosity of the cytoplasm. These data therefore provide strong support for the fact that osmotic stress functions through modulation of media viscosity.

So to summarize, reduction of the growth rate is not due to an energy burden placed on the cell at high osmolarity. It is also not due to a burden placed on the proteome. Nor can it be explained solely by a reduction in intracellular water leading to macromolecular crowding. Instead use of membrane permeant solutes leads to a very similar phenotype as observed with osmotic stress but in the complete absence of osmotic stress. Therefore, the growth slowdown is mediated by a high concentration of intracellular solutes. The high concentration of intracellular solutes is predicted to increase cytoplasmic viscosity. However, the reduction cannot be explained due to a slowdown in diffusion that disproportionately affects large metabolites such as TC.

Instead accumulation of osmolytes like trehalose seem to lead to a global reduction in metabolic activity. I therefore hypothesize that the growth rate slowdown at high osmolarities is caused not by osmotic stress but rather by an increase in cytoplasmic viscosity. The increased viscosity slows enzymatic reactions by increasing the friction between an enzyme and the solvent resulting in an increase in the activation energy.

Future efforts should now be focused on clarifying the nature of intracellular solutes. In an attempt to better understand what exactly the intracellular content is in osmotically stressed *E. coli*, I collected samples that will be analysed by quantitative mass spectrometry as described in (*89*). Furthermore, I will measure *in-vitro* enzymatic activity and determine the impact of trehalose, betaine, glycerol and EG on enzyme activity. Additionally, I am working on developing an *in-vivo* assay to determine LacZ activity in cells.

Future experiments should also aim to accurately estimate intracellular viscosity and demonstrate the relationship between viscosity and growth rate in cells osmotically stressed with and without betaine, as well as cells treated with a variety of membrane permeant solutes. Fortunately methods of intracellular viscosity measurements have been reviewed by Puchkov (*144*).

4. Utilisation of High External Osmolarity During Industrial Lactobacillus Fermentation

4.1 Introduction to Industrial Lactic Acid Bacteria Fermentation

Bacteria's potential to cause disease often receives significant attention. However, bacteria are also indispensable for human health and well being. Bacteria and other microbiological organisms have been used for millennia to produce and prevent spoilage of the food we eat. Their diverse metabolic capabilities and unique physiological characteristics allow them to convert raw materials to edible food and drink. Use of bacteria can range from fermentation of dairy products and beverages to ripening of cheeses and their use in probiotic products such as Kefir and Kombucha. The value of probiotics in maintaining human health has recently gained prominence (*155*), showing that bacteria not only transform food but are also essential for preventing disease. They are central to transform various raw materials into safe, nutritious and delicious food. Probiotics can prevent spoilage by inhibiting growth of otherwise disease causing bacteria, by consuming the growth substrate and making the environment inhospitable for other microbes. Many of the foods we now associate with specific cultures were made possible by microbes. German Sauerkraut, Korean Kim Chi and Japanese Miso are just a few of the many examples that show how inextricable food produced by a culture is from bacteria. Bacteria that were passed down through generations long before the first microscopes were invented.

Our modern world with industrial scale food production requires an industrial scale of bacterial production. However, scaling the production of bacteria is non-trivial. I will focus here specifically on challenges faced for industrial scale fermentation of Lactic Acid Bacteria (LAB). I will then assess ways in which understanding of osmotic stress

could benefit industrial LAB production.

The first step in developing a new industrial process for bacteria production is identifying potentially useful bacteria, they must then be isolated from their environments and assessed for safety, culturability, and ability to perform desired metabolic function. Next a process needs to be developed for growing the bacteria that is cost effective, robust, reproducible and allows for the bacteria to be isolated at the end of culture, stored and transported to the location where they will be used. Once the process is developed it needs to be scaled up from the litre volume to industrial size using reactors capable of producing thousands of litres of bacteria.

Various media compositions were developed to enable rapid growth of LAB for industrial culture. The media now widely used for LAB culture is MRS containing a variety of protein digests as well as a carbon source like glucose. MRS has proven very successful showing very fast growth and allowing the majority of LAB to grow. Furthermore, it can be made more selective for LAB by lowering the pH to 5.4 preventing unwanted bacterial growth (*156*). However, due to the cost associated with MRS, the media used by Chr. Hansen is a MRS like media made from industrial raw components.

Scaling the process from a small reactor containing less than 10 litres to industrial scale fermentors often encompassing thousands of litres is a very challenging process (*157*). While small lab scale production rely on batches of high quality ingredients, large scale production requires sourcing, processing and sterilizing of huge quantities of raw material. Large scale production can lead to sub-optimal growth as the composition of compounds in the media can vary based on the raw ingredients. Another major issue is fermentor mixing. Small fermentors can easily mix and distribute substances added into the fermentor. However, as the scale increases so does the mixing time. Increased mixing time can lead to gradients in nutrients, pH, temperature and osmolarity that can negatively affect fermentation. Shear stress also needs to be considered when balancing time required for mixing as mixing too fast in larger reactors can cause huge amounts of shear stress. Another important consideration is hydrostatic pressure experienced by cells near the bottom of the reactor, with potentially thousands of litres weighing down on cells at the bottom. So industrial scale fermentation can create various stresses that bacteria experience.

Here I want to focus specifically on osmotic stress that cells experience during industrial scale fermentation. In collaboration with my industrial partner Chr. Hansen, I investigated the impact of osmolarity in *L. animalis* on growth and storage survival. *L. animalis* is a probiotic LAB that may improve animal health by preventing disease.

Supplementing feedstock with *L. animalis* has been shown to reduce the burden of *Salmonella enterica* in Bovine lymph nodes (158). Furthermore it improves the health outcomes of pigs challenged with *S. enterica* (159). Use of probiotics over antibiotics for disease prevention is strongly preferred as it can stop the emergence of antibiotic resistance, and leads to healthier animals. The negative effects of preventative antibiotic supplementation led to the ban of the practice in the EU (160). Therefore, discovery and production of probiotics that can be used to supplement animal feedstock, and help maintain animal health, is desired.

This chapter will focus on two ways in which osmolarity could affect the production and storage of LAB using *L. animalis* as an example. First I will investigate how osmolarity changes during pilot scale production and assess whether osmotic changes negatively impact growth. Next I will determine what osmotic changes bacteria undergo after production which includes centrifugation, preparation for freeze drying and finally lyophilization the most extreme osmotic change during which bacteria are dehydrated.

4.2 Osmotic Stress During Lactic Acid Bacterial Culture

Fermentation of *L. animalis* consists of three steps. First frozen stock is inoculated into culture media. The culture is grown overnight to create the pre-inoculation media. The pre-inoculation media is then added to the main fermentation reactor at a ratio of 1:100. I worked at a pilot scale level looking at growth in a 35 litre reactor. Cells were grown at 37 ℃ under anaerobic conditions. Samples were collected every 30 minutes to measure the following parameters

1. HPLC measuring glucose consumption and lactic acid excretion.
2. Fluorescence Assisted Cell Sorting (FACS) measuring cell number.
3. Microscopy to measure cell size.
4. Osmolarity to determine osmotic changes.
5. OD_{600} measurements to determine growth rate and total yield.

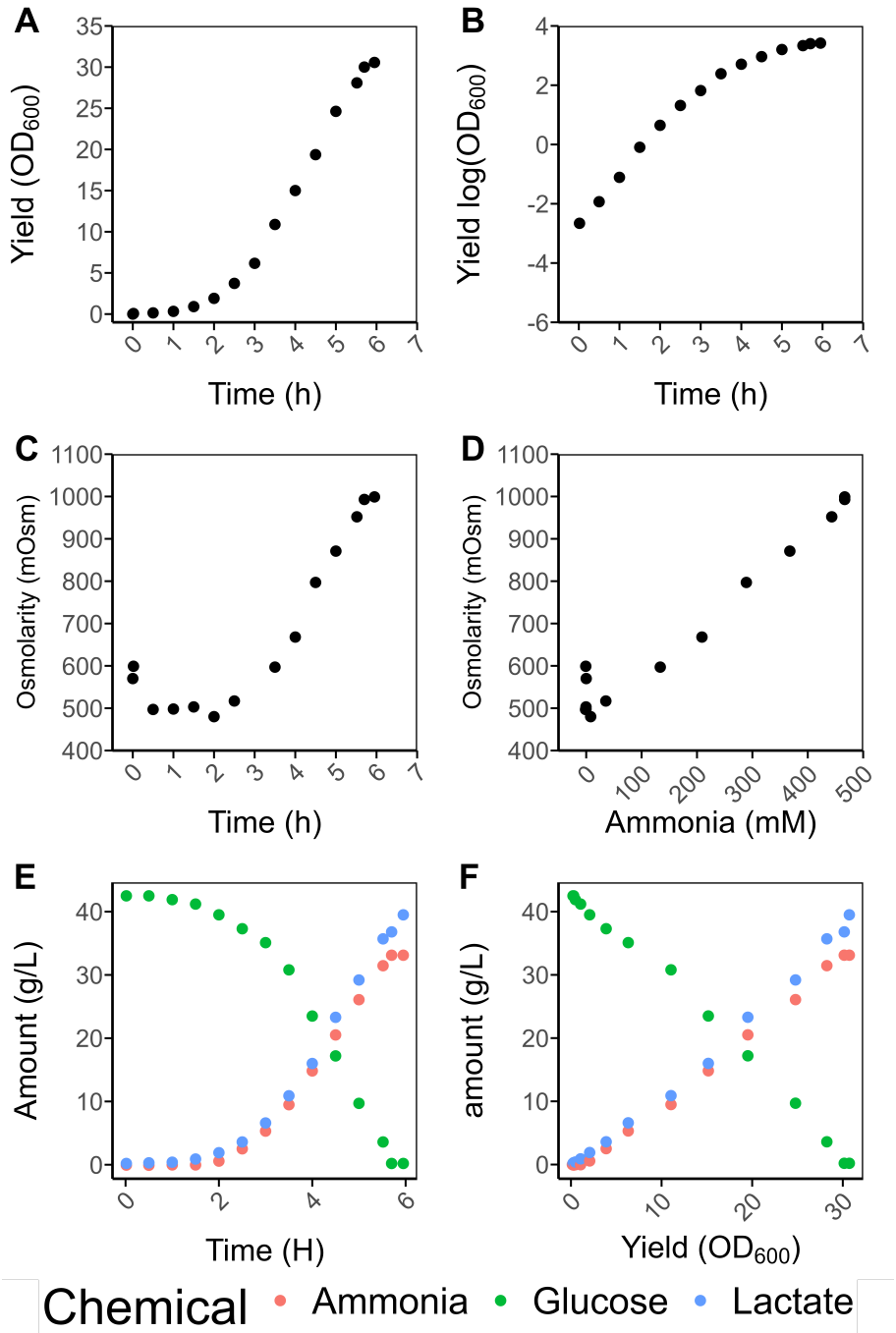

Figure 25: Measurement of growth and osmolarity changes during fermentation of *L. animalis*. **A, B)** Change in measured OD_{600} and ln(OD_{600}) over the course of fermentation. **C)** Change in osmolarity during growth. **D)** Change in osmolarity compared to ammonia addition. **E)** Concentration of ammonia, lactate, and glucose in the media by time. **F)** Concentration of ammonia, lactate, and glucose in the media relative to OD_{600}.

First looking at the change in OD_{600} we can determine that cells grow rapidly and show exponential type growth for the first two hours of the fermentation. However, it is unclear whether growth observed here is true exponential growth as the dilution

was only 10^{-2} and higher dilution could potentially lead to a better exponential curve. LAB rapidly acidify their media due to excretion of lactic acid and acidification is also observed during growth of *L. animalis* figure S15. To allow for continuous growth and prevent growth arrest at low pH, the media pH is kept constant at 5.4 by addition of ammonia to the media, resulting in the reaction of lactic acid with ammonia to produce ammonium lactate.

$$C_3H_6O_3 + NH_3 \rightarrow C_3H_9NO_3$$

As expected *L. animalis* grew well in complex media, achieving a growth rate of 1.7 h^{-1} and a doubling time of 24 minutes. The osmolarity of growth media increases in direct proportion to the amount of ammonia added. There is an unexpected initial decrease in media osmolarity as the pre-inoculation media is added from around 600 to 500 mOsm. The drop in media osmolarity is unexpected as it suggests that cells absorb nearly 100 mM of solutes when added to the fermentation media. It is impossible that cells would absorb such a high concentration of solutes. It also cannot be explained by the pre-innoculation media having a lower osmolarity as such a drop would necessitate an addition of around 6 L of water to the reactor but only 350 ml of media was added. Therefore the most likely explanation is an error in sample collection rather than a genuine experimental observation. As growth progresses the fermentation reaction hits pH 5.4 and ammonia addition starts. There is a clear relationship between glucose consumed which leads to production of lactic acid and results in addition of ammonia (figure 25 D). The osmolarity changes from 500 to 1000 mOsm corresponding to a 500 mM addition of ammonia. Furthermore we show that there is a correlation between glucose consumption, lactate production and ammonia addition with OD_{600} (figure 25 E and F). I was also interested in understanding how cell size changed during the course of the experiment, as osmolarity can affect cell size (*85*).

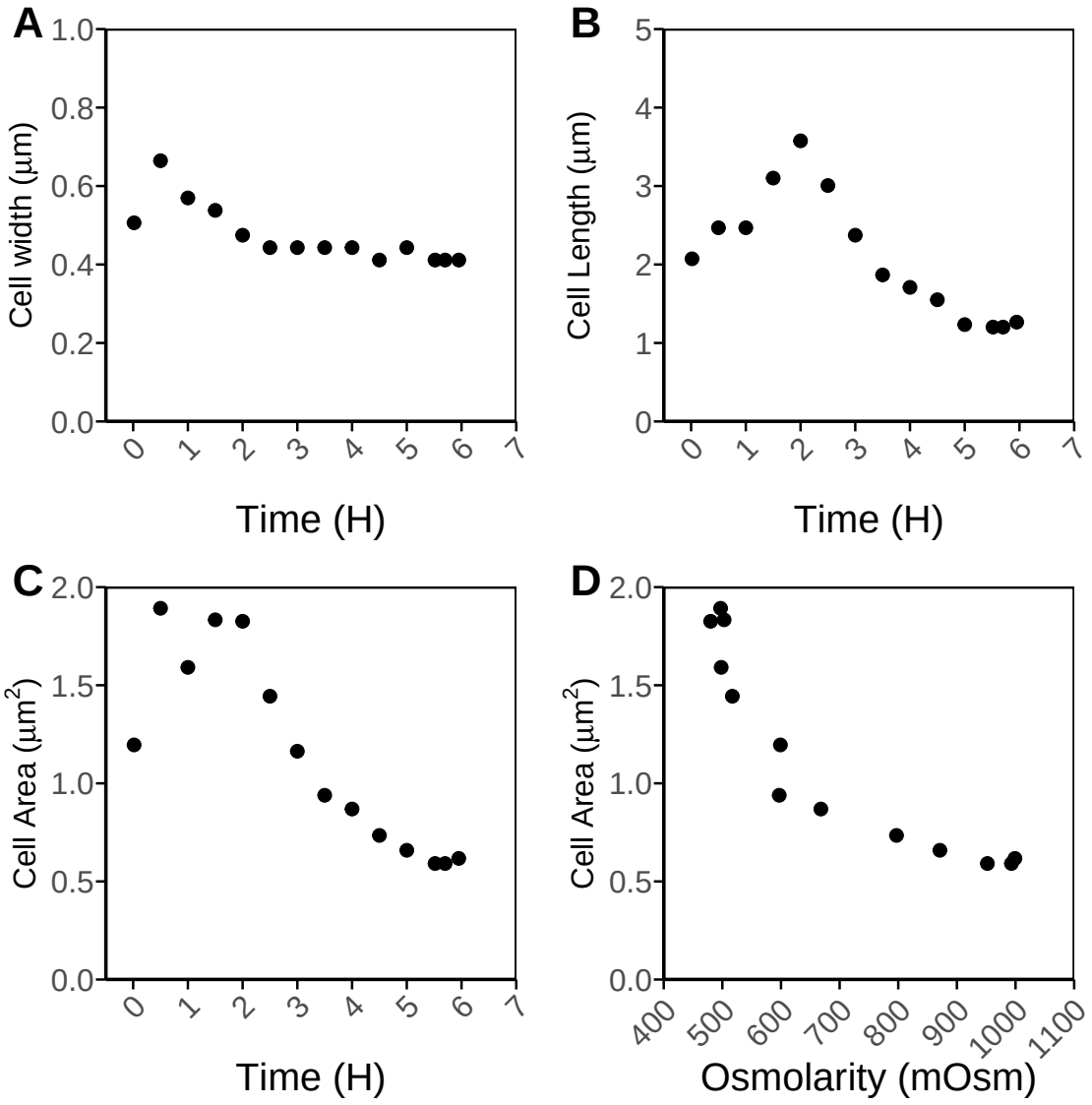

Figure 26: Measurement of cell size changes during fermentation of *L. animalis*. **A)** Change in cell width during fermentation. **B)** Change in cell length during fermentation. **A)** Change in cell area during fermentation. **A)** Change in cell area compared to change in osmolarity of the growth media.

Cell size initially increase from about 2 µm to a maximum length of 4 µm. Width increases slightly from 0.5 µm to 0.7 µm (figure 26). The maximum cell area is reached after about 2 hours of culture, and is consistent with observation of exponential growth at this time. Ammonia addition starts due to acidification of the media at about the 2 hour time point figure S15, and cell length starts decreasing again at this time. There appears to be a relationship between cell area and osmolarity. However, it is hard to disentangle the impact of growth rate and osmolarity on cell area. As soon as ammonia addition starts cells are no longer in exponential phase and therefore cell size could be related to change in growth rate. As the change in osmolarity is gradual it seems unlikely that cells are experiencing an osmotic shock causing the shrinking,

making the change in growth rate the most likely cause of the reduced growth (*161*).

I therefore wanted to understand how osmotic stress affects growth in *L. animalis* grown in complex media. To test the susceptibility of *L. animalis* to osmolarity I scaled down the fermentation reaction to allow for higher throughput. I used custom built 15ml bioreactors. These reactors allow for much faster experimental execution but lacked pH control. Therefore, media osmolarity would not change during culture. Instead cells would acidify media and then arrest growth. To better understand the impact of osmolarity on growth and yield I supplemented the media with 750 mM NaCl directly. Supplementation with NaCl has the advantage of telling me how cells respond to osmolarity during exponential growth rather than changing osmolarity gradually during fermentation. However, lactic acid is now no longer neutralised and will rapidly acidify the media influencing measurements.

Addition of 750 mM NaCl to the media causes a reduction in the growth rate from about 2.0 h^{-1} to 1.35 h^{-1} figure S16. Therefore just like *E. coli* the cells were susceptible to changes in osmolarity. One of my findings was that growth rate reduction in *E. coli* was dependent on the type of osmolyte present in the media. I was therefore curious whether addition of osmolytes would be beneficial to the growth at high osmolarity. I reviewed literature for compounds that have been identified as osmoprotectants in LAB. The review included common osmolytes such as betaine and choline and some that are not osmolytes in *E. coli* such as dimethylsulfonioacetate (DMSA) and Dimethylsulfoniopropionate (DMSP).

Compound	Shown as an osmoprotectant in any bacteria	Shown as an osmoprotectant in lactic acid bacteria	Cost rating (GBP / g)
Trehalose	*E.coli* (162, 163)	*B. thuringiensis* (164)	2.02
Glycine Betaine	*E. coli* (61, 120, 165), *Listeria monocytogenes* (166)		0.07
Proline	*E. coli* (61, 120)	*P. pentosaceus*	0.81
Ectoine / dihydroxyectoine	*Virgibacillus pantothenticus* (167)	*E. coli* (168)	10.70
Sucrose	*Sinorhizobium meliloti* (169)		0.10
Na-glutamate	*E. coli*(61, 67)	*Lactobacillus bulgaricus* (170)	0.0074
Carnitine	*Listeria monocytogenes* (171), *E. coli* (172)		10.80
Choline	*E. coli*, *Bacillus subtilis* (172)		5.61
Pipecolate		*L. lactis* (173)	2.10
DMSA	*Bacillus subtilis* (172)	*Pediococcus pentosaceus* (174)	10.65
DMSP	*Bacillus subtilis* (172)	*Pediococcus pentosaceus* (174)	520

Table 2: Compounds Shown as an osmoprotectant in any bacteria and lactic acid bacteria, with cost rating (GBP / g)

I then tested whether any of the aformentioned osmolytes could restore growth at high osmolarity in complex media. Media osmolarity was adjusted by addition of 5 M NaCl to a final concentration of 750 mM. 1.5 µl of frozen bacterial stock was added to each 15 ml reactor tube. Osmolytes were prepared as a 1 M stock in water and 10 mM of each osmolyte was added where indicated. Cells were grown overnight at 37 ℃. Growth rates were determined by estimating the region of linear growth looking at the $ln(OD_{600})$ vs time plot and fitting a linear regression through that linear region.

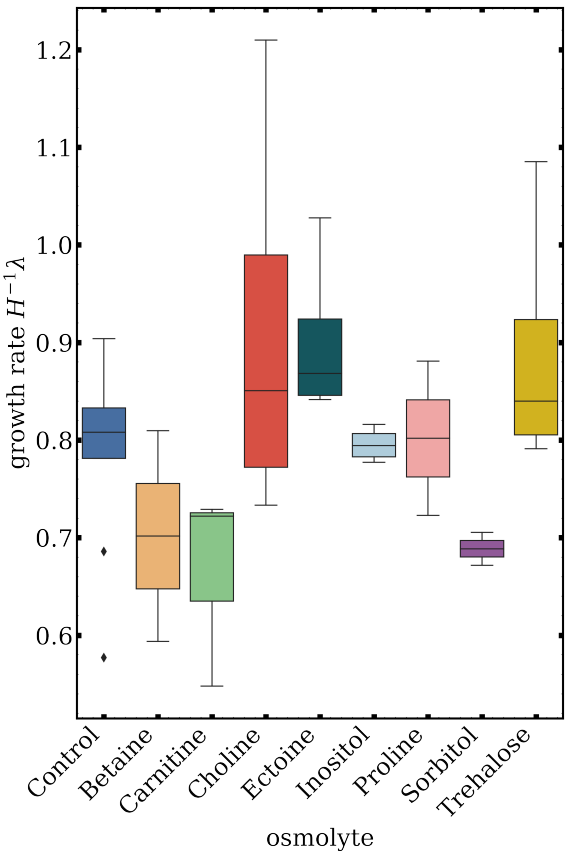

Figure 27: *L. animalis* was grown in complex media supplemented with 750 mM NaCl. 10 mM of each osmolyte was added to the media and growth rate determined.

Choline, Ectoine and Trehalose showed small improvements in their growth rate compared to the control condition (figure 27). Most other compounds had no effect or resulted in decreased growth. I selected Betaine, Choline and Ectoine for follow up as both Choline and Ectoine showed potential improvements. I also continued using betaine in my investigation as choline is converted to betaine in *E. coli*, as well as some LAB (*175*). However, none of the osmolytes showed huge improvements in growth rate. The absence of a protective effect is consistent with findings that osmolytes like betaine are already present in rich media (*123*, *176*, *177*). Therefore, further supplementation of the growth media with osmolytes seems to make little difference as was found with *E. coli* and LB (*120*).

There is no noticeable effect on the growth rate of *L. animalis* at high osmolarity when osmolytes are supplemented.However, while not noticeably changing the growth at low OD_{600} readings cells are grown to very high OD_{600} during industrial fermentation. Therefore, osmolytes may be depleted during fermentation. Furthermore, as previously discussed, importing or synthesizing osmolytes may place an energy burden on cells and therefore reduce yield. I therefore, wanted to better understand how osmolyte supplementation could affect the yield of *L. animalis*. Furthermore, it is noted that osmolytes may be protective during the freeze-drying process (*178*). As bacteria undergo freeze-drying the number of viable bacteria is greatly reduced. If osmolytes are beneficial in protecting cells during freeze-drying it could result in an improved efficiency as the desired end-product is viable bacteria. Therefore, my hypothesis was that growth at higher osmolarities might enhance yield. I based my hypothesis on the observation that in *E. coli*, I did not detect a reduction in yield with increasing osmolarity. Additionally, higher osmolarity implies increased osmolyte uptake, potentially aiding cells during freezing or drying processes.

4.3 Effect of Osmolyte Supplementation on Yield and Resilience to Freeze-Drying

I investigated how choline, betaine and ectoine affect the yield, viability, and lactic acid production capability of *L. animalis*. Yield is an extremely important measure for industrial bacteria production as it determines the efficiency of the fermentation reaction. Yield can be measured as the OD_{600} at the end of fermentation. However, the most important metric is not only how many cells are present at the end of fermentation but how many viable cells are present once the fermented cells have been stored. Using lyophilization to dry cells prior to shipping is cost effective as cells do not need to remain frozen. However, freeze-drying causes a large reduction in the number of viable cells once rehydrated. Based on previous studies I hypothesized that addition of osmolytes may increase viability after freeze-drying (*178*). I measured how resilient cells are to the freeze-drying process with and without osmolytes by measuring the CFU. Furthermore, the amount of lactic acid produced is correlated with total amount of glucose consumed.

Cells were grown as before with the exception that the reactor headspace of the bioreactor was filled with N_2 allowing for anaerobic growth. Yield was measured by spectrophotometer reading. Lactic acid was determined using a lactic acid kit. Finally, the number of viable bacteria after growth and lyophilization was determined using the CFU assay as described.

Briefly, cells were grown into the exponential phase, then collected by centrifugation. Cell pellets were suspended in cryo-buffer, flash frozen in liquid nitrogen and placed into freeze-dryer. Cells were dried overnight. After complete dehydration cells were removed from freeze-dryer and suspended in a peptide broth. After rehydration of the bacteria they were plated on complex media agar plates and grown anaerobically at 37 ℃ overnight. Colony counting was done using a custom trained splinedist neural network as described.

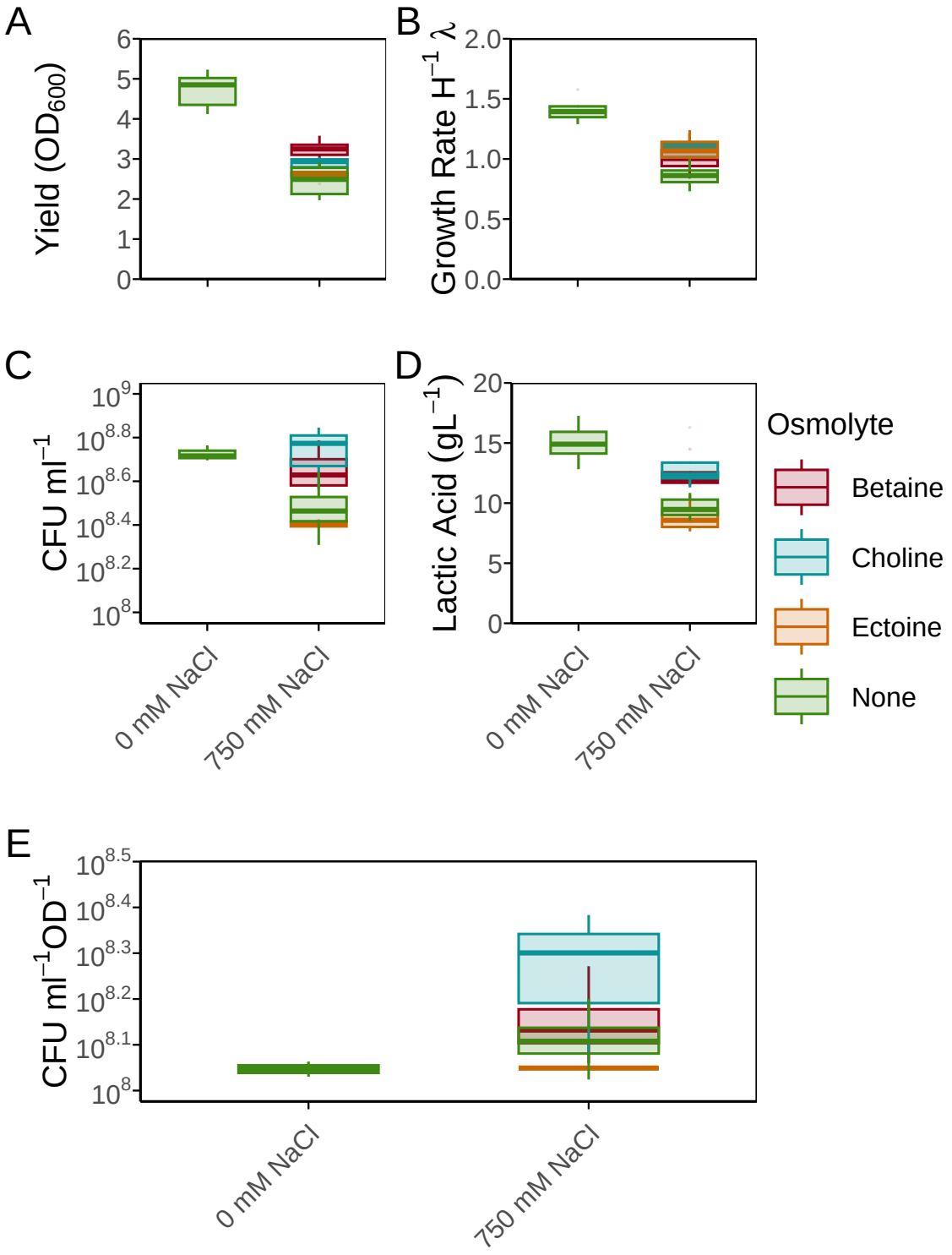

Figure 28: *L. animalis* was grown in complex media supplemented with 750 mM NaCl. 10 mM of each osmolyte was added to the media. **A)** Yield for cells grown at high osmolarity. **B)** Change in growth rate at high osmolarity. **C)** Number of CFU at high osmolarity. **D)** Amount of lactic acid produced at high osmolarity. **E)** Change in viability per unit of OD_{600} of cells.

These data indicate that osmolarity negatively affects the growth rate, lactic acid production, number of viable colonies after freeze drying and total yield as measured by OD_{600}. Addition of betaine and choline are mildly protective increasing the yield and growth rate. Surprisingly, betaine and choline greatly improved survival after freeze drying. As the number of CFU after lyophylization drop from $10^{8.7}$ to $10^{8.4}$ which is approximately 55% reduction in viability. However, cells grown with choline and betaine show improved survival after lyophilization, when betaine or choline was supplemented showing only a 37% reduction in CFU when betaine is added and a slight increase in CFU when media is supplemented with choline. When taking into account the change in yield after growth the cells showed improved survival after freeze drying (figure 28 E). Improved survival indicates that osmotic stress, specifically in the presence of betaine or choline improves viability after freeze-drying. I therefore became interested in whether accumulation of osmolytes within the cell could potentially improve resilience to freeze-drying. The data indicates that addition of choline and betaine is beneficial at protecting cells during the freeze drying process. However, an issue with the collected data is the lack of pH control, meaning that the media acidifies during growth. Therefore the nature of the protective effect conferred by betaine and choline was unclear. In the next section I will attempt to replicate the ability of osmolytes to improve survival during freeze-drying while using pH control.

4.4 Addition of Osmolytes Does Not Increase Growth or Yield During pH Controlled Batch Fermentation of *L. animalis*

Freeze-drying removes all cellular water and reversibly inactivates the bacteria to allow for room temperature storage and transport. A variety of organisms undergo complete dehydration in nature in a phenomena called anhydrobiosis, the reversible arrest of metabolic activity due to loss of cellular water. Organisms undergoing anhydrobiosis generally fill themselves with polyols such as trehalose, glycerol or sucrose (*179*). The sugars stabilize membranes and proteins in the dry state by hydrogen bonding of polar residues in the macromolecular structures. Furthermore, the sugars allow for glass formation (vitrification) and could potentially account for their stabilizing effects. Current, consensus is that both direct interaction and vitrification can contribute to the protective effect during dehydration (*180*). Notably both betaine and choline contain three methyl groups. Therefore, like polyols, betaine and choline may stabilize proteins and membranes during dehydration (*71*, *181*).

I speculated that a small increase in osmolarity may be beneficial to survival after

freeze drying, as it allows for import or synthesis of protective osmolytes. Various studies have looked at the impact of osmolytes on the survival of cells after desiccation. *Enterobacter sakazakii* accumulates high concentrations of trehalose during drying (*182*). Kets showed that salt stress can significantly improve survival after drying, which is further enhanced by betaine supplementation in various LAB cultures (*178*, *183*). Welsh found a moderate increase in survival to freeze-drying after accumulation of intracellular betaine (*184*). Meanwhile, other authors showed that freeze-dried bacteria survive better after osmotic stress (*177*). Another study found that supplementation of the cryo-buffer with betaine was as effective or more effective than bovine serum albumin and sucrose at preserving viability after freeze-drying for a wide range of prokaryotes (*185*). It is also known that trehalose is essential for the viability of *E. coli* at low temperatures (*186*).

As I also observed an increase in viability after freeze-drying, I attempted to repeat the experimental data under the fermentation conditions used for industrial production. *L. animalis* was grown in 2 l bioreactors with pH maintained at 5.4 by addition of ammonia. Cells were grown in complex media at 37 ℃ in media supplemented with NaCl and betaine, choline or ectoine.

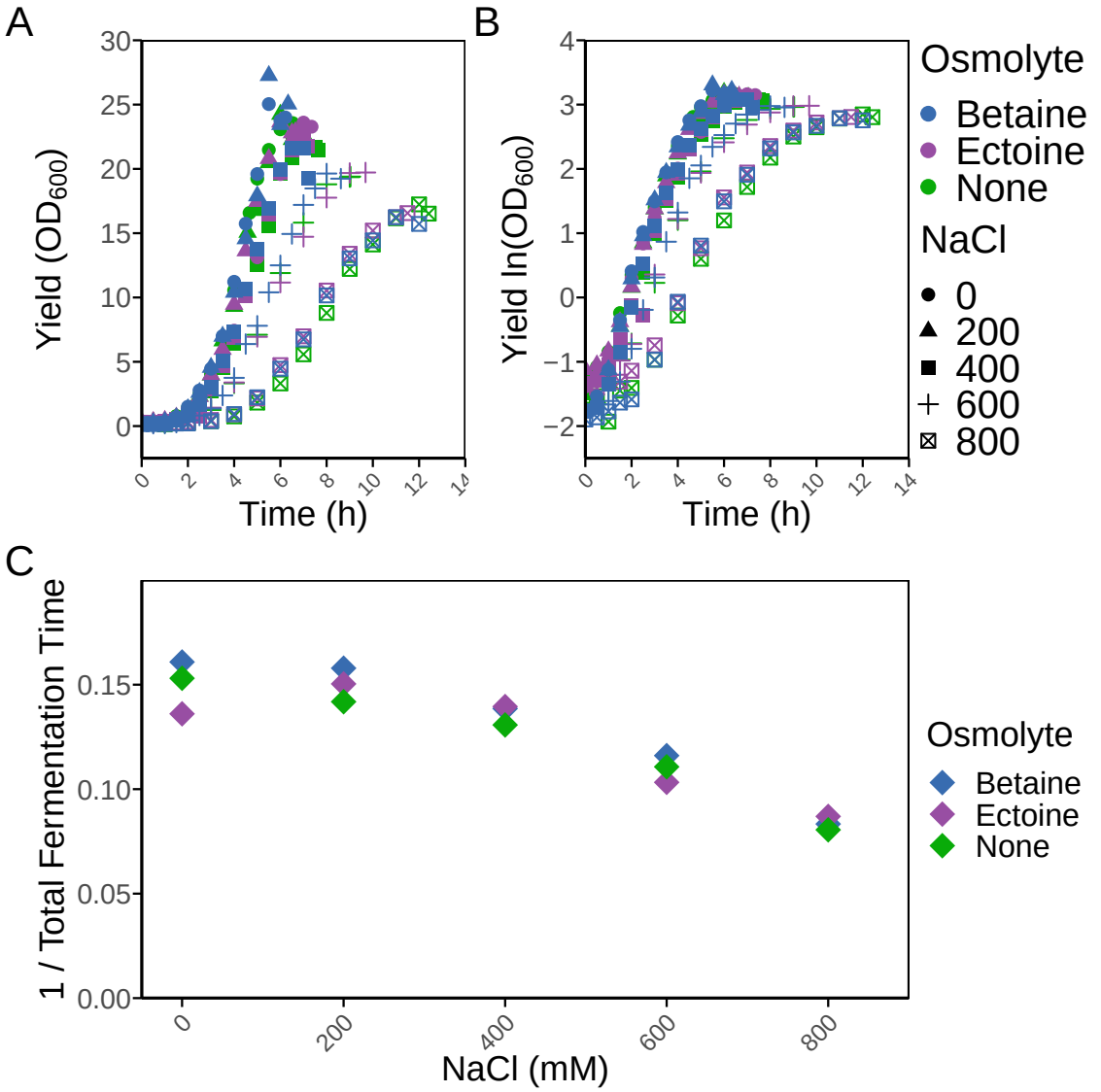

Figure 29: *L. animalis* was grown in complex media containing various NaCl concentrations. Growth curves were established by sampling OD_{600} every 30 minutes. **A)** OD_{600} measurements for various different NaCl concentration with addition of 10 mM Betaine or Choline or 1 mM Ectoine. **B)** Same data presented as the natural log of the yield. **C)** Change in 1 / fermentation time with osmolarity in the presence or absence of 10 mM Betaine of 1 mM Ectoine.

Surprisingly, under pH control addition of osmolytes had no effect on the growth of *L. animalis* at various osmolarities. Due to the infrequent sampling of every 30 minutes and short exponential phase calculating growth was not possible. Instead looking at the growth curve for cells is instructive, giving both an indication of how many cells are generated and how quick the fermentation is. The total time to complete fermentation is also a useful measure of growth as it includes both exponential growth and growth during addition of ammonia. The end of fermentation could be determined precisely, as continuous pH measurements allowed us to know when the cells consumed all the

glucose and stopped excreting lactic acid. Remarkably, the time taken to complete fermentation closely resembles the pattern observed in *E. coli* when betaine is introduced to the media. Initially, there is a flat region, indicating only minimal impact on fermentation time with the addition of 200 mM NaCl, followed by a reduction in the growth rate with increasing NaCl concentration. Addition of betaine and ectoine did not affect fermentation time. Potentially suggesting that betaine and ectoine are not taken up by *L. animalis*, however, other LAB have documented betaine transporters (*187*). Far more likely is that there is already a saturating amount of betaine present in the growth media, and there is evidence that complex media contains betaine (*176*). Overall there was a reduction in the yield with increasing osmolarity as well as an increase in total fermentation time.

4.5 Loading Cells with Osmolytes Does Not Increase Survival of *L. animalis* in Frozen-Formulated and Freeze-Dried Cells

Osmolytes and cryoprotectants share many similarities (*188*), therefore stimulating the uptake of osmolytes by increasing the osmolarity of the growth media may be a viable strategy to improving survival after freezing and freeze-drying. I investigated the effect of growth at high osmolarity on viability by measuring the CFU as well as metabolically active cells by FACS using a live/dead cell stain. Cells were prepared using three different methods. First, cells were either taken directly at the end of fermentation and frozen in the complex media (Frozen Culture). Second, Cells were concentrated by centrifugation and supernatant was removed. Cells were then formulated in cryo-buffer supplied by Chr. Hansen, and frozen by dropping into liquid nitrogen (Frozen Formulated). Finally cells were concentrated, formulated and flash frozen like in the previous experiment but then underwent a freeze drying process (Freeze-Dry Formulated). Viability was determined by CFU counting. Additionally, number of active cells was determined by FACS. Active cells refers to cells that are able to maintain their cell membrane potential. CFU and FACS assays were performed by Chr. Hansen technicians.

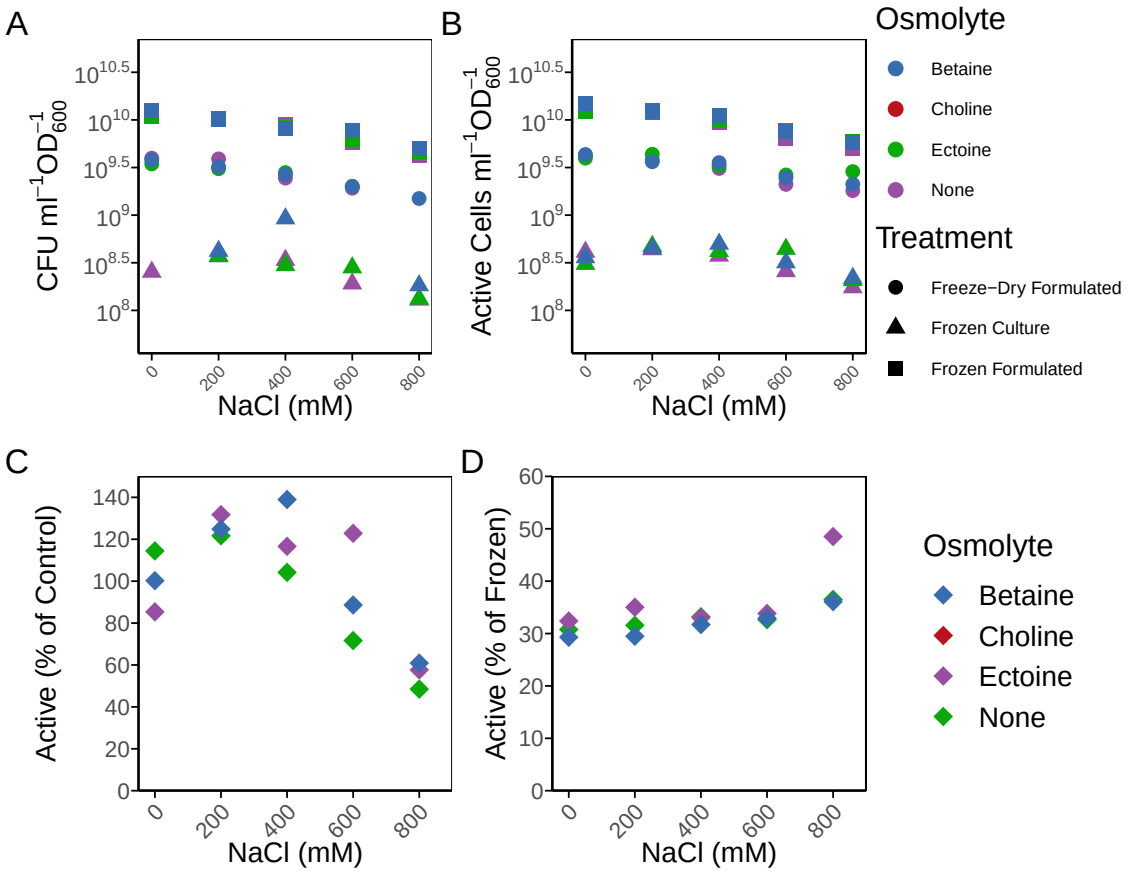

Figure 30: *L. animalis* was grown in complex media containing various NaCl concentrations. End of fermentation was determined by glucose run out. Once fermentation stopped cells were collected and processed. **A)** CFU for culture frozen directly, formulated then frozen or formulated then freeze dried. **B)** FACS determination of active cells for culture frozen directly, formulated then frozen or formulated then freeze dried. **C)** FACS comparison of number of active cells compared to the 0 NaCl condition. **D)** Comparison of active number of cells after freeze-drying.

FACS and CFU counting yielded similar results, showing that FACS is a suitable way to determine viability. Here, I show that increasing media osmolarity decreases number of viable cells in all cases even when correcting for the reduced yield as measured by OD_{600}. Therefore any protective effect that osmolyte accumulation may have on survival of freezing and freeze-drying is outweighed by a general reduction in viability with increasing osmolarity. Increasing NaCl concentration from 0 to 800 mM NaCl caused a 72% reduction in the number of viable bacteria after freezing. When correcting for the lower yield there is still a 59% reduction in viability of the frozen cells per unit OD_{600} (figure 30 A & B). There is a slight increase in viability in cells frozen directly in the growth media with an approximate 20 % increase in viability with addition of 200 mM NaCl. However, as osmolarity is increased further viability rapidly drops to around 60% when 800 mM of NaCl is added to the growth media (figure 30 C), supplementation of the media with osmolytes does not seem to have any further

protective effect. It is important to note that cells frozen directly cannot be compared easily to the frozen-formulated or freeze-dried cells as they did not go through a concentration step.

Finally, I wanted to see whether increasing osmolarity could increase survival of the freeze drying process. I compare the number of viable cells after concentration, formulation and freezing and then again after freeze-drying the frozen product, to calculate the change in viability after freeze-drying. This tells me what proportion of cells survived freeze-drying. As intracellular osmolyte concentration is correlated to size of osmotic stress I hypothesized that cells would survive freeze-drying process better if grown at high osmolarity due to high accumulation of osmolytes. There is indeed a small increase in survival of freeze-dried bacteria from about 30 to 38% at high osmolarity (figure 30 D), suggesting that accumulation of osmolytes may protect *L. animalis* during the lyophilization process. However, the modest increase in viability is not enough to offset the 72% reduction in viable cells with increasing osmolarity. Therefore, increasing growth osmolarity to stimulate uptake of osmolytes is not a viable strategy to protect cells.

A potential caveat of our study is that the osmolarity of the cryo-buffer was not adjusted to match the osmolarity of the growth media. Cells may therefore have lost some of their accumulated osmolytes due to the change in osmolarity experienced when being transferred from their growth media to the cryo-buffer. Loss of osmolytes could explain why cells frozen directly in the growth media show an initial increase in the number of viable cells. Another possible interpretation of the data is that the cryo-buffer and the internally accumulated osmolytes serve similar functions. This seems unlikely as commonly used cryoprotectants such as sucrose and trehalose do not readily have access to the intracellular space. Instead potential protective effects could be due to membrane stabilization of vitrification during dehydration (*179*, *188*).

Therefore, when grown under anaerobic conditions and pH control the impact of increased media osmolarity is a reduction in the yield as well as a reduction in viability after freezing. There is a modest improvement in survival after freeze-drying but not enough to counteract the viability loss during freezing. The question then is does increased osmolarity negatively affect growth and viability during normal culture?

Osmotic stress induced by ammonia addition is fairly small for *L. animalis* cultured in complex media, increasing from 500 to 1000 mOsm. While it may be tempting to try and extrapolate the effect on growth and viability based on the NaCl supplemented data, it is unclear whether at osmolarities ranging from 500 to 1000 mOsm would show the same type of relationship. Supplementing the media with an additional 200 mM

NaCl did not seem to have an effect on fermentation time and only led to a very small reduction in viable cells after freezing and freeze drying. The small increase in osmolarity that cells experience during fermentation from addition of ammonia figure 25, is therefore unlikely to affect growth or viability.

Increased osmolarity also negatively affects survival after freezing and freeze drying especially if cells are formulated with a cryo-buffer. Addition of osmolytes to the media does not protect growth at higher osmolarities and is therefore of no benefit when added to the media. The absence of a protective effect could be because complex media is a rich media and is naturally high in osmolytes such as betaine (*176*). In conclusion, there does not seem to be an easy way in which to increase bacterial growth or yield during normal fermentation as addition of ammonia is required to prevent pH induced growth inhibition. Ideally we would be able to maintain media osmolarity while still controlling pH, however there is no feasible way to do this without also diluting the media.

4.6 Squeezing Intracellular Water and Rapid Loading of Osmolytes to Improve Survival of the Freeze-Dry Process

Prokaryotes, especially in arid environments are well suited to anhydrobiosis (*117*). Lactic acid bacteria can also tolerate desiccation. As dehydrated bacteria are easier to store, dehydrating bacteria is highly desirable. Typically bacteria are dehydrated either by spray-drying or freeze-drying. Spray drying uses hot gas to rapidly evaporate water contained in cells. Freeze-drying on the other hand involves freezing cells first and then removing water under very low pressure using sublimation. As dried cells are metabolically inactive they do not need to be frozen which can be a major issue when trying to transport a large amount of bacteria, greatly reducing the total weight as well as cooling costs. However, as shown before freeze-drying causes a large reduction in viability with only around 30% of *L. animalis* surviving the process.

Improving survival after freeze drying is therefore an easy way to increase total number of viable cells in the final product. One of the main ways in which organisms capable of anhydrobiosis protect themselves is accumulation of osmolytes such as trehalose (*117*, *179*, *180*). Therefore, I wanted to attempt loading *L. animalis* with betaine immediately prior to freeze-drying by varying the osmolarity of the cryo-buffer in which cells are suspended. Furthermore, water content in the cell may be related to survival after freeze-drying as one of the main reasons for reduced viability after

freezing is ice water crystallisation (*189*, *190*). I proposed that subjecting cells to a large osmotic shock before freezing could be beneficial, leading to either betaine accumulation or reducing ice formation by causing water loss.

To test whether a large osmotic shock is beneficial before freeze-drying, *L. animalis* was grown anaerobically at 37 ℃ in complex media, in a miniature bioreactor. Cells were collected and 15 ml of cell culture was centrifuged at 8000 g for 5 minutes at 4 ℃. The supernatant was discarded and cells were suspended in 1 ml of water containing various sucrose or NaCl concentration and containing 10 mM of osmolyte when indicated. Cells were suspended in the mixture at room temperature for 15 minutes, then flash frozen in liquid nitrogen. Freeze-drying was done as previously described in a lablyo-mini overnight. Dried cells were rehydrated by addition of 15 ml of peptide solution and CFU counting was performed as described, to estimate viability based on osmolarity of the freezing buffer.

To gain insights into the effects of osmolarity of the cryo-buffer, I conducted measurements of cell volume to determine whether intracellular water loss was occurring using equation (1.1). The standard freeze-drying buffer had a measured osmolarity of about 1 osmole. If a major cause of the viability reduction is the formation of intracellular ice crystals it stands to reason that using an osmotic shock to ”squeeze” water out of the cell results in increased viability. I also supplemented betaine in the various solutions as a recovery in cell volume would indicate betaine uptake. If the volume recovery is linked to better survival it stands to reason that improved volume recovery is due to accumulation of betaine.

To measure the change in cell volume, cells were grown identical to the CFU study in normal complex media without pH control anaerobically at 37 ℃ overnight. Stationary phase cultures were collected and cells were attached to a tunnel slide as described in the methods section 2.7. Cells were flushed with various concentrations of sucrose or NaCl and 10 mM of betaine is added where indicated and continuous images were taken at 2 second interval for 15 minutes to mimic the conditions of the CFU analysis.

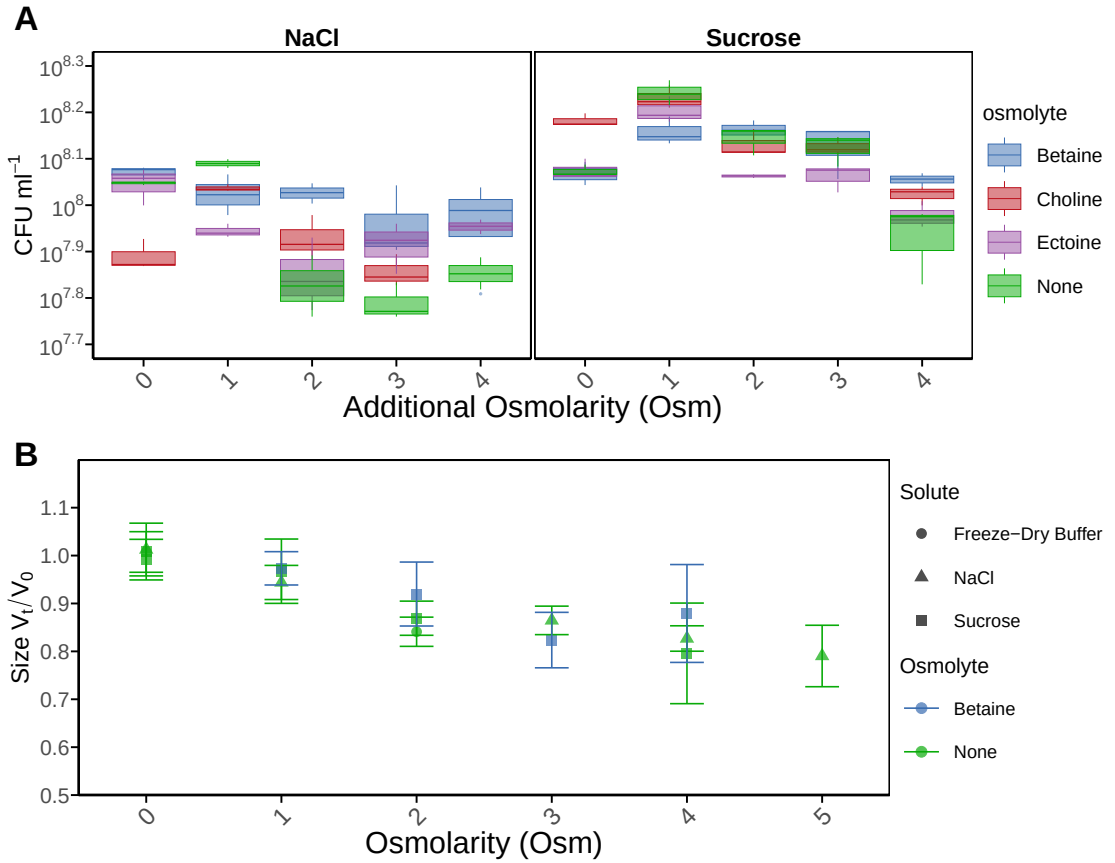

Figure 31: *L. animalis* was grown in complex media for 16 hours in a bioreactor without pH control. **A)** CFU for cells frozen at various osmolarities where osmolarity was altered with either NaCl or Sucrose. **B)** Cell size changes determined by microscopy after application of water containing various concentrations of NaCl or sucrose.

Viability of cells was identical in pure water and water containing 1 osmole of NaCl (figure 31). Increasing the osmolarity past 1 osmole reduced the number of CFU by nearly 50% with the largest decrease seen at 3 osmole. Indicating that causing an osmotic shock prior to lyophilization is not beneficial to survival. Addition of osmolytes specifically betaine had a protective effect on the survival at higher osmolarities but had no effect at low osmolarities. Addition of sucrose on the other hand was clearly protective at 1 osmole with an increase in viability of around 50%. However, further increasing the sucrose concentration past 1 osmole caused a reduction in viability. Improved survival shows that there is an osmolarity independent protective effect of sucrose on survival in freeze drying potentially through membrane stabilisation or formation of a protective matrix around cells (*179*, *188*). However, as concentration of sucrose was increased past 1 M there is a reduction in viability, suggesting a biphasic effect of sucrose with around 1 M sucrose having a protective effect but increasing it further causes a reduction in viability.

I wanted to better understand what was happening to intracellular water concentra-

tion in the cells and therefore measured cell size in response to addition of different concentrations of NaCl and sucrose. Addition of pure water had surprisingly little impact on cell size. The absence of volume change was surprising as transition from the growth media to water represents a significant hypo-osmotic shock of about 500 mOsm. In *E. coli* during exponential growth such a shock causes a 10-15% increase in the cell volume (*191*). However, in *L. animalis* in the stationary phase no increase in volume was observed. The absence of volume change could be due to the cells being in stationary phase and therefore the intracellular solute concentration is quite low resulting in only a modest hypo-osmotic shock when transferred to water. Another likely explanation is that *L. animalis* is gram positive bacterium and therefore has a much thicker cell wall meaning that it is less likely to deform with increase in turgor pressure.

As osmolarity increased there was a reduction in cell volume that was approximately linear until 3 osmole and then showed an asymptote. This is consistent with findings such as those by Cayley who shows that there is a limit to intracellular free water that can be removed by hyper-osmotic shock (*58*). The size reduction is approximately similar for NaCl and sucrose as well as using the standard freeze-dry buffer. The identical reduction in cell size further confirms that protective effects of the freeze dry-buffer does not originate from cellular water loss but other protective attributes of the components. Addition of betaine, choline and ectoine did seem slightly protective at higher osmolarities but were not beneficial at around 1 osmole. Therefore, modulating the osmolarity and osmolyte content of the cryo-buffer does not seem to have a beneficial impact on survival after lyophilization.

4.7 Impact of Osmolarity on Growth of *L. animalis*

Here I have demonstrated that during growth *L. animalis* experiences a change in media osmolarity from 500 mOsm to about 1000 mOsm due to addition of ammonia to the growth media. Exploring the effect of a large change in osmolarity by addition of 750 mM NaCl results in a reduction in yield, CFU after freeze-drying, growth rate, and lactic acid production. Addition of betaine and choline improved the yield and survival after freeze-drying when pH was not controlled. Under pH control conditions I show that addition of osmolytes has little impact on the growth characteristics of *L. animalis*. Furthermore, I demonstrate that addition of up to 400 mM additional NaCl has little effect on the fermentation time. Suggesting that cells grown in complex media are most likely well equipped to deal with osmotic stress present in the media. However, further increasing osmolarity to 600 or 800 mM NaCl led to a large reduction in growth rate and yield. With final optical density being 30% lower for cells grown in 800 mM

NaCl and fermentation time increasing from 6 to 12 hours figure 29.

I wanted to investigate whether accumulation of osmolytes would confer an increased resistance to freezing or freeze-drying. Intracellular osmolyte concentration scales with osmotic stress, so I tried loading osmolytes by increasing media osmolarity. However, number of viable cells decreased with increasing osmolarity. There was a small improvement in survival if cells were frozen directly as osmolarity increased. However, the protective effect was absent if cells were concentrated and suspended in a cryo-buffer before freezing or freeze drying. Cells exposed to osmotic stress showed a slight improvement in survival after freeze-drying but not nearly enough to offset the massive reduction in viability they experience after freezing.

Finally, I looked at how the osmolarity of the cryo-buffer affects survival after freeze drying. I found that the osmolarity of the cryo-buffer was not related to survival after freeze drying and that supplementation of the cryo-buffer with betaine did not protect cells. Furthermore, I found that cell size of stationary phase *L. animalis* varied with osmolarity and that addition of betaine had no impact on the total cell size change experienced by the cells.

Therefore, there is no easy way to optimize the growth or viability of *L. animalis* using osmolarity. While the cells experience a small change in osmolarity during fermentation, the media most likely already contains sufficient osmolytes and further supplementation is not beneficial. One of the most remarkable changes in osmolarity is during freeze-drying of bacteria. We tested whether modulation of the media osmolarity with or without the addition of betaine, choline or ectoine had an impact on the ability of cells to survive freezing or freeze-drying and saw no beneficial effect. Increasing media osmolarity to stimulate osmolyte uptake greatly reduced viability after freezing and did not offer relevant protection during freeze-drying.

These comprehensive studies show that growth at high osmolarities for *L. animalis* is not recommended. However, I did not explore the impact of high osmolarity on viability during long-term storage. Previous research has shown that increasing media osmolarity can improve the longevity of bacteria in storage (*192*). Furthermore, future investigations should take into account the rich nature of complex media. Use of a more minimal media could be beneficial to better understand the direct contribution of osmolytes to maintenance of growth and yield at higher osmolarities (*193*).

5. Concluding Remarks on Osmotic Stress During Bacterial Culture

Prokaryotes are masters of adaptation able to survive extremes of temperature, pH, osmolarity and even radioactivity (*194*). These physical challenges require innovative solutions for life to exist and thrive. In this thesis I focused on how bacterial cells deal with osmotic stress. Increasing the media osmolarity leads to rapid efflux of water from the cell as described by equation (1.1). This sudden increase in media osmolarity could present a variety of problems for the cell such as loss of turgor pressure (*2*), an increased energy burden (*106*), sudden macromolecular crowding (*1*), loss of diffusive motion within the cell (*73*, *113*), or a proteome burden (*47*).

E. coli can deal with osmotic stress by accumulation of organic osmolytes. However, it seems like the accumulation of osmolytes themselves poses a challenge to growth. I present evidence that none of the aforementioned problems are responsible for growth rate slowdown in *E. coli*. There is no energetic or proteome burden placed on the cell. Nor is the growth rate reduction solely caused by loss of cytoplasmic water. Cells resisted significant efforts to load more osmolytes into the cytoplasm to restore cellular water. In fact when succeeding to increase intracellular osmolytes, with overexpression of trehalose, I observed a decrease in growth rate when betaine is present in the media appendix A.8. Furthermore, I show that similar changes in growth rate can be obtained by loading the cell with membrane permeant solutes such as glycerol or EG that do not induce osmotic stress at all. These findings indicate that the decrease in growth rate is not due to the osmotic stress itself but due to the effect of high concentration of osmolytes. I propose here that as there is no proteome reallocation the only way the growth rate slowdown can be explained is by a global slowdown in metabolic flux.

As the rate of metabolic flux depends on enzyme efficiency the logical conclusion is that accumulation of osmolytes negatively affects enzyme activity. However, organic osmolytes such as betaine and trehalose are thought to stabilize enzyme structure,

and do not have perturbing effects on cellular macromolecules(*68*, *195*). Here I presented evidence from various sources that applying Kramer's theory on reaction rates in viscous media can explain the reduction of reaction rate and therefore growth rate (*134*, *142*, *143*, *145*, *147*, *196*). An increase of solution viscosity results in increased friction for conformational change of protein structure that enzymes undergo during catalysis. Sampedro and colleagues demonstrated that increasing the solution viscosity directly increases the activation energy required for a reaction to occur and that this results in a reduced maximal enzyme velocity, as well as a decrease in enzyme efficiency (*147*). The *in-vitro* studies investigating enzymatic catalysis with increasing trehalose show the same trends as bacteria with increasing osmolarity. The reduced catalytic efficiency at different temperatures and trehalose concentrations also show corresponding trends to bacterial growth rates when grown in various NaCl concentration at different temperatures.

Overall, these data suggest that the cause of the slowdown at increased osmolarity is due to accumulation of osmolytes in the cytoplasm. The accumulation of osmolyte negatively impacts enzyme activity. This theory explains why there is minimal proteome reallocation as the majority of cytoplasmic enzymes experience reduced activity, rather than osmolarity disproportionately affecting a single pathway or enzyme. Future experiments can confirm this theory by measuring intracellular viscosity of cells grown at various osmolarities. There have been various attempts to quantify the viscosity of *E. coli* cytoplasm. Using either rotational or translational diffusion allows for estimation of viscosity using the generalized Stokes-Einstein equation equation (3.6). Attempts to quantify microviscosity within cells are reviewed here (*144*, *197*, *198*). Using membrane permeant solutes such as glycerol should allow for easy manipulation of intracellular viscosity and comparison to change in growth rate.

Having explored potential causes of growth slowdown at elevated media osmolarity, chapter 4 looks at the impact of media osmolarity on industrial fermentation of LAB. I find that media osmolarity during fermentation increases based on ammonia addition for pH control. Just as with *E. coli* there is a decrease in growth rate with increasing media osmolarity. Addition of osmolytes only yielded marginal improvement in the growth rate. Suggesting that the growth media already contains sufficient osmolytes. Future studies should confirm the presence of osmolytes in the growth media. However, addition of osmolytes results in an increase in yield, lactic acid production and number of viable bacteria after freeze-drying as measured by CFU in small scale experiments without pH control.

To further explore the impact of osmolyte addition and osmolarity on the growth of LAB, *L. animalis* was grown with the addition of 0, 200, 400, 600, or 800 mM NaCl un-

der pH control. Fermentation time increased from 6 to 12 hours and yield as measured by OD_{600} decreased. Addition of betaine and ectoine did not reduce fermentation time at any of the osmolarities tested. Survival of cells if frozen directly may have been increased slightly. However, concentration of cells and freezing in a freezing buffer resulted in a decrease in number of viable cells with increasing NaCl concentration. Addition of betaine or ectoine did not result in increased viability at any osmolarity and osmolyte addition did not have any protective effect on survival after freeze drying. Finally, I demonstrated that the protective effect of the freezing buffer was not related to the reduction in intracellular water and in fact increasing the osmolarity of the freezing buffer past 1 M resulted in a reduction of cellular viability. Therefore we can conclude that LAB during industrial fermentation are exposed to small osmotic changes but enhanced protection is not required as the growth media is already rich in osmolytes. The small change in osmolarity experienced during fermentation is not likely to have an adverse effect on cell culture or survival. However, if cells are exposed to large changes in osmolarity there is an increase in the time for fermentation and a decrease in the number of viable cells.

This thesis aimed to understand the impact of increased media osmolarity on the growth of bacterial cells and apply that knowledge to investigate industrial applications of high osmolarity. I presented a potential solution to the cause of reduced growth at increasing osmolarity. Furthermore, I show that osmolarity only changes slightly during fermentation of LAB and increasing osmolarity does not have a protective effect on viability after freezing or freeze drying. Future studies should validate the link between cytoplasmic viscosity and growth and understand whether changes in viscosity can fully account for growth rate changes observed at increased osmolarity.

Bibliography

1. S. Cayley, M. T. Record, *Biochemistry* **42**, 12596–12609, ISSN: 0006-2960, 1520-4995, (2022; https://pubs.acs.org/doi/10.1021/bi0347297) (Nov. 1, 2003).
2. H. Walter, *Z. Bot* **16**, 1931 (1924).
3. Y. Fan, O. Pedersen, *Nature Reviews Microbiology* **19**, 55–71, ISSN: 1740-1526, 1740-1534, (2023; https://www.nature.com/articles/s41579-020-0433-9) (Jan. 2021).
4. I. Levin-Reisman *et al.*, *Science* **355**, 826–830, ISSN: 0036-8075, 1095-9203, (2023; https://www.science.org/doi/10.1126/science.aaj2191) (Feb. 24, 2017).
5. W. H. Organization, *The top 10 causes of death*, Sept. 12, 2020, (2022; https://www.who.int/news-room/fact-sheets/detail/the-top-10-causes-of-death).
6. C. J. Murray *et al.*, *The Lancet* **399**, 629–655, ISSN: 01406736, (2022; https://linkinghub.elsevier.com/retrieve/pii/S0140673621027240) (Feb. 2022).
7. R. P. Evershed *et al.*, *Nature* **455**, 528–531, ISSN: 0028-0836, 1476-4687, (2022; http://www.nature.com/articles/nature07180) (Sept. 2008).
8. S. B. McClure *et al.*, *PLOS ONE* **13**, ed. by J. J. Loor, e0202807, ISSN: 1932-6203, (2022; https://dx.plos.org/10.1371/journal.pone.0202807) (Sept. 5, 2018).
9. P. E. McGovern *et al.*, *Proceedings of the National Academy of Sciences* **101**, 17593–17598, ISSN: 0027-8424, 1091-6490, (2022; http://www.pnas.org/cgi/doi/10.1073/pnas.0407921102) (Dec. 21, 2004).
10. L. Capasso, *The Lancet* **352**, 1864, ISSN: 01406736, (2022; https://linkinghub.elsevier.com/retrieve/pii/S0140673605799396) (Dec. 1998).
11. Aristotle, *Oxford Classical Texts: Aristotelis: De Generatione Animalium*, ed. by H. J. Drossaart Lulofs (Oxford University Press, Jan. 1, 1965), ISBN: 978-0-19-814563-9.

12. G. Pappas, I. J. Kiriaze, M. E. Falagas, *International Journal of Infectious Diseases* **12**, 347–350, ISSN: 12019712, (2022; https://linkinghub.elsevier.com/retrieve/pii/S1201971207002123) (July 2008).
13. R. J. Littman, *Mount Sinai Journal of Medicine: A Journal of Translational and Personalized Medicine* **76**, 456–467, ISSN: 00272507, (2022; https://onlinelibrary.wiley.com/doi/10.1002/msj.20137) (Oct. 2009).
14. P. Prioreschi, *A History of Medicine: Roman medicine* (Horatius Press, 1996), ISBN: 1-888456-03-5.
15. A. van Leeuwenhoek, *Philosophical Transactions of the Royal Society of London* **12**, 821–831, ISSN: 0261-0523, 2053-9223, (2022; https://royalsocietypublishing.org/doi/10.1098/rstl.1677.0003) (Mar. 25, 1677).
16. N. Lane, *Philosophical Transactions of the Royal Society B: Biological Sciences* **370**, 20140344, ISSN: 0962-8436, 1471-2970, (2023; https://royalsocietypublishing.org/doi/10.1098/rstb.2014.0344) (Apr. 19, 2015).
17. J. R. Porter, *Bacteriological Reviews* **37**, 284–288, ISSN: 0005-3678, (2022; https://journals.asm.org/doi/10.1128/br.37.3.284-288.1973) (Sept. 1973).
18. A. Ariatti, P. Mandrioli, *Aerobiologia* **9**, 101–107, ISSN: 0393-5965, 1573-3025, (2022; http://link.springer.com/10.1007/BF02066251) (Dec. 1993).
19. R. Garcia, J. Adrian, *Food Reviews International* **25**, 115–125, ISSN: 8755-9129, (2022; http://www.tandfonline.com/doi/abs/10.1080/87559120802682656) (Apr. 2009).
20. G. Vantomme, J. Crassous, *Chirality* **33**, 597–601, ISSN: 0899-0042, 1520-636X, (2022; https://onlinelibrary.wiley.com/doi/10.1002/chir.23349) (Oct. 2021).
21. A. Brack, Ed., *The molecular origins of life: assembling pieces of the puzzle* (Cambridge University Press, Cambridge, 1998), 417 pp., ISBN: 978-0-521-56412-0.
22. D. Pitt, J.-M. Aubin, *Canadian Journal of Surgery* **55**, E8–E9, ISSN: 0008428X, (2022; http://www.canjsurg.ca/lookup/doi/10.1503/cjs.007112) (Oct. 1, 2012).
23. J. A. Barnett, L. Barnett, *Yeast research: a historical overview*, in collab. with A. S. for Microbiology, OCLC: ocn657027867 (ASM Press, Washington, DC, 2011), 379 pp., ISBN: 978-1-55581-516-5.
24. S. M. Blevins, M. S. Bronze, *International Journal of Infectious Diseases* **14**, e744–e751, ISSN: 12019712, (2022; https://linkinghub.elsevier.com/retrieve/pii/S1201971210023143) (Sept. 2010).

25. Y. Kawaguchi *et al.*, *Frontiers in Microbiology* **11**, 2050, ISSN: 1664-302X, (2023; https://www.frontiersin.org/article/10.3389/fmicb.2020.02050/full) (Aug. 26, 2020).
26. J. E. Lane-Claypon, *Journal of Hygiene* **9**, 239–248, ISSN: 0022-1724, (2023; https://www.cambridge.org/core/product/identifier/S0022172400016260/type/journal_article) (Sept. 1909).
27. M. Schaechter, *Frontiers in Microbiology* **6**, ISSN: 1664-302X, (2023; http://journal.frontiersin.org/article/10.3389/fmicb.2015.00289/abstract) (Apr. 21, 2015).
28. X. Fang, C. J. Lloyd, B. O. Palsson, *Nature Reviews Microbiology* **18**, 731–743, ISSN: 1740-1526, 1740-1534, (2023; https://www.nature.com/articles/s41579-020-00440-4) (Dec. 2020).
29. J.-C. Lachance *et al.*, *Molecular Systems Biology* **17**, ISSN: 1744-4292, 1744-4292, (2023; https://onlinelibrary.wiley.com/doi/10.15252/msb.202010099) (July 2021).
30. D. Miroli, *PhD Thesis*, 199 (2019).
31. J. Monod, *Annual Review of Microbiology* **3**, 371–394, ISSN: 0066-4227, 1545-3251, (2022; https://www.annualreviews.org/doi/10.1146/annurev.mi.03.100149.002103) (Oct. 1949).
32. A. Campbell, *Bacteriological Reviews* **21**, 263–272, ISSN: 0005-3678, (2023; https://journals.asm.org/doi/10.1128/br.21.4.263-272.1957) (Dec. 1957).
33. F. C. Neidhardt, *Nature Reviews Microbiology* **4**, 876–876, ISSN: 1740-1526, 1740-1534, (2023; http://www.nature.com/articles/nrmicro1554) (Dec. 2006).
34. M. Schaechter, O. Maaloe, N. O. Kjeldgaard, *Journal of General Microbiology* **19**, 592–606, ISSN: 0022-1287, (2022; https://www.microbiologyresearch.org/content/journal/micro/10.1099/00221287-19-3-592) (Dec. 1, 1958).
35. H. Bremer, P. P. Dennis, *EcoSal Plus* **3**, ecosal.5.2.3, ISSN: 2324-6200, (2023; https://journals.asm.org/doi/10.1128/ecosal.5.2.3) (Feb. 12, 2008).
36. J. Mitchison, *Experimental Cell Research* **13**, 244–262, ISSN: 00144827, (2023; https://linkinghub.elsevier.com/retrieve/pii/0014482757900058) (Oct. 1957).
37. S. Cooper, C. E. Helmstetter, *Journal of Molecular Biology* **31**, 519–540, ISSN: 00222836, (2023; https://linkinghub.elsevier.com/retrieve/pii/0022283668904257) (Feb. 1968).

38. C. E. Helmstetter, *Frontiers in Microbiology* **6**, ISSN: 1664-302X, (2023; http://journal.frontiersin.org/Article/10.3389/fmicb.2015.00238/abstract) (Mar. 25, 2015).

39. H. Yoshikawa, N. Sueoka, *Proceedings of the National Academy of Sciences* **49**, 559–566, ISSN: 0027-8424, 1091-6490, (2023; https://pnas.org/doi/full/10.1073/pnas.49.4.559) (Apr. 1963).

40. R. Ecker, M. Schaechter, *Biochimica et Biophysica Acta (BBA) - Specialized Section on Nucleic Acids and Related Subjects* **76**, 275–279, ISSN: 09266550, (2023; https://linkinghub.elsevier.com/retrieve/pii/0926655063900409) (Jan. 1963).

41. X. Dai *et al.*, *Nature Microbiology* **2**, 16231, ISSN: 2058-5276, (2021; http://www.nature.com/articles/nmicrobiol2016231) (Feb. 2016).

42. B. J. Paul, W. Ross, T. Gaal, R. L. Gourse, *Annual Review of Genetics* **38**, 749–770, ISSN: 0066-4197, 1545-2948, (2022; https://www.annualreviews.org/doi/10.1146/annurev.genet.38.072902.091347) (Dec. 1, 2004).

43. M. Kaczanowska, M. Rydén-Aulin, *Microbiology and Molecular Biology Reviews* **71**, 477–494, ISSN: 1092-2172, 1098-5557, (2023; https://journals.asm.org/doi/10.1128/MMBR.00013-07) (Sept. 2007).

44. M. Scott, C. W. Gunderson, E. M. Mateescu, Z. Zhang, T. Hwa, *Science* **330**, 1099–1102, ISSN: 0036-8075, 1095-9203, (2021; https://www.sciencemag.org/lookup/doi/10.1126/science.1192588) (Nov. 19, 2010).

45. C. You *et al.*, *Nature* **500**, 301–306, ISSN: 0028-0836, 1476-4687, (2021; http://www.nature.com/articles/nature12446) (Aug. 2013).

46. S. Hui *et al.*, *Molecular Systems Biology* **11**, 784, ISSN: 1744-4292, 1744-4292, (2023; https://onlinelibrary.wiley.com/doi/10.15252/msb.20145697) (Feb. 2015).

47. M. Mori *et al.*, *Molecular Systems Biology* **17**, ISSN: 1744-4292, 1744-4292, (2022; https://onlinelibrary.wiley.com/doi/10.15252/msb.20209536) (May 2021).

48. T. M. Wendrich, G. Blaha, D. N. Wilson, M. A. Marahiel, K. H. Nierhaus, *Molecular Cell* **10**, 779–788, ISSN: 10972765, (2021; https://linkinghub.elsevier.com/retrieve/pii/S1097276502006561) (Oct. 2002).

49. S. Klumpp, M. Scott, S. Pedersen, T. Hwa, *Proceedings of the National Academy of Sciences* **110**, 16754–16759, ISSN: 0027-8424, 1091-6490, (2021; http://www.pnas.org/cgi/doi/10.1073/pnas.1310377110) (Oct. 15, 2013).

50. C. Wu *et al.*, *Proceedings of the National Academy of Sciences* **119**, e2201585119, ISSN: 0027-8424, 1091-6490, (2023; https://pnas.org/doi/full/10.1073/pnas.2201585119) (May 17, 2022).

51. A. Farewell, F. C. Neidhardt, *Journal of Bacteriology* **180**, 4704–4710, ISSN: 0021-9193, 1098-5530, (2022; https://journals.asm.org/doi/10.1128/JB.180.17.4704-4710.1998) (Sept. 1998).

52. S. M. Chiang, H. E. Schellhorn, *Archives of Biochemistry and Biophysics* **525**, 161–169, ISSN: 00039861, (2023; https://linkinghub.elsevier.com/retrieve/pii/S0003986112000586) (Sept. 2012).

53. Y. Xu *et al.*, *Nature Communications* **11**, 1496, ISSN: 2041-1723, (2023; https://www.nature.com/articles/s41467-020-15350-5) (Mar. 20, 2020).

54. D. C. Sévin, J. N. Stählin, G. R. Pollak, A. Kuehne, U. Sauer, *PLOS ONE* **11**, ed. by H. Shi, e0148888, ISSN: 1932-6203, (2023; https://dx.plos.org/10.1371/journal.pone.0148888) (Feb. 5, 2016).

55. J. M. Wood, *Science's STKE* **2006**, pe43–pe43, ISSN: 1525-8882, (2021; https://stke.sciencemag.org/lookup/doi/10.1126/stke.3572006pe43) (Oct. 10, 2006).

56. J. M. Wood, *Annual Review of Microbiology* **65**, 215–238, ISSN: 0066-4227, 1545-3251, (2023; https://www.annualreviews.org/doi/10.1146/annurev-micro-090110-102815) (Oct. 2011).

57. T. Pilizota, J. W. Shaevitz, *Biophysical Journal* **107**, 1962–1969, ISSN: 00063495, (2021; https://linkinghub.elsevier.com/retrieve/pii/S0006349514008972) (Oct. 2014).

58. S. Cayley, B. A. Lewis, H. J. Guttman, M. Record, *Journal of Molecular Biology* **222**, 281–300, ISSN: 00222836, (2021; https://linkinghub.elsevier.com/retrieve/pii/0022283691902120) (Nov. 1991).

59. D. McLaggan, J. Naprstek, E. Buurman, W. Epstein, *Journal of Biological Chemistry* **269**, 1911–1917, ISSN: 00219258, (2023; https://linkinghub.elsevier.com/retrieve/pii/S0021925817421132) (Jan. 1994).

60. T. Lamark, O. B. Styrvold, A. R. StrÃ¸m, *FEMS Microbiology Letters* **96**, 149–154, ISSN: 03781097, 15746968, (2023; https://academic.oup.com/femsle/article-lookup/doi/10.1111/j.1574-6968.1992.tb05408.x) (Sept. 1992).

61. U. Dinnbier, E. Limpinsel, R. Schmid, E. P. Bakker, *Archives of Microbiology* **150**, 348–357, ISSN: 0302-8933, 1432-072X, (2021; http://link.springer.com/10.1007/BF00408306) (Aug. 1988).

62. A. R. Strom, I. Kaasen, *Molecular Microbiology* **8**, 205–210, ISSN: 0950-382X, 1365-2958, (2022; https://onlinelibrary.wiley.com/doi/10.1111/j.1365-2958.1993.tb01564.x) (Apr. 1993).

63. W. Epstein, in *Progress in Nucleic Acid Research and Molecular Biology* (Elsevier, 2003), vol. 75, pp. 293–320, ISBN: 978-0-12-540075-6, (2021; https://linkinghub.elsevier.com/retrieve/pii/S0079660303750089).

64. C. Stock *et al.*, *Nature Communications* **9**, 4971, ISSN: 2041-1723, (2023; https://www.nature.com/articles/s41467-018-07319-2) (Nov. 26, 2018).

65. A. Amir, D. R. Nelson, *Proceedings of the National Academy of Sciences* **109**, 9833–9838, ISSN: 0027-8424, 1091-6490, (2023; https://pnas.org/doi/full/10.1073/pnas.1207105109) (June 19, 2012).

66. H. Jiang, S. X. Sun, *Physical Review Letters* **105**, 028101, ISSN: 0031-9007, 1079-7114, (2023; https://link.aps.org/doi/10.1103/PhysRevLett.105.028101) (July 7, 2010).

67. W. Epstein, *FEMS Microbiology Letters* **39**, 73–78, ISSN: 03781097, 15746968, (2021; https://academic.oup.com/femsre/article-lookup/doi/10.1111/j.1574-6968.1986.tb01845.x) (July 1986).

68. P. H. Yancey, M. E. Clark, S. C. Hand, R. D. Bowlus, G. N. Somero, *Science* **217**, 1214–1222, ISSN: 0036-8075, 1095-9203, (2023; https://www.science.org/doi/10.1126/science.7112124) (Sept. 24, 1982).

69. K. Lippert, E. Galinski, *Applied Microbiology and Biotechnology* **37**, ISSN: 0175-7598, 1432-0614, (2023; http://link.springer.com/10.1007/BF00174204) (Apr. 1992).

70. P. H. Yancey, *American Zoologist* **41**, 699–709, ISSN: 0003-1569, (2021; https://academic.oup.com/icb/article-lookup/doi/10.1093/icb/41.4.699) (Aug. 2001).

71. P. H. Yancey, *Journal of Experimental Biology* **208**, 2819–2830, ISSN: 1477-9145, 0022-0949, (2023; https://journals.biologists.com/jeb/article/208/15/2819/15754/Organic-osmolytes-as-compatible-metabolic-and) (Aug. 1, 2005).

72. K. Stevenson, *Edinburgh Research Archive*, 128, (https://hdl.handle.net/1842/36666) (Feb. 12, 2019).

73. X. Dai *et al.*, *mBio* **9**, ed. by S. Y. Lee, in collab. with S. Pedersen, M. Record, ISSN: 2161-2129, 2150-7511, (2021; https://journals.asm.org/doi/10.1128/mBio.02375-17) (Mar. 7, 2018).

74. T. E. Proseus, G.-L. Zhu, J. S. Boyer, *Journal of Experimental Botany* **51**, 1481–1494, ISSN: 1460-2431, 0022-0957, (2023; https://academic.oup.com/jxb/article-lookup/doi/10.1093/jexbot/51.350.1481) (Sept. 2000).

75. P. B. Green, *Plant Physiology* **43**, 1169–1184, ISSN: 0032-0889, 1532-2548, (2023; https://academic.oup.com/plphys/article/43/8/1169-1184/6093756) (Aug. 1, 1968).

76. D. J. Cosgrove, *Nature* **407**, 321–326, ISSN: 0028-0836, 1476-4687, (2023; https://www.nature.com/articles/35030000) (Sept. 2000).

77. G. Misra, E. R. Rojas, A. Gopinathan, K. C. Huang, *Biophysical Journal* **104**, 2342–2352, ISSN: 00063495, (2023; https://linkinghub.elsevier.com/retrieve/pii/S0006349513005158) (June 2013).
78. E. R. Rojas, K. C. Huang, *Current Opinion in Microbiology* **42**, 62–70, ISSN: 13695274, (2022; https://linkinghub.elsevier.com/retrieve/pii/S1369527417300395) (Apr. 2018).
79. I. Kuznetsova, K. Turoverov, V. Uversky, *International Journal of Molecular Sciences* **15**, 23090–23140, ISSN: 1422-0067, (2023; http://www.mdpi.com/1422-0067/15/12/23090) (Dec. 12, 2014).
80. A. Christiansen, Q. Wang, M. S. Cheung, P. Wittung-Stafshede, *Biophysical Reviews* **5**, 137–145, ISSN: 1867-2450, 1867-2469, (2023; http://link.springer.com/10.1007/s12551-013-0108-0) (June 2013).
81. M. Senske *et al.*, *Journal of the American Chemical Society* **136**, 9036–9041, ISSN: 0002-7863, 1520-5126, (2023; https://pubs.acs.org/doi/10.1021/ja503205y) (June 25, 2014).
82. Y. Wang, M. Sarkar, A. E. Smith, A. S. Krois, G. J. Pielak, *Journal of the American Chemical Society* **134**, 16614–16618, ISSN: 0002-7863, 1520-5126, (2023; https://pubs.acs.org/doi/10.1021/ja305300m) (Oct. 10, 2012).
83. S. S. Stadmiller, A. H. Gorensek-Benitez, A. J. Guseman, G. J. Pielak, *Journal of Molecular Biology* **429**, 1155–1161, ISSN: 00222836, (2023; https://linkinghub.elsevier.com/retrieve/pii/S0022283617301055) (Apr. 2017).
84. B. Alric, C. Formosa-Dague, E. Dague, L. J. Holt, M. Delarue, *Nature Physics* **18**, 411–416, ISSN: 1745-2473, 1745-2481, (2022; https://www.nature.com/articles/s41567-022-01506-1) (Apr. 2022).
85. X. Dai, M. Zhu, *mSphere* **3**, ed. by G. R. Bowman, e00430–18, ISSN: 2379-5042, (2022; https://journals.asm.org/doi/10.1128/mSphere.00430-18) (Oct. 31, 2018).
86. P. Kuhnert, J. Nicolet, J. Frey, *Applied and Environmental Microbiology* **61**, 4135–4139, ISSN: 0099-2240, 1098-5336, (2023; https://journals.asm.org/doi/10.1128/aem.61.11.4135-4139.1995) (Nov. 1995).
87. F. R. Blattner *et al.*, *Science* **277**, 1453–1462, ISSN: 0036-8075, 1095-9203, (2023; https://www.science.org/doi/10.1126/science.277.5331.1453) (Sept. 5, 1997).
88. S. D. Brown, S. Jun, *Genome Announcements* **3**, e00879–15, ISSN: 2169-8287, (2023; https://journals.asm.org/doi/10.1128/genomeA.00879-15) (Aug. 27, 2015).

89. B. R. Taylor *et al.*, “A metabolic sum rule dictates bacterial response to short-chain fatty acid stress”, preprint (Microbiology, Aug. 31, 2022), (2023; http://biorxiv.org/lookup/doi/10.1101/2022.08.31.506075).

90. C. Merlin, S. McAteer, M. Masters, *Journal of Bacteriology* **184**, 4573–4581, ISSN: 0021-9193, 1098-5530, (2023; https://journals.asm.org/doi/10.1128/JB.184.16.4573-4581.2002) (Aug. 15, 2002).

91. T. D. Brock, *Robert Koch: a life in medicine and bacteriology* (ASM Press, Washington, D.C, 1999), 364 pp., ISBN: 978-1-55581-143-3.

92. M. Armstrong Lumley, R. Burgess, L. J. Billingham, D. F. McDonald, D. W. Milligan, *British Journal of Haematology* **97**, 481–484, ISSN: 0007-1048, 1365-2141, (2023; https://onlinelibrary.wiley.com/doi/abs/10.1046/j.1365-2141.1997.492695.x) (May 1997).

93. S. Mandal, V. Uhlmann, “SplineDist: Automated Cell Segmentation With Spline Curves”, preprint (Bioinformatics, Oct. 28, 2020), (2023; http://biorxiv.org/lookup/doi/10.1101/2020.10.27.357640).

94. N. Otsu, *IEEE Transactions on Systems, Man, and Cybernetics* **9**, 62–66, ISSN: 0018-9472, 2168-2909, (2023; http://ieeexplore.ieee.org/document/4310076/) (Jan. 1979).

95. N. R. Pal, S. K. Pal, *Pattern Recognition* **26**, 1277–1294, ISSN: 00313203, (2023; https://linkinghub.elsevier.com/retrieve/pii/003132039390135J) (Sept. 1993).

96. S. Minaee *et al.*, Publisher: arXiv Version Number: 5, (2023; https://arxiv.org/abs/2001.05566) (2020).

97. O. Ronneberger, P. Fischer, T. Brox, Publisher: arXiv Version Number: 1, (2023; https://arxiv.org/abs/1505.04597) (2015).

98. L. Von Chamier *et al.*, *Nature Communications* **12**, 2276, ISSN: 2041-1723, (2023; https://www.nature.com/articles/s41467-021-22518-0) (Apr. 15, 2021).

99. W. F. Wolkers, H. Oldenhof, Eds., *Cryopreservation and Freeze-Drying Protocols* (Springer New York, New York, NY, 2015), vol. 1257, ISBN: 978-1-4939-2192-8, (2023; https://link.springer.com/10.1007/978-1-4939-2193-5).

100. T. Chang, G. Zhao, *Advanced Science* **8**, 2002425, ISSN: 2198-3844, 2198-3844, (2023; https://onlinelibrary.wiley.com/doi/10.1002/advs.202002425) (Mar. 2021).

101. U. Barboza Perez, E. Krasnopeeva, J. Rosko, T. Pilizota, “Tunnel Slide Preparation for Motor Speed Recordings v1”, preprint, (2023; https://www.protocols.io/view/tunnel-slide-preparation-for-motor-speed-recording-bcjdiui6).

102. J. Rosko, V. A. Martinez, W. C. K. Poon, T. Pilizota, *Proceedings of the National Academy of Sciences* **114**, E7969–E7976, ISSN: 0027-8424, 1091-6490, (2021; http://www.pnas.org/lookup/doi/10.1073/pnas.1620945114) (Sept. 19, 2017).

103. C. Stringer, T. Wang, M. Michaelos, M. Pachitariu, *Nature Methods* **18**, 100–106, ISSN: 1548-7091, 1548-7105, (2023; https://www.nature.com/articles/s41592-020-01018-x) (Jan. 2021).

104. J. K. Lanyi, *Bacteriological Reviews* **38**, 272–290, ISSN: 0005-3678, (2023; https://journals.asm.org/doi/10.1128/br.38.3.272-290.1974) (Sept. 1974).

105. C. Waymouth, *In Vitro* **6**, 109–127, ISSN: 0073-5655, 1475-2689, (2023; http://link.springer.com/10.1007/BF02616113) (Sept. 1970).

106. A. Oren, *Microbiology and Molecular Biology Reviews* **63**, 334–348, ISSN: 1092-2172, 1098-5557, (2023; https://journals.asm.org/doi/10.1128/MMBR.63.2.334-348.1999) (June 1999).

107. M. Cashel, J. Gallant, *Journal of Molecular Biology* **34**, 317–330, ISSN: 00222836, (2023; https://linkinghub.elsevier.com/retrieve/pii/0022283668902568) (June 1968).

108. K. Potrykus, M. Cashel, *Annual Review of Microbiology* **62**, 35–51, ISSN: 0066-4227, 1545-3251, (2023; https://www.annualreviews.org/doi/10.1146/annurev.micro.62.081307.162903) (Oct. 1, 2008).

109. W. A. Haseltine, R. Block, *Proceedings of the National Academy of Sciences* **70**, 1564–1568, ISSN: 0027-8424, 1091-6490, (2023; https://pnas.org/doi/full/10.1073/pnas.70.5.1564) (May 1973).

110. K. Potrykus, H. Murphy, N. Philippe, M. Cashel, *Environmental Microbiology* **13**, 563–575, ISSN: 14622912, (2022; https://onlinelibrary.wiley.com/doi/10.1111/j.1462-2920.2010.02357.x) (Mar. 2011).

111. M. Scott, T. Hwa, *Current Opinion in Biotechnology* **22**, 559–565, ISSN: 09581669, (2021; https://linkinghub.elsevier.com/retrieve/pii/S0958166911000772) (Aug. 2011).

112. M. Basan *et al.*, *Nature* **528**, 99–104, ISSN: 0028-0836, 1476-4687, (2021; http://www.nature.com/articles/nature15765) (Dec. 2015).

113. M. C. Konopka *et al.*, *Journal of Bacteriology* **191**, 231–237, ISSN: 0021-9193, 1098-5530, (2022; https://journals.asm.org/doi/10.1128/JB.00536-08) (Jan. 2009).

114. K. Stevenson, A. F. McVey, I. B. N. Clark, P. S. Swain, T. Pilizota, *Scientific Reports* **6**, 38828, ISSN: 2045-2322, (2022; http://www.nature.com/articles/srep38828) (Dec. 2016).

115. W. Scott, *Australian Journal of Biological Sciences* **6**, 549, ISSN: 0004-9417, (2023; http://www.publish.csiro.au/?paper=BI9530549) (1953).

116. S. Pirt, *Journal of Fermentation Technology* **65**, 173–177, ISSN: 03856380, (2022; https://linkinghub.elsevier.com/retrieve/pii/0385638087901610) (Jan. 1987).

117. A. H. García, *Journal of Biosciences* **36**, 939–950, ISSN: 0250-5991, 0973-7138, (2023; http://link.springer.com/10.1007/s12038-011-9107-0) (Dec. 2011).

118. J. Christian, *Australian Journal of Biological Sciences* **8**, 75, ISSN: 0004-9417, (2023; http://www.publish.csiro.au/?paper=BI9550075) (1955).

119. R. J. Britten, F. T. McClure, *Bacteriological Reviews* **26**, 292–335, ISSN: 0005-3678, (2023; https://journals.asm.org/doi/10.1128/br.26.3.292-335.1962) (Sept. 1962).

120. S. Cayley, B. A. Lewis, M. T. Record, *Journal of Bacteriology* **174**, 1586–1595, ISSN: 0021-9193, 1098-5530, (2021; https://journals.asm.org/doi/10.1128/jb.174.5.1586-1595.1992) (Mar. 1992).

121. A. Deshpande, M. Bhatia, S. Laxman, A. Bachhawat, *Microbial Cell* **4**, 112–126, ISSN: 23112638, (2021; http://microbialcell.com/researcharticles/thiol-trapping-and-metabolic-redistribution-of-sulfur-metabolites-enable-cells-to-overcome-cysteine-overload/) (Apr. 3, 2017).

122. J. V. Živković *et al.*, *Acta Medica Medianae* **61**, 35–42, ISSN: 03654478, 18212794, (2023; https://publisher.medfak.ni.ac.rs/AMM_1/2022/2022-3-broj/Abs_eng/05Jelena%20V.%20Zivkovic.pdf) (June 15, 2022).

123. S. Diamant, N. Eliahu, D. Rosenthal, P. Goloubinoff, *Journal of Biological Chemistry* **276**, 39586–39591, ISSN: 00219258, (2023; https://linkinghub.elsevier.com/retrieve/pii/S0021925820600187) (Oct. 2001).

124. J. Cairney, I. R. Booth, C. F. Higgins, *Journal of Bacteriology* **164**, 1224–1232, ISSN: 0021-9193, 1098-5530, (2023; https://journals.asm.org/doi/10.1128/jb.164.3.1224-1232.1985) (Dec. 1985).

125. B. Poolman, J. J. Spitzer, J. M. Wood, *Biochimica et Biophysica Acta (BBA) - Biomembranes* **1666**, 88–104, ISSN: 00052736, (2023; https://linkinghub.elsevier.com/retrieve/pii/S0005273604001609) (Nov. 2004).

126. N. Gul, B. Poolman, *Molecular Membrane Biology* **30**, 138–148, ISSN: 0968-7688, 1464-5203, (2023; http://www.tandfonline.com/doi/full/10.3109/09687688.2012.754060) (Mar. 2013).

127. K. B. Heller, E. C. Lin, T. H. Wilson, *Journal of Bacteriology* **144**, 274–278, ISSN: 0021-9193, 1098-5530, (2023; https://journals.asm.org/doi/10.1128/jb.144.1.274-278.1980) (Oct. 1980).

128. S. Panda, V. Y. K. Fung, J. F. J. Zhou, H. Liang, K. Zhou, *Biochemical Engineering Journal* **168**, 107957, ISSN: 1369703X, (2023; https://linkinghub.elsevier.com/retrieve/pii/S1369703X21000334) (Apr. 2021).

129. A. V. Pandit, E. Harrison, R. Mahadevan, *Microbial Cell Factories* **20**, 22, ISSN: 1475-2859, (2023; https://microbialcellfactories.biomedcentral.com/articles/10.1186/s12934-021-01509-2) (Jan. 22, 2021).

130. T. Müller, B. Walter, A. Wirtz, A. Burkovski, *Current Microbiology* **52**, 400–406, ISSN: 0343-8651, 1432-0991, (2023; http://link.springer.com/10.1007/s00284-005-0370-x) (May 2006).

131. U. Sauer *et al.*, *Journal of Bacteriology* **181**, 6679–6688, ISSN: 0021-9193, 1098-5530, (2023; https://journals.asm.org/doi/10.1128/JB.181.21.6679-6688.1999) (Nov. 1999).

132. F. W. Sears, G. L. Salinger, *Thermodynamics, kinetic theory, and statistical thermodynamics* (Addison-Wesley Pub. Co, Reading, Mass, 3d ed, 1975), 454 pp., ISBN: 978-0-201-06894-8.

133. M. Laliberté, *Journal of Chemical & Engineering Data* **52**, 321–335, ISSN: 0021-9568, 1520-5134, (2023; https://pubs.acs.org/doi/10.1021/je0604075) (Mar. 1, 2007).

134. H. Kramers, *Physica* **7**, 284–304, ISSN: 00318914, (2023; https://linkinghub.elsevier.com/retrieve/pii/S0031891440900982) (Apr. 1940).

135. P. W. Atkins, J. De Paula, *Physical chemistry for the life sciences*, OCLC: ocn695528594 (W.H. Freeman and Co. ; Oxford University Press, New York : Oxford, 2nd ed, 2011), 590 pp., ISBN: 978-1-4292-3114-5.

136. G. G. Hammes, *Nature* **204**, 342–343, ISSN: 0028-0836, 1476-4687, (2023; https://www.nature.com/articles/204342a0) (Oct. 1964).

137. B. Gavish, M. M. Werber, *Biochemistry* **18**, 1269–1275, ISSN: 0006-2960, 1520-4995, (2023; https://pubs.acs.org/doi/abs/10.1021/bi00574a023) (Apr. 1, 1979).

138. H. Frauenfelder, S. G. Sligar, P. G. Wolynes, *Science* **254**, 1598–1603, ISSN: 0036-8075, 1095-9203, (2023; https://www.science.org/doi/10.1126/science.1749933) (Dec. 13, 1991).

139. D. D. Boehr, D. McElheny, H. J. Dyson, P. E. Wright, *Science* **313**, 1638–1642, ISSN: 0036-8075, 1095-9203, (2023; https://www.science.org/doi/10.1126/science.1130258) (Sept. 15, 2006).

140. P. Agarwal, N. Doucet, C. Chennubhotla, A. Ramanathan, C. Narayanan, in *Methods in Enzymology* (Elsevier, 2016), vol. 578, pp. 273–297, ISBN: 978-0-12-811107-9, (2023; https://linkinghub.elsevier.com/retrieve/pii/S0076687916300581).

141. B. A. Chrunyk, C. R. Matthews, *Biochemistry* **29**, 2149–2154, ISSN: 0006-2960, 1520-4995, (2023; https://pubs.acs.org/doi/abs/10.1021/bi00460a027) (Feb. 27, 1990).

142. A. Ansari, C. M. Jones, E. R. Henry, J. Hofrichter, W. A. Eaton, *Science* **256**, 1796–1798, ISSN: 0036-8075, 1095-9203, (2023; https://www.science.org/doi/10.1126/science.1615323) (June 26, 1992).

143. M. Jacob, F. X. Schmid, *Biochemistry* **38**, 13773–13779, ISSN: 0006-2960, 1520-4995, (2023; https://pubs.acs.org/doi/10.1021/bi991503o) (Oct. 1, 1999).

144. E. O. Puchkov, *Biochemistry (Moscow) Supplement Series A: Membrane and Cell Biology* **7**, 270–279, ISSN: 1990-7478, 1990-7494, (2023; http://link.springer.com/10.1134/S1990747813050140) (Oct. 2013).

145. N. Periasamy, H. P. Kao, K. Fushimi, A. S. Verkman, *American Journal of Physiology-Cell Physiology* **263**, C901–C907, ISSN: 0363-6143, 1522-1563, (2023; https://www.physiology.org/doi/10.1152/ajpcell.1992.263.4.C901) (Oct. 1, 1992).

146. A. P. Demchenko, O. I. Rusyn, E. A. Saburova, *Biochimica et Biophysica Acta (BBA) - Protein Structure and Molecular Enzymology* **998**, 196–203, ISSN: 01674838, (2023; https://linkinghub.elsevier.com/retrieve/pii/0167483889902732) (Oct. 1989).

147. J. G. Sampedro, R. A. Muñoz-Clares, S. Uribe, *Journal of Bacteriology* **184**, 4384–4391, ISSN: 0021-9193, 1098-5530, (2023; https://journals.asm.org/doi/10.1128/JB.184.16.4384-4391.2002) (Aug. 15, 2002).

148. J. M. Hernández-Meza, J. G. Sampedro, *The Journal of Physical Chemistry B* **122**, 4309–4317, ISSN: 1520-6106, 1520-5207, (2023; https://pubs.acs.org/doi/10.1021/acs.jpcb.8b01656) (Apr. 19, 2018).

149. L. Weinisch *et al.*, *PLOS Biology* **16**, ed. by V. Sourjik, e2003892, ISSN: 1545-7885, (2023; https://dx.plos.org/10.1371/journal.pbio.2003892) (Jan. 22, 2018).

150. A. Sitnitsky, *Chemical Physics* **369**, 37–42, ISSN: 03010104, (2023; https://linkinghub.elsevier.com/retrieve/pii/S0301010410000534) (Mar. 2010).

151. D. Araiza-Olivera, J. G. Sampedro, A. Mújica, A. Peña, S. Uribe-Carvajal, *FEMS Yeast Research* **10**, 282–289, ISSN: 15671356, 15671364, (2023; https://academic.oup.com/femsyr/article-lookup/doi/10.1111/j.1567-1364.2010.00605.x) (Apr. 12, 2010).

152. C. Olsson, S. Genheden, V. García Sakai, J. Swenson, *The Journal of Physical Chemistry B* **123**, 3679–3687, ISSN: 1520-6106, 1520-5207, (2023; https://pubs.acs.org/doi/10.1021/acs.jpcb.9b01856) (May 2, 2019).

153. S. Wera, E. De Schrijver, I. Geyskens, S. Nwaka, J. M. Thevelein, *The Biochemical Journal* **343 Pt 3**, 621–626, ISSN: 0264-6021 (Pt 3 Nov. 1, 1999).

154. A. Medvedova, M. Kocis-Koval, L. Valik, *Acta Alimentaria*, ISSN: 0139-3006, 1588-2535, (2023; https://akjournals.com/view/journals/066/aop/article-10.1556-066.2020.00213/article-10.1556-066.2020.00213.xml) (Mar. 24, 2021).

155. H. N. Rabetafika, A. Razafindralambo, B. Ebenso, H. L. Razafindralambo, *Encyclopedia* **3**, 561–581, ISSN: 2673-8392, (2023; https://www.mdpi.com/2673-8392/3/2/40) (Apr. 30, 2023).

156. J. Corry, G. Curtis, R. Baird, in *Progress in Industrial Microbiology* (Elsevier, 2003), vol. 37, pp. 511–513, ISBN: 978-0-444-51084-6, (2023; https://linkinghub.elsevier.com/retrieve/pii/S0079635203800668).

157. J. S. Crater, J. C. Lievense, *FEMS Microbiology Letters* **365**, ISSN: 1574-6968, (2023; https://academic.oup.com/femsle/article/doi/10.1093/femsle/fny138/5026621) (July 1, 2018).

158. J. L. Vipham *et al.*, *Zoonoses and Public Health* **62**, 599–608, ISSN: 18631959, (2023; http://doi.wiley.com/10.1111/zph.12187) (Dec. 2015).

159. W. Zhang *et al.*, *Frontiers in Microbiology* **10**, 977, ISSN: 1664-302X, (2023; https://www.frontiersin.org/article/10.3389/fmicb.2019.00977/full) (May 7, 2019).

160. P. Markowiak, K. Śliżewska, *Gut Pathogens* **10**, 21, ISSN: 1757-4749, (2023; https://gutpathogens.biomedcentral.com/articles/10.1186/s13099-018-0250-0) (Dec. 2018).

161. F. C. Neidhardt, B. Magasanik, *Biochimica et Biophysica Acta* **42**, 99–116, ISSN: 00063002, (2022; https://linkinghub.elsevier.com/retrieve/pii/0006300260907575) (Jan. 1960).

162. G. Iturriaga, R. Suárez, B. Nova-Franco, *International Journal of Molecular Sciences* **10**, 3793–3810, ISSN: 1422-0067, (2023; http://www.mdpi.com/1422-0067/10/9/3793) (Sept. 1, 2009).

163. I. Kaasen, J. McDougall, A. Strøm, *Gene* **145**, 9–15, ISSN: 03781119, (2023; https://linkinghub.elsevier.com/retrieve/pii/0378111994903166) (July 1994).

164. S. B. Leslie, E. Israeli, B. Lighthart, J. H. Crowe, L. M. Crowe, *Applied and Environmental Microbiology* **61**, 3592–3597, ISSN: 0099-2240, 1098-5336, (2023; https://journals.asm.org/doi/10.1128/aem.61.10.3592-3597.1995) (Oct. 1995).

165. J. Mellies, A. Wise, M. Villarejo, *Journal of Bacteriology* **177**, 144–151, ISSN: 0021-9193, 1098-5530, (2023; https://journals.asm.org/doi/10.1128/jb.177.1.144-151.1995) (Jan. 1995).

166. M. L. Mendum, L. T. Smith, *Applied and Environmental Microbiology* **68**, 813–819, ISSN: 0099-2240, 1098-5336, (2023; https://journals.asm.org/doi/10.1128/AEM.68.2.813-819.2002) (Feb. 2002).

167. A. U. Kuhlmann, T. Hoffmann, J. Bursy, M. Jebbar, E. Bremer, *Journal of Bacteriology* **193**, 4699–4708, ISSN: 0021-9193, 1098-5530, (2023; https://journals.asm.org/doi/10.1128/JB.05270-11) (Sept. 15, 2011).

168. M. Jebbar, R. Talibart, K. Gloux, T. Bernard, C. Blanco, *Journal of Bacteriology* **174**, 5027–5035, ISSN: 0021-9193, 1098-5530, (2023; https://journals.asm.org/doi/10.1128/jb.174.15.5027-5035.1992) (Aug. 1992).

169. K. Gouffi *et al.*, *Journal of Bacteriology* **180**, 5044–5051, ISSN: 0021-9193, 1098-5530, (2023; https://journals.asm.org/doi/10.1128/JB.180.19.5044-5051.1998) (Oct. 1998).

170. F. Fonseca, C. Béal, F. Mihoub, M. Marin, G. Corrieu, *International Dairy Journal* **13**, 917–926, ISSN: 09586946, (2023; https://linkinghub.elsevier.com/retrieve/pii/S0958694603001195) (Jan. 2003).

171. A. S. Angelidis, G. M. Smith, *Applied and Environmental Microbiology* **69**, 1013–1022, ISSN: 0099-2240, 1098-5336, (2023; https://journals.asm.org/doi/10.1128/AEM.69.2.1013-1022.2003) (Feb. 2003).

172. B. Kempf, E. Bremer, *Archives of Microbiology* **170**, 319–330, ISSN: 0302-8933, 1432-072X, (2023; http://link.springer.com/10.1007/s002030050649) (Sept. 29, 1998).

173. P. Uguen, J. Hamelin, J.-P. Le Pennec, C. Blanco, *Applied and Environmental Microbiology* **65**, 291–293, ISSN: 0099-2240, 1098-5336, (2023; https://journals.asm.org/doi/10.1128/AEM.65.1.291-293.1999) (Jan. 1999).

174. A. Baliarda *et al.*, *International Journal of Food Microbiology* **84**, 13–20, ISSN: 01681605, (2023; https://linkinghub.elsevier.com/retrieve/pii/S0168160502003884) (July 2003).

175. H. Robert, C. Le Marrec, C. Blanco, M. Jebbar, *Applied and Environmental Microbiology* **66**, 509–517, ISSN: 0099-2240, 1098-5336, (2023; https://journals.asm.org/doi/10.1128/AEM.66.2.509-517.2000) (Feb. 2000).

176. R. W. Hutkins, W. L. Ellefson, E. R. Kashket, *Applied and Environmental Microbiology* **53**, 2275–2281, ISSN: 0099-2240, 1098-5336, (2023; https://journals.asm.org/doi/10.1128/aem.53.10.2275-2281.1987) (Oct. 1987).

177. F. Gaucher *et al.*, *Applied Microbiology and Biotechnology* **104**, 3145–3156, ISSN: 0175-7598, 1432-0614, (2021; http://link.springer.com/10.1007/s00253-020-10425-1) (Apr. 2020).

178. E. Kets, P. Teunissen, J. De Bont, *Applied and Environmental Microbiology* **62**, 259–261, ISSN: 0099-2240, 1098-5336, (2023; https://journals.asm.org/doi/10.1128/aem.62.1.259-261.1996) (Jan. 1996).

179. J. H. Crowe, *Journal of Experimental Biology* **211**, 2899–2900, ISSN: 1477-9145, 0022-0949, (2023; https://journals.biologists.com/jeb/article/211/18/2899/17660/TREHALOSE-AND-ANHYDROBIOSIS-THE-EARLY-WORK-OF-J-S) (Sept. 15, 2008).

180. J. H. Crowe, J. F. Carpenter, L. M. Crowe, *Annual Review of Physiology* **60**, 73–103, ISSN: 0066-4278, 1545-1585, (2023; https://www.annualreviews.org/doi/10.1146/annurev.physiol.60.1.73) (Oct. 1998).

181. M. Stasiulewicz, A. Panuszko, P. Bruździak, J. Stangret, *The Journal of Physical Chemistry B* **126**, 2990–2999, ISSN: 1520-6106, 1520-5207, (2023; https://pubs.acs.org/doi/10.1021/acs.jpcb.2c00281) (Apr. 28, 2022).

182. P. Breeuwer, A. Lardeau, M. Peterz, H. Joosten, *Journal of Applied Microbiology* **95**, 967–973, ISSN: 1364-5072, 1365-2672, (2023; https://academic.oup.com/jambio/article/95/5/967/6723913) (Nov. 2003).

183. E. P. Kets, J. A. Bont, *FEMS Microbiology Letters* **116**, 251–255, ISSN: 03781097, 15746968, (2021; https://academic.oup.com/femsle/article-lookup/doi/10.1111/j.1574-6968.1994.tb06711.x) (Mar. 1994).

184. D. T. Welsh, R. A. Herbert, *FEMS Microbiology Letters* **174**, 57–63, ISSN: 03781097, 15746968, (2023; https://academic.oup.com/femsle/article-lookup/doi/10.1111/j.1574-6968.1999.tb13549.x) (May 1999).

185. D. Cleland, P. Krader, C. McCree, J. Tang, D. Emerson, *Journal of Microbiological Methods* **58**, 31–38, ISSN: 01677012, (2023; https://linkinghub.elsevier.com/retrieve/pii/S0167701204000600) (July 2004).

186. O. Kandror, A. DeLeon, A. L. Goldberg, *Proceedings of the National Academy of Sciences* **99**, 9727–9732, ISSN: 0027-8424, 1091-6490, (2021; http://www.pnas.org/cgi/doi/10.1073/pnas.142314099) (July 23, 2002).

187. D. Obis *et al.*, *Journal of Bacteriology* **181**, 6238–6246, ISSN: 0021-9193, 1098-5530, (2023; https://journals.asm.org/doi/10.1128/JB.181.20.6238-6246.1999) (Oct. 15, 1999).

188. P. Wessman, S. Håkansson, K. Leifer, S. Rubino, *Journal of Visualized Experiments*, 4058, ISSN: 1940-087X, (2023; https://www.jove.com/t/4058/formulations-for-freeze--drying-of-bacteria-and-their-influence-on-cell-survival) (Aug. 3, 2013).

189. F. Fonseca, C. Béal, G. Corrieu, *Journal of Dairy Research* **67**, 83–90, ISSN: 0022-0299, 1469-7629, (2023; https://www.cambridge.org/core/product/identifier/S002202999900401X/type/journal_article) (Feb. 2000).

190. A. Fowler, *Annals of the New York Academy of Sciences* **1066**, 119–135, ISSN: 0077-8923, (2023; http://doi.wiley.com/10.1196/annals.1363.010) (Dec. 1, 2005).

191. R. Buda *et al.*, *Proceedings of the National Academy of Sciences* **113**, E5838–E5846, ISSN: 0027-8424, 1091-6490, (2021; http://www.pnas.org/lookup/doi/10.1073/pnas.1522185113) (Oct. 4, 2016).

192. A. S. Carvalho *et al.*, *International Dairy Journal* **14**, 835–847, ISSN: 09586946, (2021; https://linkinghub.elsevier.com/retrieve/pii/S0958694604000378) (Oct. 2004).

193. A. Wegkamp, B. Teusink, W. De Vos, E. Smid, *Letters in Applied Microbiology* **50**, 57–64, ISSN: 02668254, 1472765X, (2021; https://onlinelibrary.wiley.com/doi/10.1111/j.1472-765X.2009.02752.x) (Jan. 2010).

194. N. Merino *et al.*, *Frontiers in Microbiology* **10**, 780, ISSN: 1664-302X, (2022; https://www.frontiersin.org/article/10.3389/fmicb.2019.00780/full) (Apr. 15, 2019).

195. T. Arakawa, S. Timasheff, *Biophysical Journal* **47**, 411–414, ISSN: 00063495, (2023; https://linkinghub.elsevier.com/retrieve/pii/S0006349585839321) (Mar. 1985).

196. M. Rholam, S. Scarlata, G. Weber, *Biochemistry* **23**, 6793–6796, ISSN: 0006-2960, 1520-4995, (2023; https://pubs.acs.org/doi/abs/10.1021/bi00321a079) (Dec. 18, 1984).

197. J. A. Dix, A. Verkman, *Annual Review of Biophysics* **37**, 247–263, ISSN: 1936-122X, 1936-1238, (2023; https://www.annualreviews.org/doi/10.1146/annurev.biophys.37.032807.125824) (June 1, 2008).

198. M. K. Kuimova, *Physical Chemistry Chemical Physics* **14**, 12671, ISSN: 1463-9076, 1463-9084, (2023; http://xlink.rsc.org/?DOI=c2cp41674c) (2012).

199. F. C. Neidhardt, P. L. Bloch, D. F. Smith, *Journal of Bacteriology* **119**, 736–747, ISSN: 0021-9193, 1098-5530, (2023; https://journals.asm.org/doi/10.1128/jb.119.3.736-747.1974) (Sept. 1974).

A. Appendix

A.1 Additional Information on Strain Creation

Strain MZ1 was generated by homologous recombination inserting sfGFP under otsB promoter. The construct was generated by Dario Miroli.

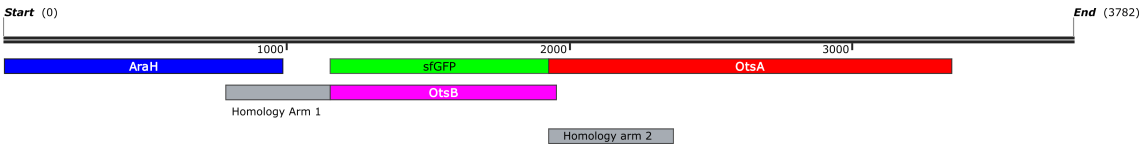

Figure S1: Homology regions were designed to replace the OtsB gene with sfGFP while staying under the native Ots promoter

Correct insertion was verified by use of Polymerase Chain Reaction (PCR) using one primer located in the bacterial nucleoid and one primer in sfGFP. The region was also sequenced by Sanger sequencing.

A.2 Plate Reader Supplementary Methods and Calibration

A.2.1 Manual Growth Rate Inspection

To ensure that only accurate data was used to calculate growth rates. Data for every well was manually inspected to observe a linear growth rate and correct annotation of the exponential and stationary phases.

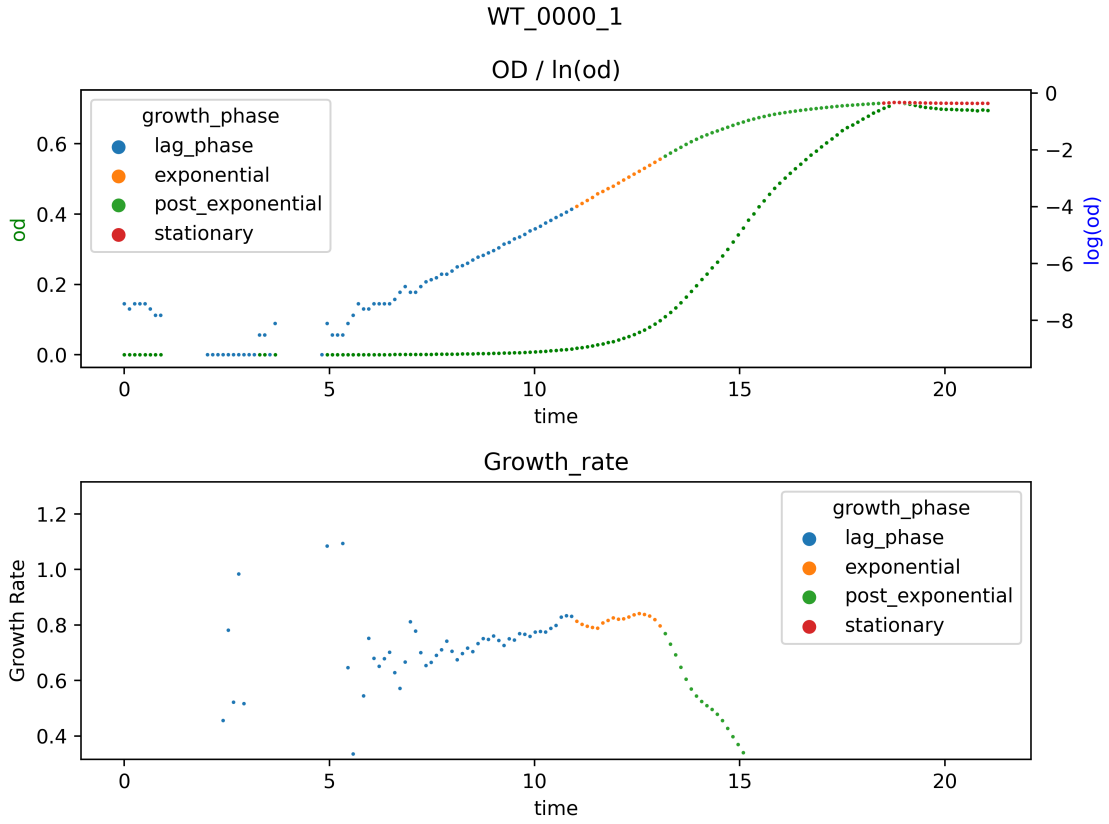

Figure S2: Graph generated to confirm correct annotation of growth rate. The upper panel shows the OD_{600} in green and $ln(OD)$ overlaid in multi colour corresponding to the program predicted growth phases. The lower panel shows the instantaneous growth rate with yellow showing the region of the program used to calculate the growth rate.

A.2.2 Validation of Yield Analysis

The solute used to modify osmolarity did not have an impact on the growth rate. However, a linear decrease in the maximal observed OD_{600} is seen when sucrose is used as the solute.

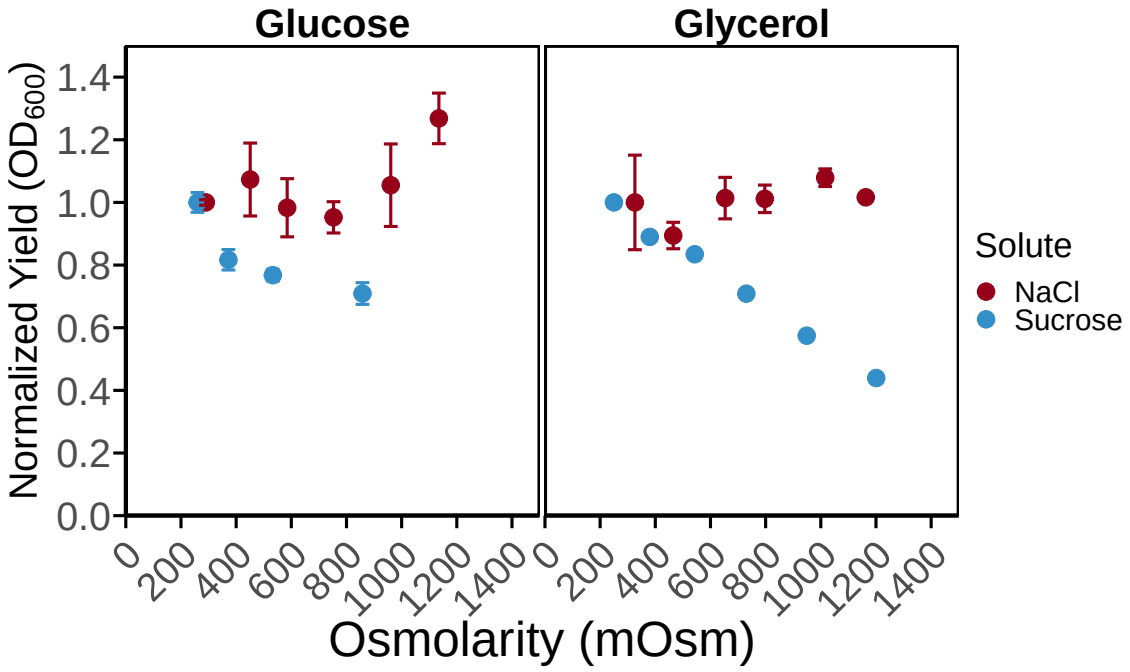

Figure S3: Comparison of Yield using NaCl or Sucrose to vary osmolarity. WT cells grown in M63 media with either Glycerol or Glucose as the carbon source. Yield Corresponds to maximum observed OD_{600}.

Meanwhile using NaCl to modify the osmolarity did not have an impact on the yield. The decrease in yield was an artefact based on the change in refractive index of the media as sucrose concentration was increased. The change of refractive index can be calculated by observing the specific refractive index increment dn/dc and the sucrose concentration used c.

$$\Delta n = (dn/dc) \cdot c \tag{A.1}$$

This effect is a particular problem only for sucrose. Using NaCl results in refractive index changes of less than 5% at relevant concentrations figure S4. As the solute used to induce osmotic stress is not important I continued using NaCl to induce osmotic stress rather than sucrose. I confirmed that the change in the refractive index is not significant for NaCl or EG for a wide range of molarities.

A.2.3 Investigation of Yield Changes with Different Solutes

To confirm that the reduction in yield was caused by a change in the refractive index I compared a change in OD_{600} observed with plastic beads to that observed with bacteria. I added 10 µl of beads to media containing various amounts of sucrose. I

also used a fixed concentration of *E. coli* and diluted them in media. I then measured the observed OD_{600}. I also investigated the impact of EG and NaCl on OD_{600}.

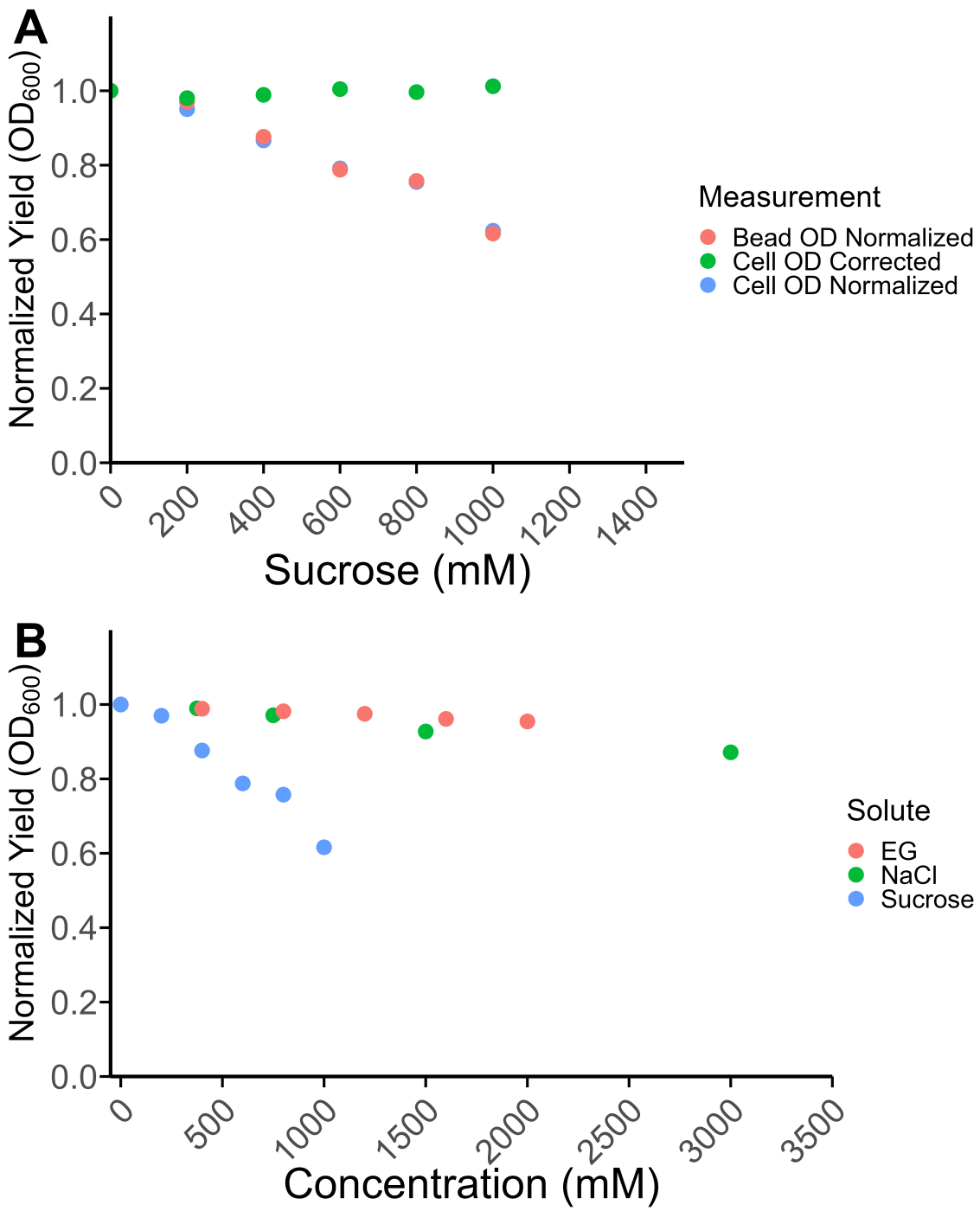

Figure S4: Sucrose impacts yield measurements due to change in refractive index. **A)** Measurement of OD_{600} of a fixed number of cells diluted in varying sucrose concentration (blue) and OD_{600} of 1 µm plastic beads diluted in the same media (red). When correcting for change in refractive index the OD_{600} of cells does not change (green). **B)** Measurement of how various solutes affect refractive index of media by measurement of plastic beads at various concentration of EG (red), NaCl (green) or Sucrose (blue).

I noted that the decrease in refractive index caused by sucrose could fully account for an observed decrease in yield. Furthermore, I show that NaCl does not cause a significant decrease in yield at relevant concentrations.

A.2.4 Linear Range of Plate reader

To confirm that I was actually measuring the yield and not just saturating the plate reader detector I performed serial dilutions of plastic beads and measured OD_{600}

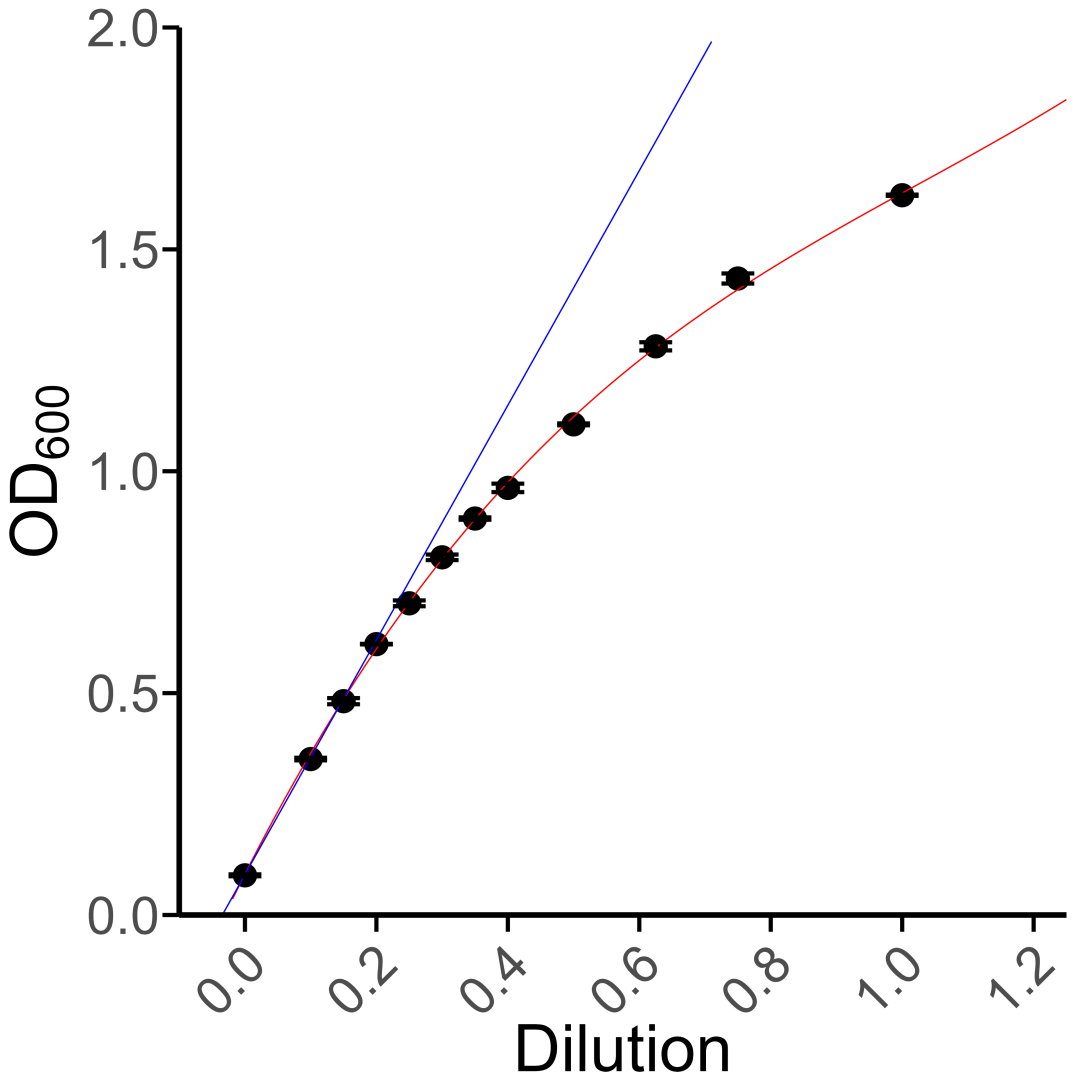

Figure S5: The plate reader showed linear measurements for OD_{600} up to about 0.6 after which the OD_{600} reading followed non linear dynamics that was fit by a polynomial equation.

The linear range of the plate reader is between 0 and 0.6 putting some of my measurements outside of the linear range. However, yield changes should still be detectable as the plate reader is still sensitive to change in OD_{600} outside of the linear range. To

confirm the accuracy of my results I manually grew cells in M63 media with glucose. Again there was no noticeable change in yield.

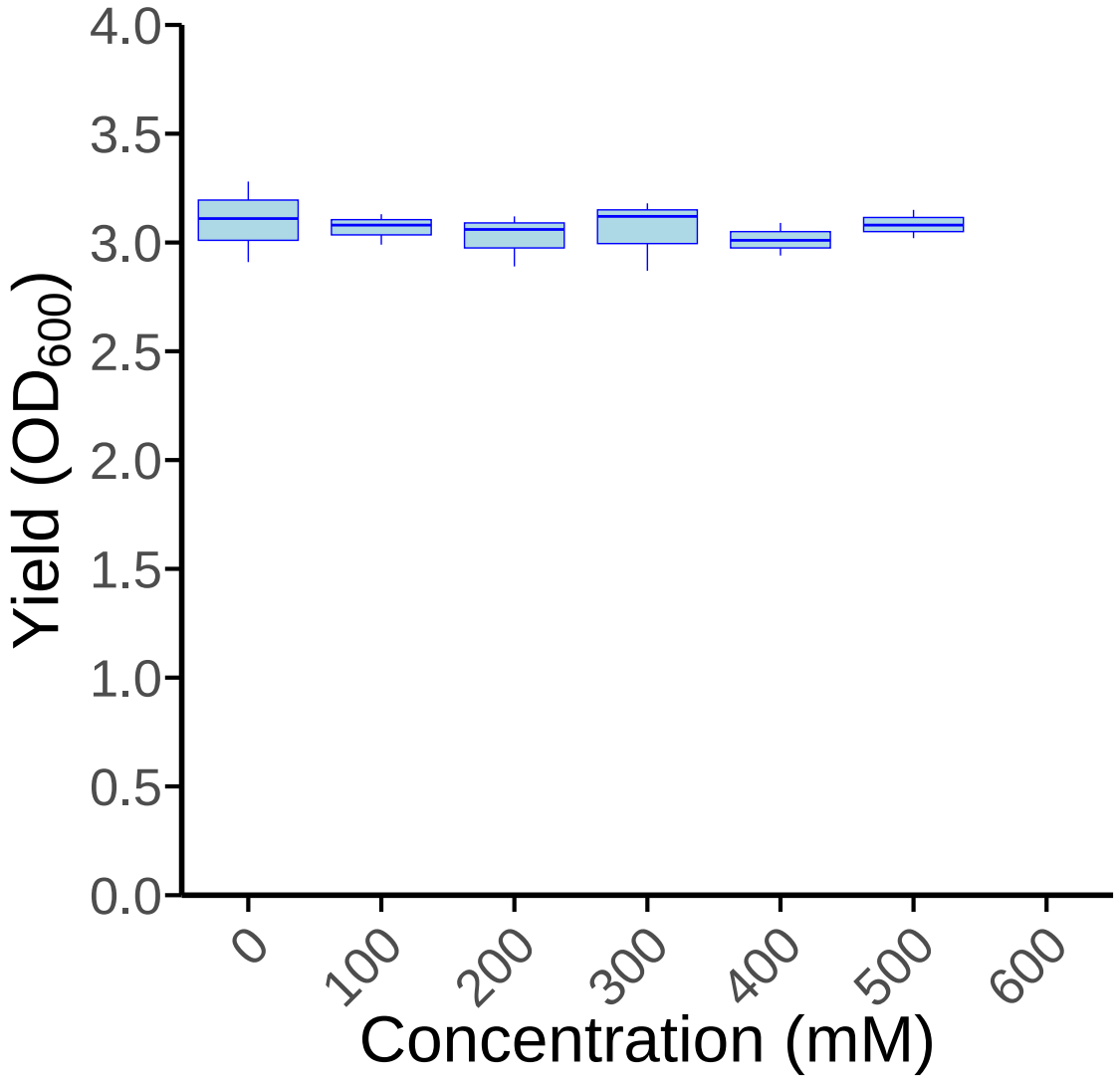

Figure S6: Measurement of WT yield remains constant when grown in flasks in M63 media using glucose as a carbon source.

A.2.5 Investigation of Overflow Metabolism in High Osmolarity Media

To further investigate the energy metabolism of WT and trehalose deficient cells I grew the WT and trehalose deficient MZ3 strain in M63 base media with 10 mM of glucose and ammonium. I measured whether there is a significant increase in overflow metabolism that could potentially explain the reduction in yield or growth rate. The acetate excretion rate is significantly elevated at high osmolarity for a given growth rate compared to a similar growth rate when nutrient conditions are varied (*112*).

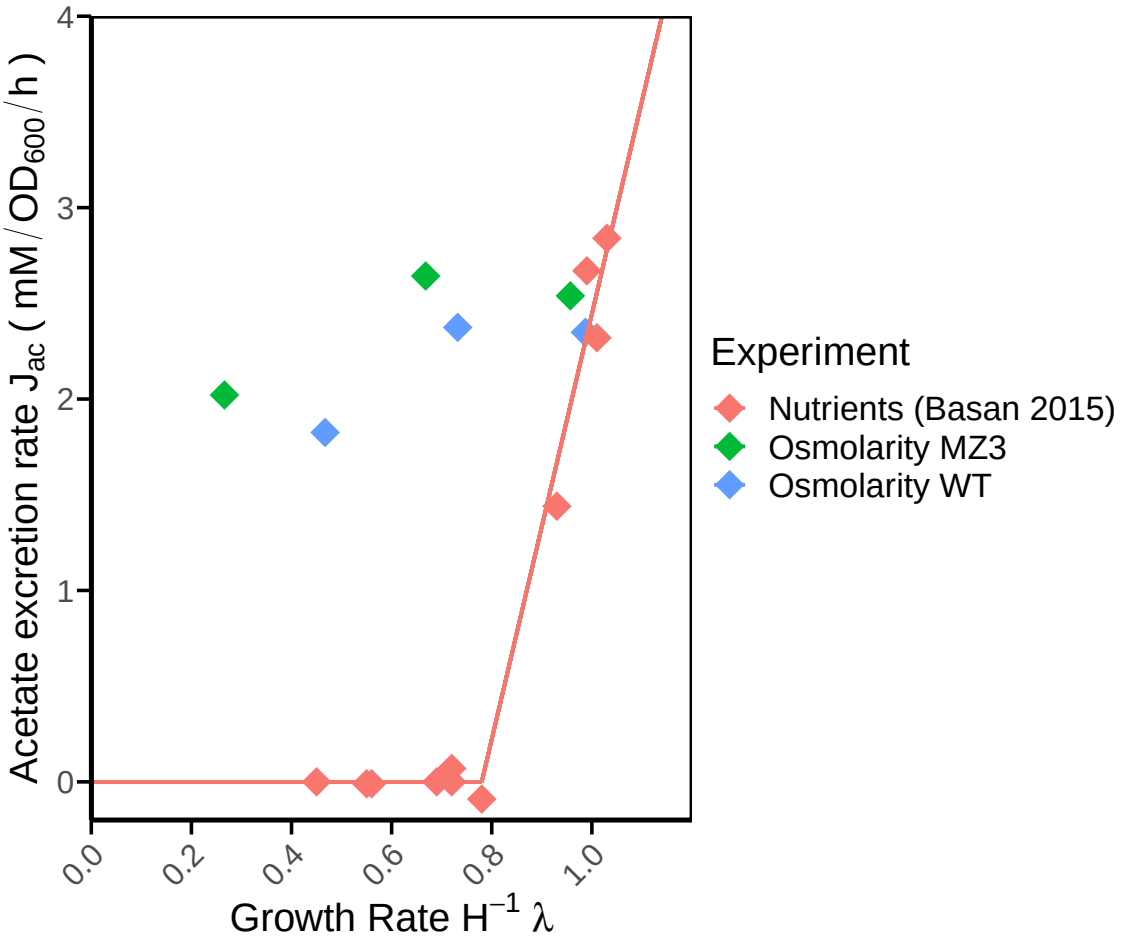

Figure S7: Measurement of rate of acetate excretion in WT and MZ3 cells grown in the presence of 0, 200 or, 400 mM NaCl. Data for acetate excretion rates under various nutrient conditions was taken from (*112*). Despite slow growth at higher osmolarity cells excrete acetate at a rate only slightly lower than at normal osmolarity.

Cells at high osmolarity excrete higher amount of acetate than cells at similar growth rate when growth is reduced by varying nutritional conditions. However, the higher rates of acetate excretion at lower growth rates do not seem to have a significant impact on the yield as WT cells show only slightly lower acetate excretion rates than MZ3 cells but show no difference in yield.

A.3 Derivation and Characterization of Normalized sfGFP Values

Observation of gene expression during bacterial growth is challenging as gene expression varies with growth rate. Here I attempt to characterize expression of osmotic stress genes by using strain MZ1 which expresses sfGFP under the native OtsB promoter. Measuring and quantifying expression levels provided two major challenges.

First cell number varied rapidly due to exponential growth. Secondly, WT bacteria show auto-fluorescence. To estimate promoter induction I had to correct for bacteria number by dividing by OD_{600} reading. I corrected for auto-fluorescence by subtracting the corrected GFP value of WT cells at equal OD from the reading equation (A.2).

$$\Delta\text{sfGFP} = \frac{\text{sfGFP}_{\text{mz1}}}{\text{OD}_{\text{mz1}}} - \frac{\text{sfGFP}_{\text{wt}}}{\text{OD}_{\text{wt}}} \tag{A.2}$$

Based on this I could now estimate sfGFP expression during growth of my strain. I then used the OD_{600} reading to estimate points of exponential and post-exponential growth as well as when cells enter stationary phase. I used binning to estimate the corrected GFP value for cells at various osmolarities figure S8.

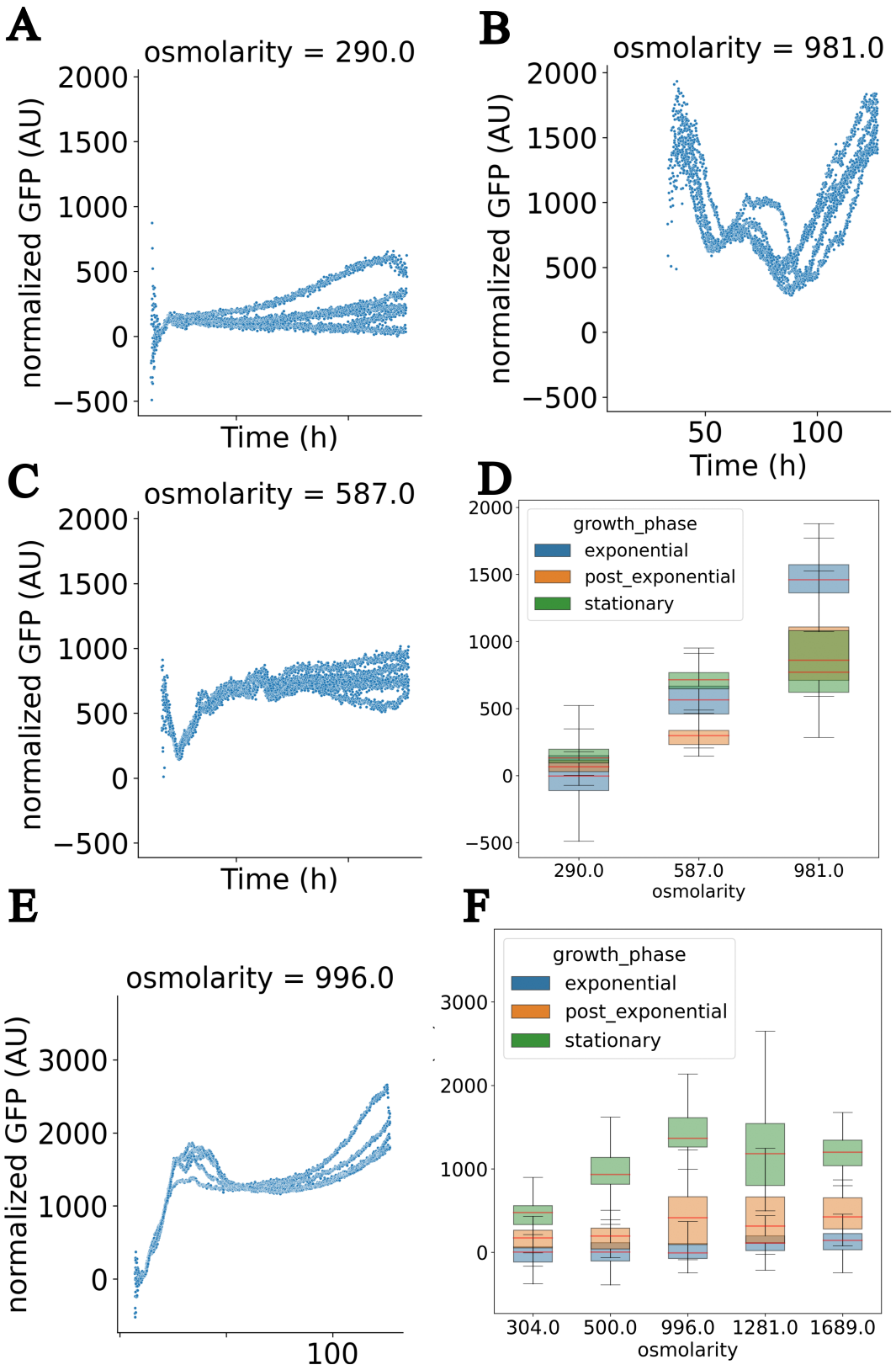

Figure S8: Expression of sfGFP was studied by calculating sfGFP/OD and subtracting the background value from WT cells to calculate mean sfGFP expression at a given OD. **A-C)** The normalized sfGFP calculated using equation (A.2) value plotted versus time for cells grown in M63 media with glucose. Each plot contains values from five repeats D) Example of binning sfGFP values according to growth phase. **E)** Example of cell grown in M63 media with glucose and CAA. **F)** Binning of values by growth phase for cells grown in M63 media with CAA

Here I demonstrate a fluorescence based approach to estimate gene expression during bacterial exponential growth. This plate based method allows for high throughput determination of gene expression.

A.4 Change in Growth Rate with Osmolarity is Trehalose Dependent

The impact of osmolarity seems to vary depending on the carbon source used by *E. coli*. Extrapolating growth rates shown on 4 different carbon sources shows that glucose and fructose seem to decrease together in parallel while mannose and glycerol seem to be converging at about 2000 mOsm. However, deletion of OtsA and OtsB making the trehalose cells deficient drastically changes the ability of cells growing on mannose to grow at high osmolarities.

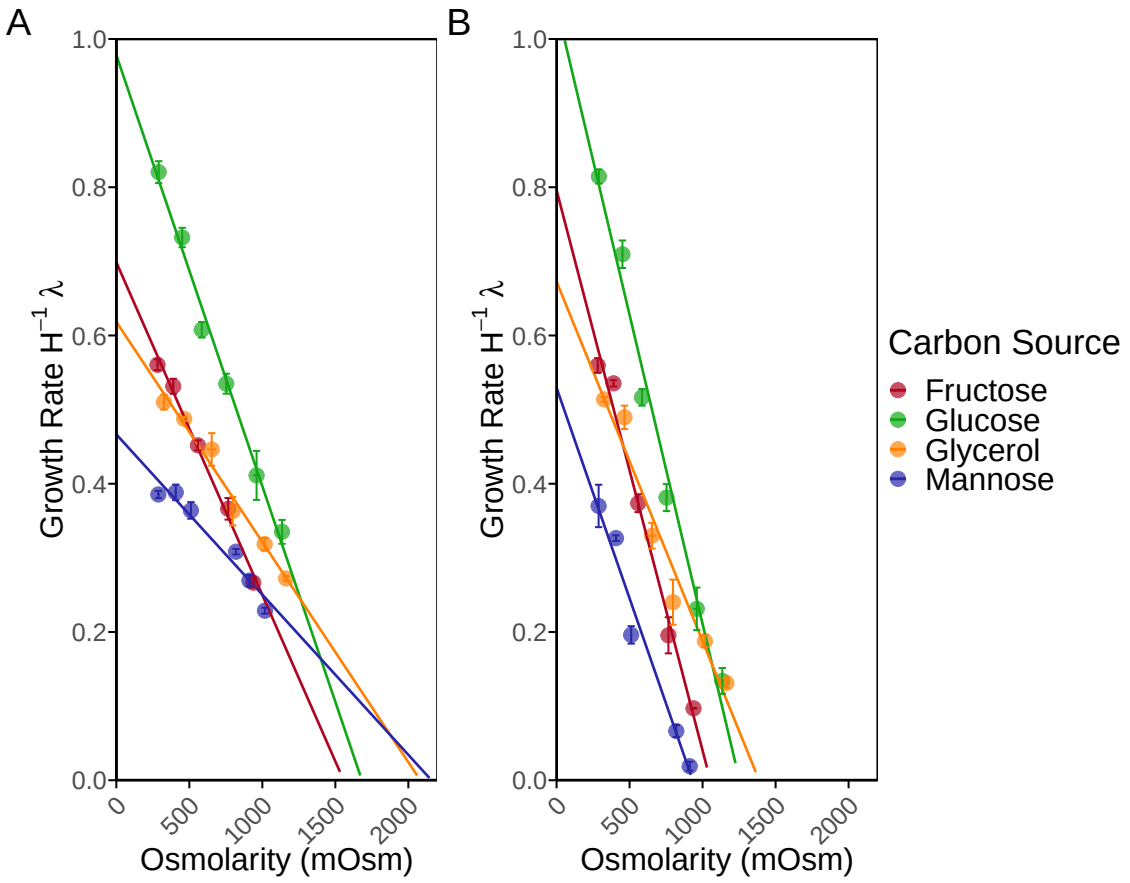

Figure S9: Fitting a linear regression to cells grown on M63 media and osmolarity is varied using NaCl. **A)** Linear regression for WT grown in different carbon sources. **B)** Linear regression for trehalose deficient cells grown in different carbon sources.

This demonstrates that growth response to osmotic stress is dependent on both the

carbon source used for growth as well as the cells ability to generate trehalose.

A.5 Proline represses Induction of OtsB Promoter at High Osmolarities

I noticed early on that the expression pattern of cells grown in media containing CAA was different to cells grown without. Instead of OtsB expression occurring during the exponential phase and then dropping in the stationary phase there was very little expression during exponential growth followed by high expression in stationary phase when grown with CAA. It is important that I also noted later that CAA most likely contain betaine which contributes to the reduction in OtsB expression. CAA is a mix of various amino acids produced by the hydrolysis of casein. So to understand if a specific amino acid was responsible for the change in OtsB expression I tested various batches of amino acid mixtures. Optimal concentration of amino acids were taken from (*199*). Here I show that both mix A containing Aspartate, Cysteine, Glutamate, Glycine and Histidine showed a moderate effect at suppressing OtsB expression. However, mix B containing Leucine, Methionine, Proline, Serine and Threonine was most effective. Individual amino acids of mix B were tested and proline was found to be the cause of trehalose synthesis repression. Cells were grown in media containing 400 mM NaCl as well as amino acids where indicated.

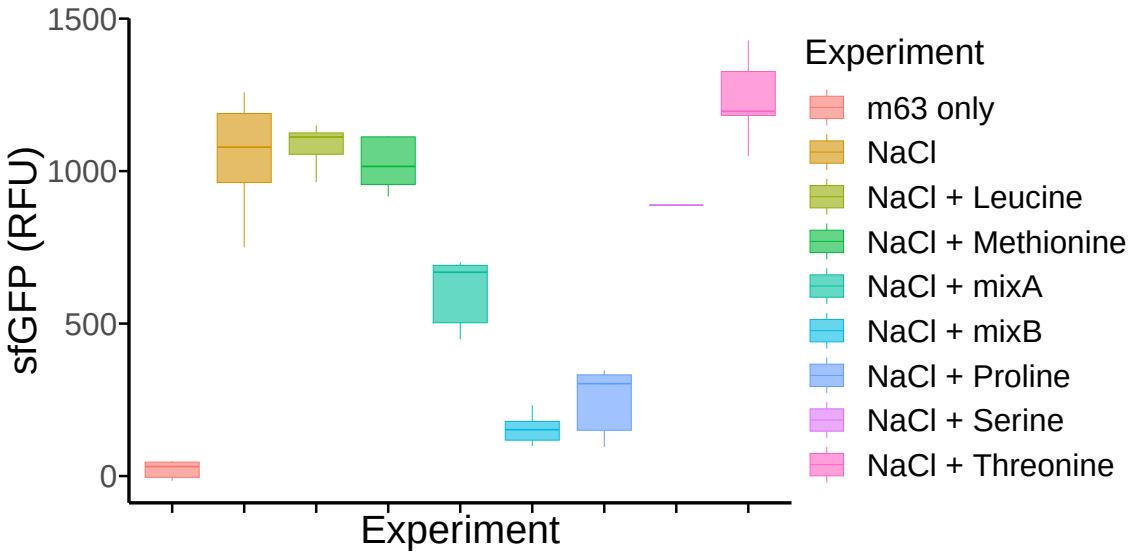

Figure S10: Proline but not a variety of other amino acids repressed the expression of sfGFP induced by addition of 400 mM NaCl.

I found that Proline reduced expression of sfGFP expression in MZ1 cells suggesting that proline suppresses the expression of trehalose synthesis. This is not surpris-

ing as it is known that under osmotic stress condition proline is accumulated and most likely presents a better alternative to *E. coli* than generating large amounts of trehalose (*119*). What is interesting is that Mix A containing Aspartate, Cysteine, Glutamate, Glycine and Histidine also showed moderate effectiveness at suppressing sfGFP expression at 400 mM NaCl.

A.6 Difference in Osmotic response of MG1655 and NCM3722 Strains

In this work I use both the NCM3722 and MG1655 strain of *E. coli*. Here I compared the growth rates of MG1655 and NCM in MOPS using 10 mM of Glucose as the carbon source and 10 mM of ammonium chloride as the nitrogen source and with or without betaine.

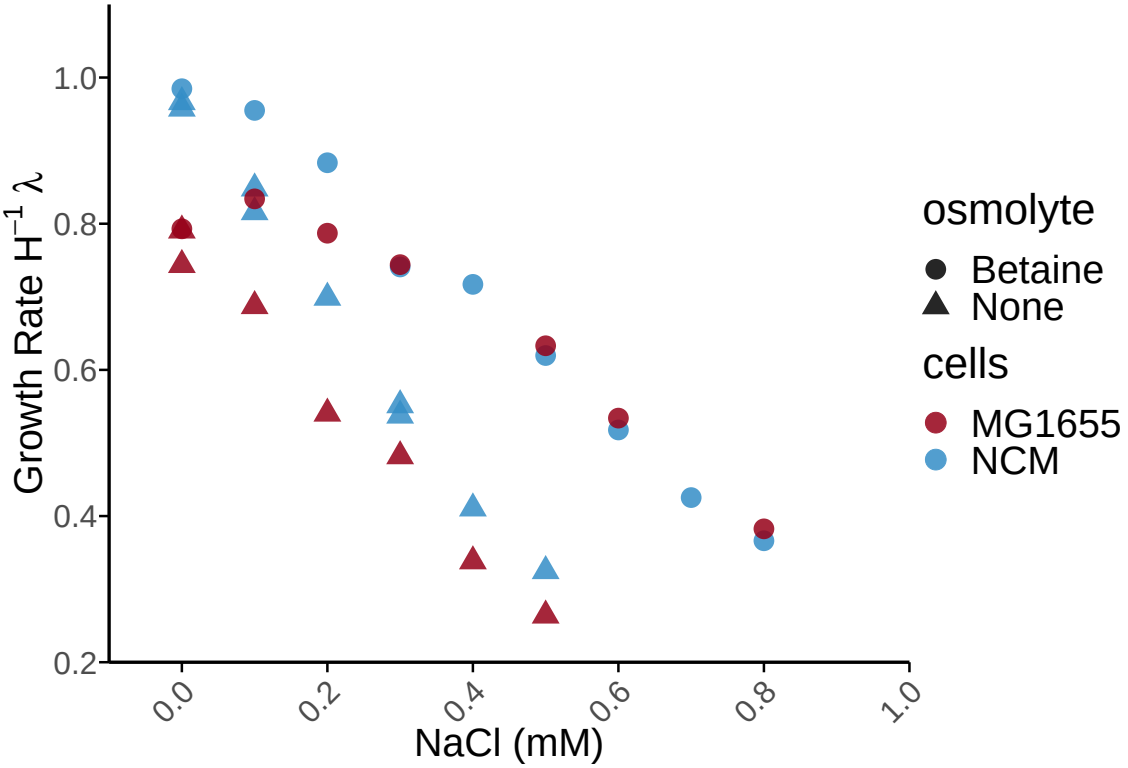

Figure S11: Growth Rate of MG1655 and NCM cells grown in MOPS either in a plate reader or shaking incubator.

NCM3722 cells grow a lot faster than MG1655 under normal osmolarity conditions. However, as osmolarity increases there is a convergence of growth rates without betaine which is interesting and potentially due to the effect of the RpoS mutation in NCM3722 cells (*88*). When betaine is supplemented we see a really drastic change in the behaviour of NCM and MG1655 cells. MG1655 cells show an initial maintenance

of their growth rate with betaine in the media as reported previously (*1*). NCM3722 cells on the other hand do not demonstrate this initial flat region instead showing near linear decrease with increasing NaCl concentration. The growth rates for betaine over lap and start descending at the same time.

The difference in growth rate between NCM and MG1655 is not well understood and cannot be explained by proteome reallocation alone (*47*). This behaviour could indicate that the difference in growth rates may be osmotic in nature. It is difficult to speculate without knowing the exact cause for slow down of growth during increased osmolarity but it seems like MG1655 cells are perhaps in a constant state of readiness for an osmotic or other shock growing slightly slower than NCM cells. This hypothesis is supported by the higher expression of RpoS regulated genes in MG1655 even during exponential growth (*47*). It may be that having a baseline level of readiness is beneficial to responding to acute stresses encountered by MG1655 in their natural environment.

A.7 Change in Cytoplasmic Water Content Analysis

Cayley and Record argue that the growth rate of *E. coli* under osmotic stress is reduced due to a reduction in cytoplasmic water content (*1*, *58*). This suggests that the growth rate slowdown in *E. coli* is caused by inability to make or import enough osmolytes to restore cytoplasmic water content. However, this is inconsistent with observations that there is no proteome bottleneck under osmotic stress and that overexpression of the choline or betaine transporters does not lead to an improvement in growth at higher osmolarity. Their main claim rests on their observation that in their condition the amount of intracellular water correlates with the growth rate. However as was shown by Taylor and coworkers the intracellular water content varies with nutrient limitation as well. This indicates that the change in growth rate can also cause a change in intracellular water.

One of the issues with comparing the data for these figures was the different units of the data. Luckily, two of the measurement conditions were in similar media and showed similar growth rates (minimal media with glucose). I therefore assumed that the cytoplasmic water in these two conditions was the same and used this two normalize data from Taylor to Cayley's scale. I used a conversion factor of 2.3 to convert from $\mu l/ml/od$ to $\mu l/mg\,dry\,weight$.

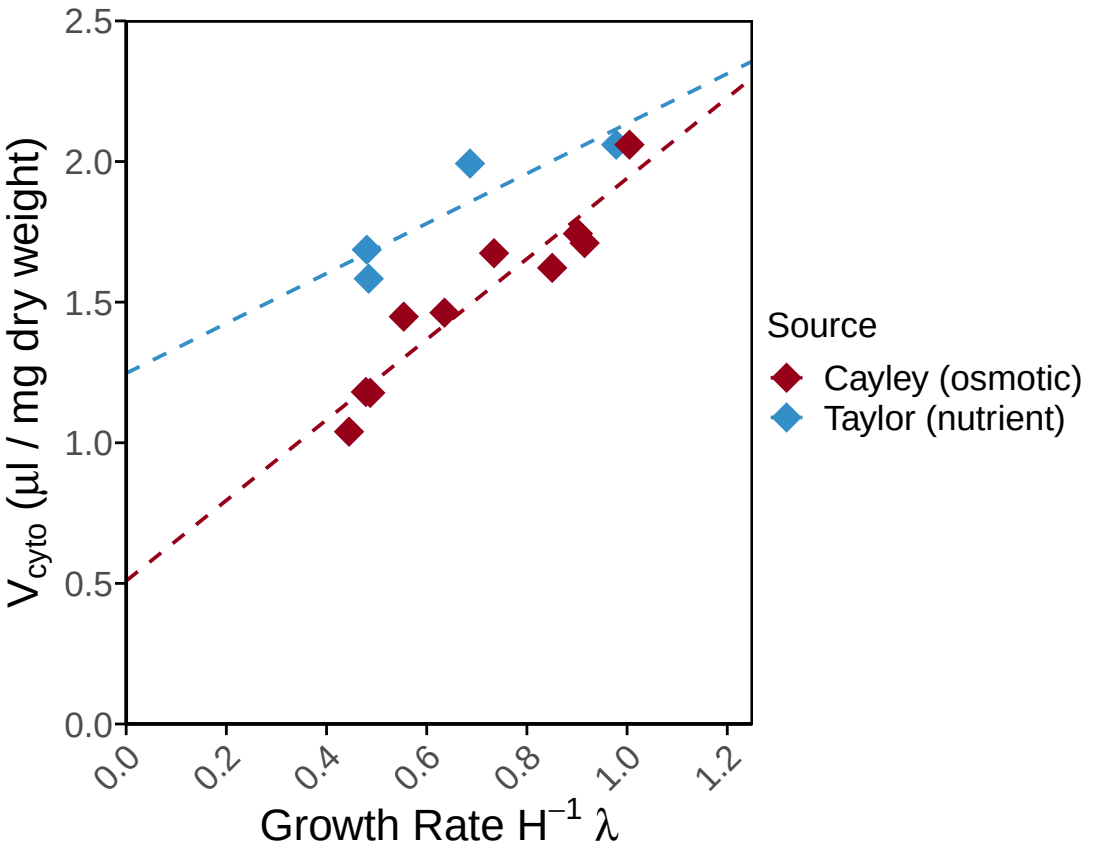

Figure S12: Comparison of Change in Intracellular water in MBM media with change in osmolarity. Also includes data in cells grown in 500 mM MBM media with addition of proline, betaine or choline (*58*, *120*), shown in red. Growth in phosphate media where growth rate is varied by changing carbon source (Glucose, Fructose, Mannose, and sorbitol) (*89*) shown in blue.

Here I show that there is significant cytoplasmic water loss as growth rate decreases regardless of whether the growth rate is varied by switching the carbon source or by varying the osmolarity of the media. Nonetheless, the reduction in cytoplasmic water does seem more pronounced with osmotic stress. However, these data indicate that cytoplasmic water concentration doesn't solely depend on external osmolarity. Instead this seems to be an actively regulated parameter by the cell that is tuned in different growth conditions. Furthermore, care needs to be taken comparing these data as they rely on the assumption that I have correctly converted the data from Taylor based on a single point of conversion.

A.8 Trehalose Over-expression Reduces Growth In High Osmolarity Media

Trehalose Over-expression in normal osmolarity condition causes a reduction in the growth rate as accumulation of useless metabolites forces depletion of endogenous metabolites (*89*). Taylor proposes that loss of endogenous metabolites is caused by cells maintaining a total internal metabolite pool that is related to the external osmolarity. They do not show that this is true for higher osmolarity but it would be logical for the cell to be constrained by the osmotic pressure it can generate. This again raises the question as to why there should be a growth defect at higher osmolarities. In theory higher external osmolarities would allow cells to maintain higher intracellular metabolite pools. However, *E. coli* cells do not indiscriminately accumulate metabolites but specifically accumulate compounds such as trehalose and betaine. Furthermore, compatible osmolytes are remarkably conserved across many different domains of life (*71*). Suggesting that the nature of these compounds makes them specifically beneficial to accumulate.

I tested trehalose overexpression in NCM derived strains HE 647 that has the Ots operon under Ptet regulation on the chromosome and HE 650 which has the same construct on a high copy number plasmid resulting in large trehalose overexpression upon CTC addition. Cells were grown in MOPS with glucose as the carbon source. 0.5 mM betaine was added when indicated. Trehalose concentration was not measured but instead assumed to be constant with osmolarity and measured trehalose values from Taylor are used (*89*).

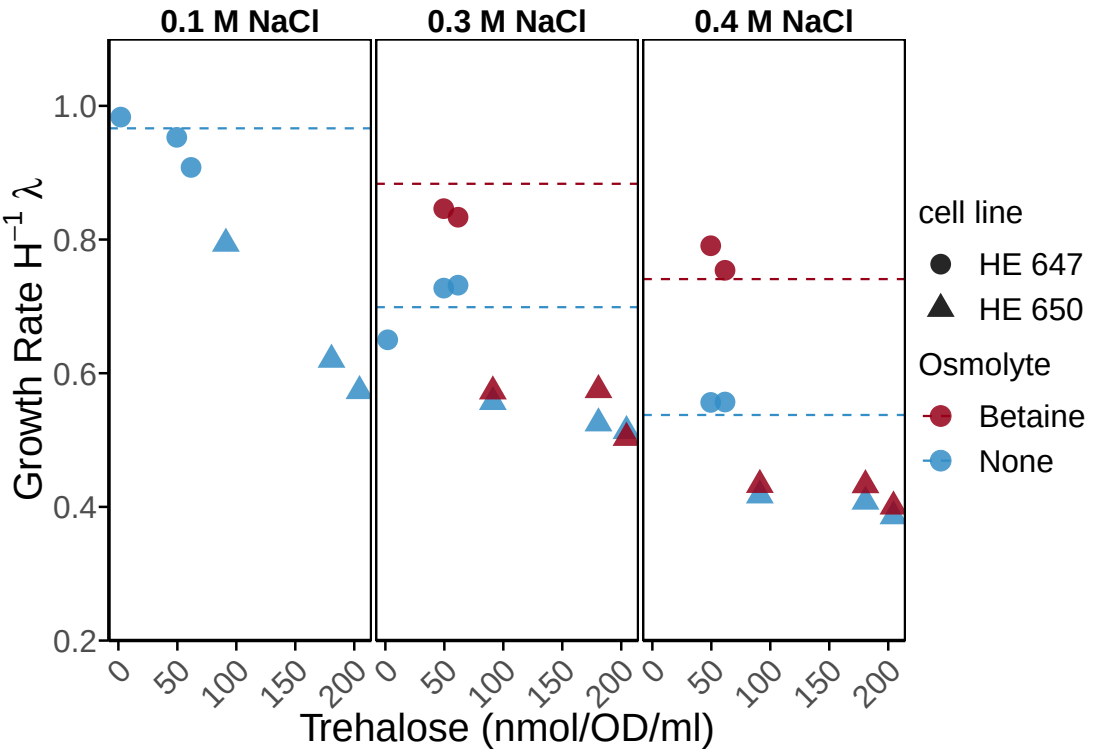

Figure S13: Trehalose overexpression was induced by addition of CTC. Growth was measured at normal osmolarity of 0.1 M NaCl (280 mOsm), 0.3 M NaCl (680 mOsm), and 0.4 M NaCl (880 mOsm). When indicated 0.5 mM of betaine was added to the media. Dashed lines indicate wild-type growth rates of the parent strain at a given osmolarity with or without betaine.

As expected with the notion that metabolites already add up correctly at various osmolarity, induction of trehalose overexpression failed to increase the growth rate. At normal osmolarity (0.1 M NaCl) there is a clear reduction in growth with increasing trehalose production. At 0.3 M NaCl there is a reduction in the growth rate as expected with increasing osmolarity. There is a small reduction of growth observed at 0.3 M NaCl when there is no expression of trehalose, consistent with my data from the MZ3 cell line. However, expression of just 100 nmol/OD/ml already causes a reduction in growth rate which is much less than the 600 mOsm change these cells experienced. The reduction in growth rate also does not appear to be linear as observed at normal osmolarity. Instead there is a rapid drop in growth rate. Over-expression of trehalose when betaine is in the media on the other hand leads to a worse outcome for the cells with cells growing as if no betaine were present. This effect is especially noticeable at 0.4 M NaCl with cells dropping from a growth rate of 0.78 to around 0.4 even in the presence of betaine. This suggests that overexpression of trehalose pushes out betaine at levels far below what is expected from the difference in osmotic pressure. For example at 0.4 M NaCl it would be expected that the intracellular solute pool

would need to accumulate an additional 800 mOsm of solute. However, expression of just 100 nmol/OD/ml led to worse growth and prevented any betaine accumulation. This data comes with the major caveat that trehalose expression is assumed constant across osmolarity in the HE 647 / 650 strains. As the native promoter has been replaced by pTet these cells should not be making any trehalose in the absence of CTC and trehalose expression should not be osmolarity controlled. However, in that case I would expect to see an initially lowered growth rate at 0 trehalose, which then increases up to the point where the internal and external change in osmolarity are equal. Then there should be a decrease for any additional trehalose as metabolites are lost. Instead these data suggest that trehalose expression at high osmolarity is surprisingly causing a further reduction in growth rate.

A.9 Ethylene Glycol and Glycerol are Membrane Permeant

To verify whether ethylene glycol and glycerol can freely permeate the cell membrane microscopy was used. Non-permeable solutes cause a rapid change in the *E. coli* cell shape (*57*). However, glycerol is known to freely cross the cell membrane via the Glycerol facilitator protein (GlpF) protein (*127*). I therefore, investigated cell size changes by attaching *E. coli* to a microscopy slide and flushing various concentration of glycerol or EG over them. Cell size was determined using a custom built GUI interface relying on a neural net for segmentation of cells from the background.

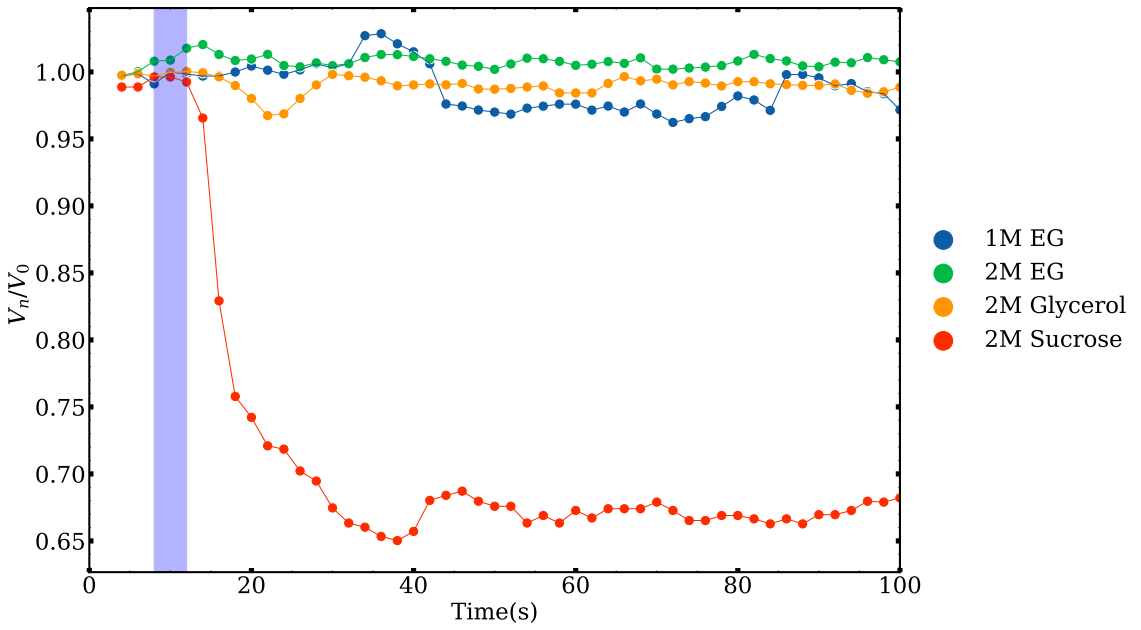

Figure S14: Cells attached to a microscopy slide were challenged by flushing of high osmolarity solutions of EG, glycerol or sucrose over them. The blue shaded region represents the time during which flushing occurs. Cell volume changes were observed over a period of 100 seconds.

As expected sucrose caused a rapid immediate reduction in cell volume while glycerol and EG showed no reduction in cell size indicating that there is no change in osmotic pressure as solutes diffuse freely across the cell membrane.

A.10 Linear regression for RNA / protein ratio

Results of performing linear regression value for the change in RNA / Protein ratio shown in figure 21 D.

Table 3: Regression Summary

Osmolyte	Term	Estimate	Std. Error	p-value	R^2
Betaine	Y-intercept	0.22	0.02	9.04×10^{-5}	0.56
Betaine	Growth Rate Slope	0.09	0.03	0.03	0.56
Choline	Y-intercept	0.22	0.02	1.6×10^{-4}	0.82
Choline	Growth Rate Slope	0.09	0.02	0.01	0.82
Proline	Y-intercept	0.19	0.03	0.01	0.60
Proline	Growth Rate Slope	0.12	0.06	0.12	0.60
Trehalose	Y-intercept	0.19	0.01	2.4×10^{-4}	0.95
Trehalose	Growth Rate Slope	0.10	0.01	0.01	0.95

Linear regression value for the change in $RP \times ER$ compared to change in growth rate shown in figure figure 21 E.

Table 4: Regression Summary

Osmolyte	Term	Estimate	Std. Error	p-value	R^2
Betaine	Y-intercept	0.62	1.04	0.59	0.73
Betaine	Growth Rate Slope	4.35	1.53	0.07	0.73
Choline	Y-intercept	-0.45	0.43	0.36	0.97
Choline	Growth Rate Slope	6.10	0.59	0.00	0.97
Proline	Y-intercept	0.63	1.05	0.59	0.76
Proline	Growth Rate Slope	5.20	1.71	0.06	0.76
Trehalose	Y-intercept	0.55	0.39	0.25	0.95
Trehalose	Growth Rate Slope	4.63	0.60	0.00	0.95

A.11 Calculation of ATP cost for osmolytes

ATP costs for different osmolytes were calculated by Oren (*106*).

Table 5: Amount of ATP required for osmolyte synthesis

Osmolyte	ATP
Glycerol	31
Ectoine	55
Glycine Betaine (via Glycine)	54
Glycine Betaine (via Choline)	59
Glucosyl-glycerol	85
Sucrose/Trehalose	110

A.12 Impact of pH and Base Addition on Osmolarity

As LAB rapidly acidify their surrounding by excretion of lactic acid into the media their growth is inhibited by the low pH. To allow for growth of more LAB the pH of the media can be controlled by addition of ammonia to the media. However, this alters the osmolarity of the media as solutes in the media are increased and therefore there is a natural limit to the amount of ammonia that can be added.

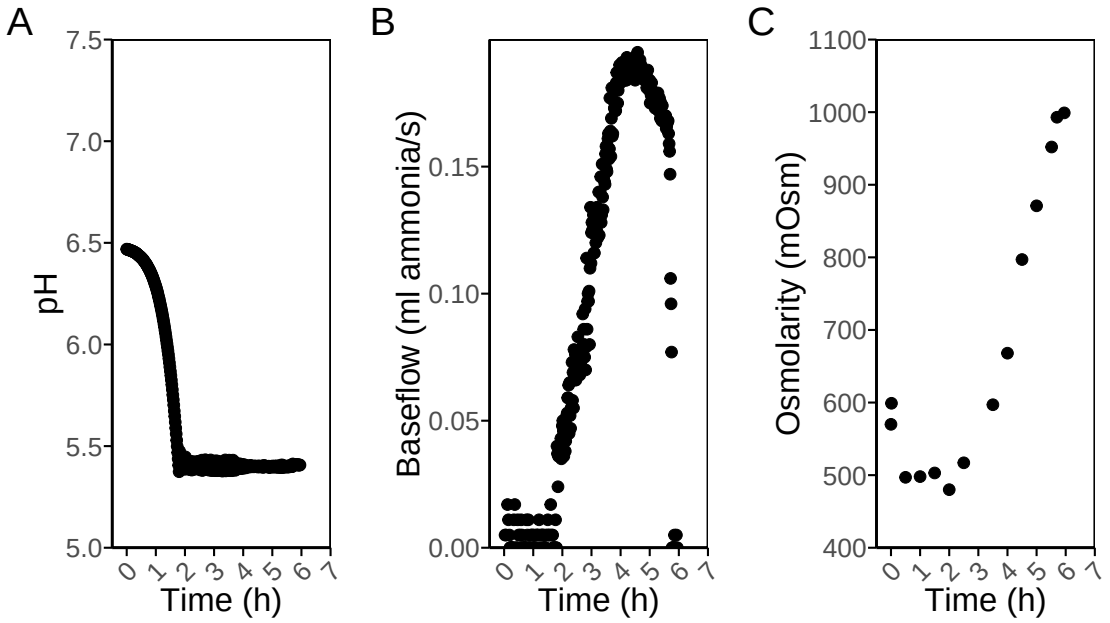

Figure S15: The media pH was monitored during batch fermentation of *L. animalis*. **A)** pH during fermentation. **B)** Amount of ammonia added to keep pH at set point. **C)** Change in osmolarity during fermentation.

As can be seen the rate at which ammonia is added increases over the course of the experiment as cells grow exponentially more and more ammonia needs to be added to keep pH constant. This leads to a rapid increase in the media osmolarity from about 500 mOsm to over 1000 mOsm.

A.13 Investigation of *L. animalis* Growth Rate at High Osmolarity

L. animalis cells were grown in a 15 ml bioreactor at 37 ℃ with gentle stirring in complex media media. Osmolarity of the media was changed by addition of 750mM NaCl.

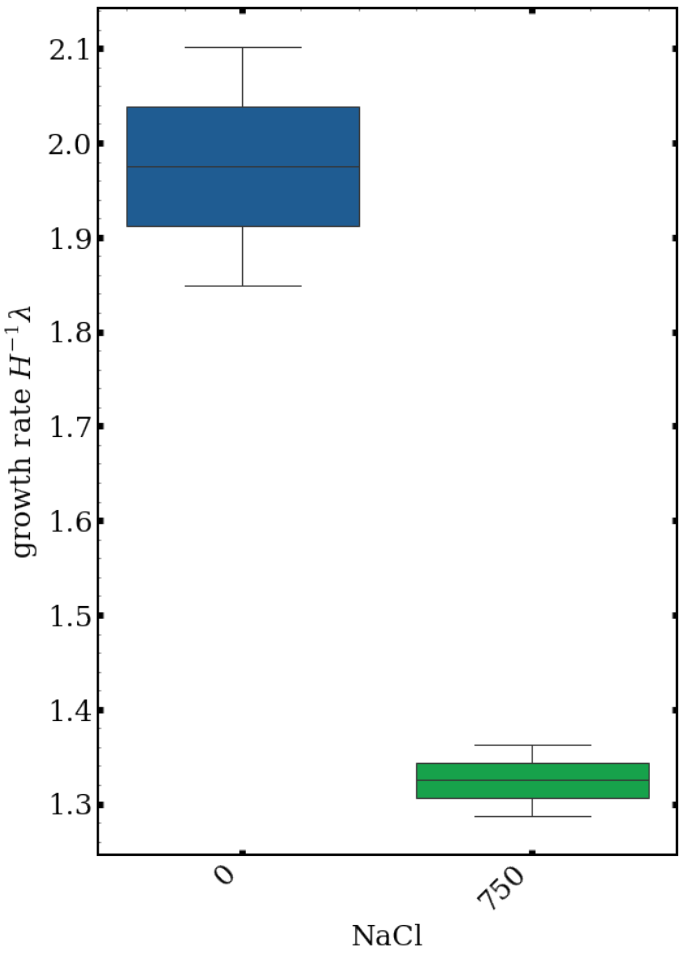

Figure S16: Comparison of growth rates of *L. animalis* in either base complex media media or media containing 750mM NaCl